2019

Long-Acting Intraductal Drug Delivery Systems for the Breast

Mibin Joseph
South Dakota State University

LONG- ACTING INTRADUCTAL DRUG DELIVERY SYSTEMS FOR THE BREAST

BY

MIBIN JOSEPH

A dissertation submitted in partial fulfillment of the requirements for the

Doctor of Philosophy

Major in Pharmaceutical Science

South Dakota State University

2019

DISSERTATION ACCEPTANCE PAGE

Mibin Kuruvilla Joseph

This dissertation is approved as a creditable and independent investigation by a candidate for the Doctor of Philosophy degree and is acceptable for meeting the dissertation requirements for this degree. Acceptance of this does not imply that the conclusions reached by the candidate are necessarily the conclusions of the major department.

Omathanu Perumal
Advisor Date

Omathanu Perumal
Department Head Date

Dean, Graduate School Date

ACKNOWLEDGEMENTS

I would like to thank Dr. Omathanu Perumal for giving me this opportunity. It was a great learning experience working with him and I truly value all the professional advice given to me during my time here. I greatly appreciate his guidance and his open-door policy for meetings which helped me in finishing my studies in a timely manner.

I thank all the committee members for their valuable suggestions and serving in my Ph.D. committee. I thank Emily Trias, Simon Newkirk, Amanda Zubke and ARW staff for their support throughout graduate studies. I thank Drs. Joshua Reineke, Michael Hildreth, Komal Raina and Xiangming Guan for their help at various stages of the project. I thank Drs.Satya Sadhu, Manju Saraswathi and Ranjit Averineni for their guidance during my first year here at SDSU. I would like to thank the department of pharmaceutical science for financial support for this project.

Most importantly, I thank my parents and my sisters for their encouragement and moral support.

TABLE OF CONTENTS

LIST OF FIGURES

LIST OF TABLES

ABBREVIATIONS

AI	Aromatase inhibitor
AURKA	Aurora Kinase A
BRCA	BReast CAncer gene
Cy 5.5	Cyanine 5.5
CYP 450	Cytochrome P450
DCIS	Ductal carcinoma in situ
DCM	Dichloromethane
DLS	Dynamic light scattering
EDX	Endoxifen
EGFR	Epidermal growth factor receptor
ER	Estrogen receptor
5-FU	5-Fluorouracil
HER-2	Human epidermal growth factor receptor 2
HDAC	Histone deacetylase
Hsp90	heat shock protein 90
4HT	4Hydroxytamoxifen
IC 50	inhibitory concentration 50
ID	Intraductal
IGF-1R	insulin-like growth factor receptor 1
ISG	In situ gel
IV	Intravenous

MK 167	human Ki-67 gene
MNU	N-methyl-N-nitrosourea (MNU)
MSG	PLGA microspheres in thermogel
MS	Microsphere
mTOR	mammalian target of rapamycin
NP	Nanoparticle
NMP	N-methyl-2-pyrrolidone
PARP-1	poly-ADPribose-polymerase-1
PDGFR	Platelet-derived growth factor receptor
PDI	Polydispersity index
PEG	Polyethylene glycol
PLD	PEGylated liposomal doxorubicin
PLGA	poly lactic-co-glycolic acid
PR	Progesterone receptor
PS	Polystyrene
PVA	Polyvinyl alcohol
SC	Stratum corneum
SEM	Scanning electron microscope
SERM	Selective estrogen receptor modulator
Src	proto-oncogene tyrosine-protein kinase
TMX	Tamoxifen
VEGF	Vascular endothelial growth factor

ABSTRACT

LONG- ACTING INTRADUCTAL DRUG DELIVERY SYSTEMS FOR THE BREAST

MIBIN KURUVILLA JOSEPH

2019

Breast cancer is the second most commonly diagnosed cancer in women in the US. Ductal carcinoma in situ (DCIS) is a premalignant lesion that has not metastasized through the regional lymph nodes to other organs. Currently, all breast cancers including localized breast cancers are treated with the same aggressive therapy. Localized drug delivery by direct intraductal injections into the mammary ducts can achieve high drug concentration at the target site. However, poor retention of drugs in the ducts limits the successful translation of this approach to the clinic. To this end, the main goal of this dissertation is to develop intraductal delivery systems that can sustain drug levels in the breast and reduce the frequency of intraductal injections.

The first objective was to test the influence of particle size and formulations using polystyrene (PS) particles (100-1000nm) and poly lactic-co-glycolic acid (PLGA) formulations [microspheres (MS) and in-situ gel (ISG) and nanoparticles (NP)] and to test the retention in the breast and regional lymph nodes. *In vivo* imaging study in rats showed that PS 1000nm was retained in the breast for 3 days compared to PS 500 nm and PS100 nm, which were retained for 2 days. The retention t ½ PS-1000nm particles was ~4-fold higher compared to 500nm, 100nm and free dye. PLGA MS and NP showed average particle size of 8.66 μm and 200 respectively. *In vivo* fluorescence imaging study in rats showed that PLGA ISG and MS were retained in the ducts for 4 days compared to PLGA

NP and free dye, which were retained for 2 days and 4 hours respectively. The breast retention t ½ of PLGA MS and ISG was > 4-fold higher compared to PLGA NP and free dye. Furthermore, PLGA MS and NP were transported and retained in the regional lymph nodes for 48 and 24 hours respectively. PLGA formulations followed a similar biodistribution trend when tested in pig. PLGA ISG and MS were retained for 4 days and the free dye was retained only for few hours.

The second objective was to develop intraductal formulations of tamoxifen (TMX) and study the *in vivo* biodistribution of TMX and its major active metabolites [4-hydroxytamoxifen (4HT) and endoxifen (EDX)] following intraductal delivery. The optimized PLGA MS and NP showed particle sizes of 9.12 μm and 274.1 nm respectively. *In vitro* release study showed that PLGA MS and ISG sustained release of TMX for > 3 weeks, while PLGA NP sustained TMX release for 2 weeks. PLGA MS and ISG T retained TMX in the breast for 2 weeks compared to PLGA NP and free TMX, which were retained 6 and 3 days respectively. The retention t ½ of TMX was delayed by >200 hours for PLGA MS and ISG compared to PLGA NP and free TMX. 4HT, a potent metabolite of TMX was generated in the mammary glands with PLGA MS and ISG and the levels were maintained above therapeutic levels for 2 weeks. No 4HT was detected in free TMX and PLGA NP groups after 2 and 7 days respectively. At the end of the treatment period (2 weeks), the amount of 4HT in the breast was 1.5 and 3.3-fold higher than free TMX group for PLGA MS and PLGA ISG respectively, and the concentration of 4HT was found to be above the therapeutic levels of 4HT in the breast. PLGA MS and ISG delayed the plasma t ½ by> 70 hours compared to free TMX. PLGA MS and ISG sustained TMX, 4HT and EDX levels in the plasma (<5ng/ml) for 2 weeks and showed ~2 fold lower systemic exposure

compared to free TMX. The C_{max} for free TMX was ~ 3- fold higher compared to PLGA MS and ISG. PLGA MS and ISG showed significantly lower levels of TMX, 4HT and EDX in the organs. Intraductal TMX did not show any measurable levels of TMX, EDX and 4HT in the uterus.

The final objective of the dissertation was to develop and test intraductal formulations of 4HT *in vivo.* To further prolong drug release upto a month, a combination of 4HT loaded PLGA microspheres and *in situ* gel (MSG) was used. *In vitro* release study showed that PLGA MSG sustained 4HT release for ~1 month. MSG retained 4HT for ~1 month compared to free 4HT, which was retained only for 1 week. EDX a metabolite of 4HT was generated in the mammary glands treated with MSG. At day 28, EDX levels were 22-fold higher in MSG mammary glands compared to free 4HT. Pharmacokinetic studies in rats showed that MSG sustained 4HT and EDX levels in the plasma for 2 weeks. MSG delayed the plasma $t_{½}$ of 4HT and EDX by >3 fold compared to free 4HT. No 4HT was detected in the regional lymph nodes in the free 4HT group. On the other hand, MSG sustained therapeutic levels of 4HT in the regional lymph nodes for 14 days and was undetectable at day 28.

Taken together, the findings from this dissertation demonstrate the feasibility of developing long acting intraductal formulations to prolong drug retention in the breast and reduce systemic drug distribution.

INTRODUCTION

A. BREAST ANATOMY AND PHYSIOLOGY

The human breast is a modified cutaneous exocrine gland and the skin over the breast connects to the underlying breast tissue through a facial layer and fibrous extensions of Coopers ligaments.[1, 2] The human breast lies on the anterior thoracic wall with its base extending from the second to the sixth rib.[3] Anatomically, the breast lies between the between the skin and underlying organs. The skin and nipple are attached to the breast through suspensory ligaments of cooper which are fibrous strands extending from the dermis into the breast. However, the peripheral boundaries of the mature human breast are not clearly defined with the exception at the deep surface where the gland overlies pectoralis fascia. Laterally, the breast extends over portions of serratus anterior muscle, over external oblique muscle inferiorly and over rectus sheath superiorly and medially into the sternum. The breast tissue comprises of epithelial and parenchymal cells and the stroma. The epithelial cells constitute 10-15% of the overall breast volume and the remainder of the volume is filled with components of the stroma. The breast is divided into upper inner, upper outer, lower inner and lower outer quadrant using two perpendicular planes intersecting at the nipple or nipple centroid line.[4]

The human breast is composed of glandular (secretory) and adipose (fatty) tissues supported by Cooper's ligaments (connective tissues) (Figure1). The secretory tissue is drained by a network of ducts that stores and transports milk during lactation[5]. The human breast consists of 15-20 lobes and each lobe is further divided into 20 to 40 lobules containing 10-100 alveoli (0.12mm in diameter)[6]. These lobules are composed of tubule

alveolar glands and it drains into a major lactiferous duct. The lactiferous ducts drain into lactiferous sinus (2-4mm)[7] which ultimately opens through orifices onto the nipple.[3]

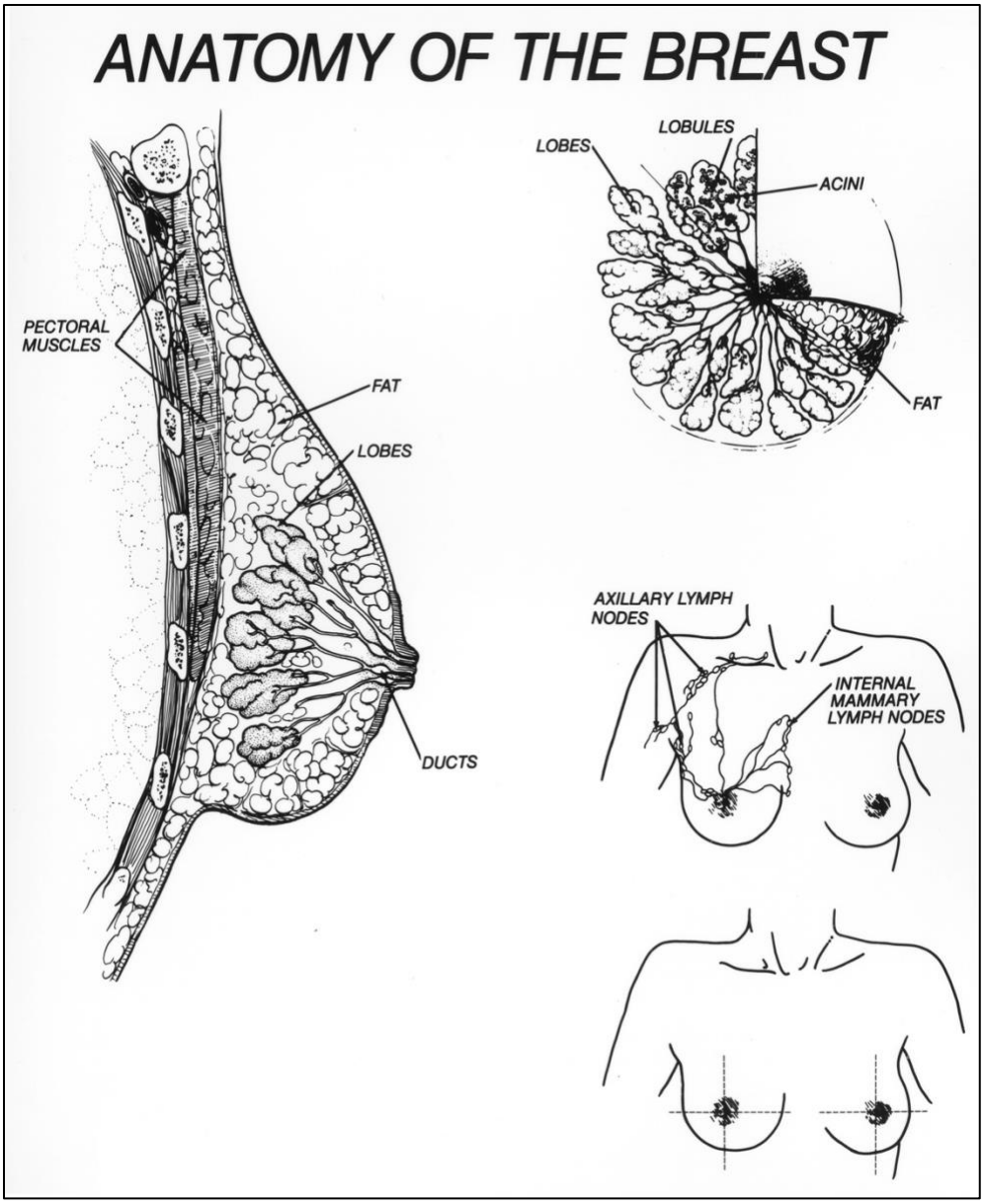

Figure 1: Anatomy of the breast

Reproduced from https://visualsonline.cancer.gov/details.cfm?imageid=2170

Breast Ductal System

The human breast comprises of 15-20 mammary ductal networks but all of these ducts do not terminate as ductal orifices at the nipple (Figure2). [8] The ductal networks can be grouped into true mammary ducts and sebaceous glands. Studies [9, 10] have confirmed that only 5-9 ducts terminate at the nipple and are accessible from the outside. Even though the ductal systems are in close juxtaposition to each other, they are not connected. [8] There is increasing evidence that breast cancer originates from a single ductal system. The sick lobe theory describes DCIS as a lobar disease and the *in situ* tumor foci are localized in the single lobe of the breast. [11] Therefore, the variabilities within each of these ducts needs to be considered in designing appropriate treatment strategies. [8] For example, in patients with a genetic predisposition to breast cancer (BRCA1, BRCA 2), the specific ducts express surrogate markers before any histological changes appear. By utilizing these surrogate markers, high risk ducts can be accessed and treated effectively.

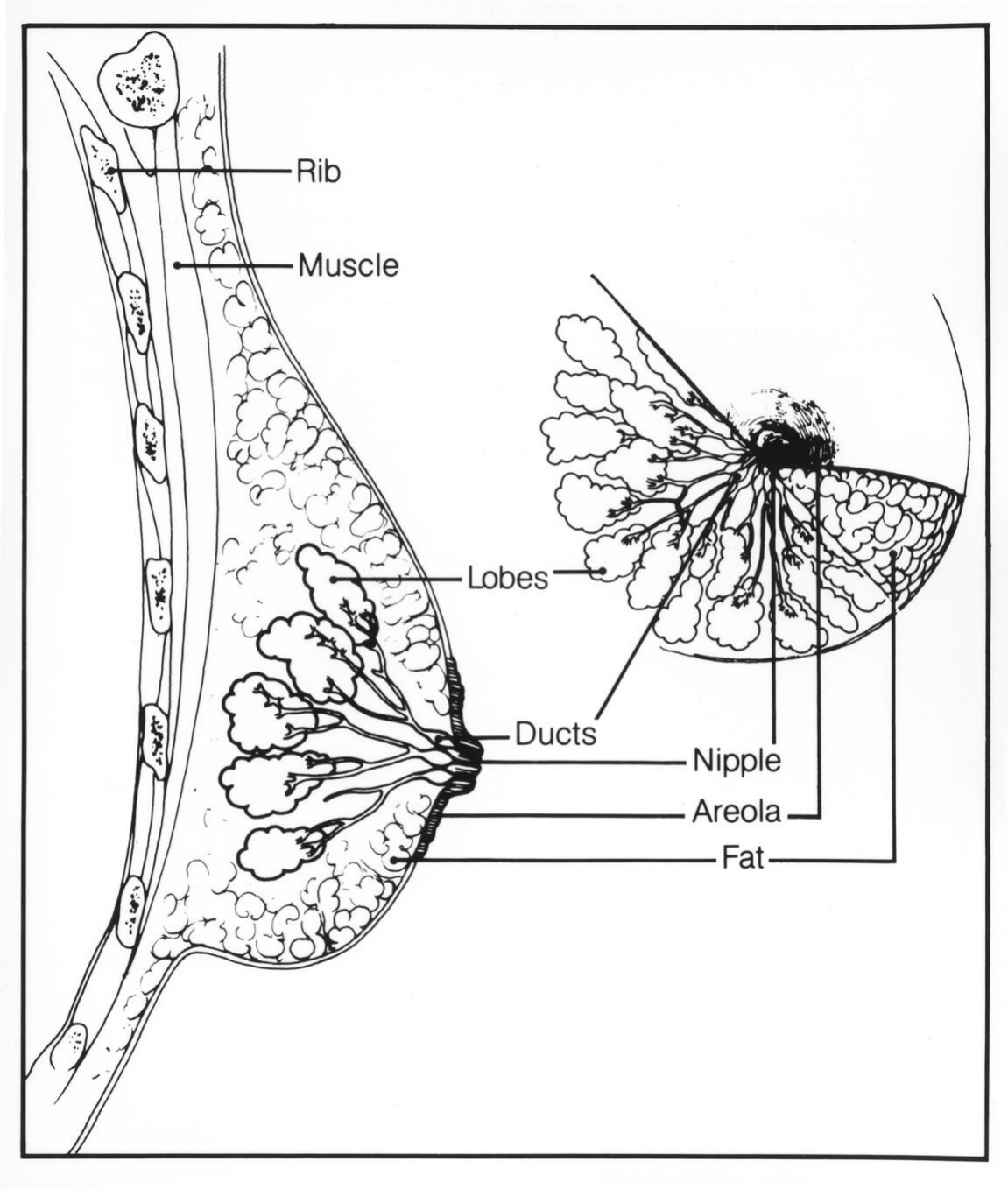

Figure 2: Breast duct anatomy

Reproduced from https://visuals.nci.nih.gov/details.cfm?imageid=1810

Vascular and Lymphatic components in breast

Three major arteries supply blood to the breast. About 60% of the blood supply is through the internal mammary artery arising from the internal thoracic artery. Around 30% of the blood supply is provided by the axillary and thoracoacromial arteries, and the remainder through the posterior intercostal arteries[12].

The lymphatic system plays a prominent role in maintaining tissue fluid homeostasis. The extravasated blood plasma and proteins are collected in the interstitial space and this forms the lymph fluid. The lymphatic system is primarily divided into lymphatic capillaries, collecting vessels, lymph nodes, and lymphatic trunks and ducts. Studies by Sappey[13] in the early 1870's demonstrated that breast lymphatics are separate from the underlying torso with the lymphatics in the subareolar plexus and a small number of large lymphatic vessels draining into the axillary lymph nodes (Figure 3). In the superficial layer of the skin, the lymphatics capillaries are 20-70 μm in diameter and they drain into pre-collectors that are up to 70 - 150 μm in diameter. These capillaries drain to lymph collectors in the subcutaneous space and are 150 - 350 μm in diameter. The lumen of lymphatic vessels are wider and more irregular than vascular capillaries and these are composed of single layer of endothelial cells and a discontinuous basement membrane of 10-50μm in diameter. [14] Axillary lymph nodes accounts for more than 75% of lymphatic drainage of the breast.[1, 15, 16] The number of nodes in the axillary region are determined to be 20 to 30. The lymph nodes are classified in accordance with their relationship to the pectoralis minor muscle. [3, 17] Level I lymph nodes (axillary vein, external mammary and scapular groups) are located

lateral to the pectoralis minor muscle. Lymph nodes found in the superficial and deep regions of pectoralis muscle are termed as level II lymph nodes (central and interpectoral group). Level III lymph nodes are located medial to the pectoralis minor muscle (subclavicular group).

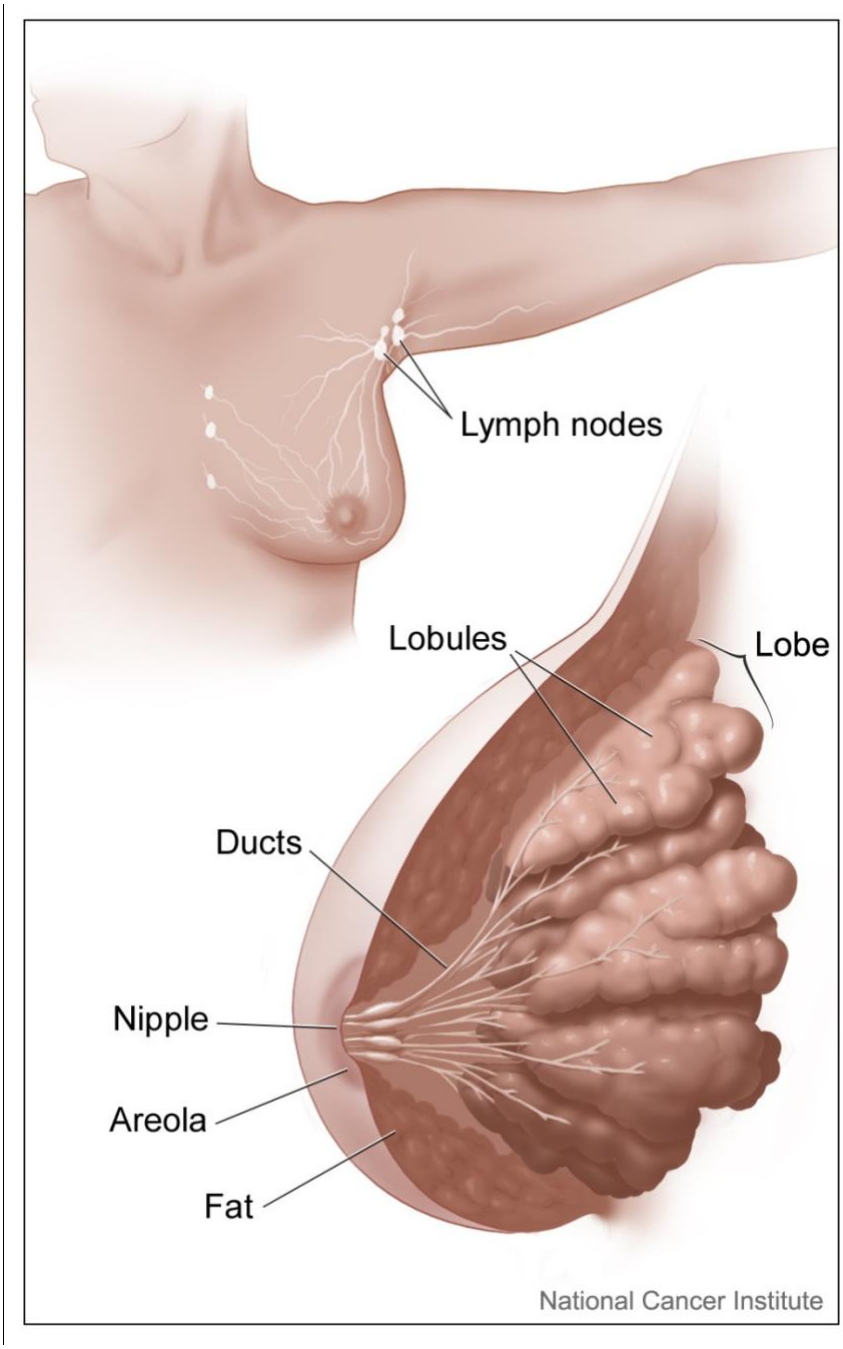

Figure 3: Breast and adjacent lymph nodes

Reproduced from https://visualsonline.cancer.gov/details.cfm?imageid=4347

B. BREAST CANCER

Breast cancer accounts for 30% of all new cancer diagnosis in women and it is the second most commonly diagnosed cancer amongst females in the US. [18] In 2019 alone, the American Cancer Society estimates 268,600 new cases of invasive breast cancer and 62,930 new cases of non-invasive (in situ) breast cancer. The majority of breast cancer originates in the epithelial cells lining the milk ducts. These malignant cells are characterized by uncontrolled cell division of epithelial cells within the ducts (in situ carcinoma) and if overlooked, eventually breaches the basement membrane and becomes invasive. [19, 20]

The exact cause of breast cancer is still unknown, but there are several risk factors which contribute to its development. There is a correlation between increased risk of developing breast cancer with an increase in age. The incidence rate of breast cancer doubles with every 10 years of age until menopause. [21] Other factors include limited blood supply to the ducts, [22] age at menarche and menopause, age at first pregnancy, and family history. [21] Women with mutations in two genes, BRCA1 and BRCA2 are associated with increased risk of developing breast cancer. It is found that about 5-10% of breast cancer cases are due to this mutation and there is an 80% chance that these women will develop breast cancer during their lifetime. [21, 23] Cells that lack BRCA1 and BRCA 2 have deficiency in repairing the double strand breaks of DNA. The resulting genomic instability contributes to the underlying mechanism to breast cancer. [24] Breast cancer incidence rates are increasing in countries with historically higher incidence rates such as in Europe, as well as in regions with lower incidence rates which includes some countries in Latin America,

Asia and Africa. [25] Some of the factors that accounts for this rising trend are altered reproductive patterns such as age at first pregnancy, breast feeding duration, number of childbirths and lifestyle changes. [26, 27,28]

The majority of the breast cancers are localized and there is a lack of clear understanding of tumors that will eventually become invasive breast cancer. [29] Lymphatic system also plays a key role in cancer metastasis and breast cancer mortalities are primarily due to metastasis to other organs through the regional lymph nodes. The is pathological examination of lymph nodes is used for determining the stage of the cancer and metastasis. [30] Generally, lymphatic drainage of the breast occurs to the adjacent lymph nodes and not to lymph nodes on the contralateral breast. Hence, there is minimal chance of cancer metastasis to the contralateral nodes. [17] However, extensive blockage of lymphatic vessels results in subcutaneous lymphatic permeation to occur on the opposite breast.

Types of Breast Cancer

Breast cancer can be classified based on the stage of cancer[31](Table 1), epithelial origin and molecular subtypes.

Based on the epithelial origin[32] breast cancers can be grouped into:

I. *DCIS (Ductal carcinoma in situ)* is designated as Stage 0 in the AICC (American Joint Commission on Cancer) staging of breast cancer. DCIS is the abnormal proliferation of epithelial cells lining the mammary ducts (Figure 4). In situ refers to the fact that the malignant cells have not breached the basement membrane out into the stroma in the breast.

II. *IDC (Invasive ductal carcinoma)* remains the most prevalent type of invasive breast cancer and accounts for 70-80% of all cases (Figure 5). In IDC, the malignant cells spread throughout the breast tissue, blood vessels and the lymphatic system and metastasize to regional lymph nodes, and in advanced cases to the rest of the body. Around 75% of IDC are ER (estrogen receptor) and PR (progesterone receptor) positive and 15-20% expresses growth factor receptor HER2 (human epidermal growth factor receptor 2).

III. *ILC (infiltrating lobular carcinoma)* is the second most common IDC. It is generally ER positive and found to occur more frequently in older women. ILC is characterized by a lack of cellular adhesion due to alterations in E-cadherin, a protein that aids in cell adhesion that is deleted or mutated.[32] The lack of cellular adhesion gives rise to a single pattern of cells microscopically which is a distinguishing feature of ILC.

Table 1: Breast cancer classification based on stage of the cancer

Stage	**Classification**
Stage 0	In situ
Stage 1	Early stage – Invasive
Stage II	Early stage – Invasive
Stage III	Locally advanced
Stage IV	Metastatic

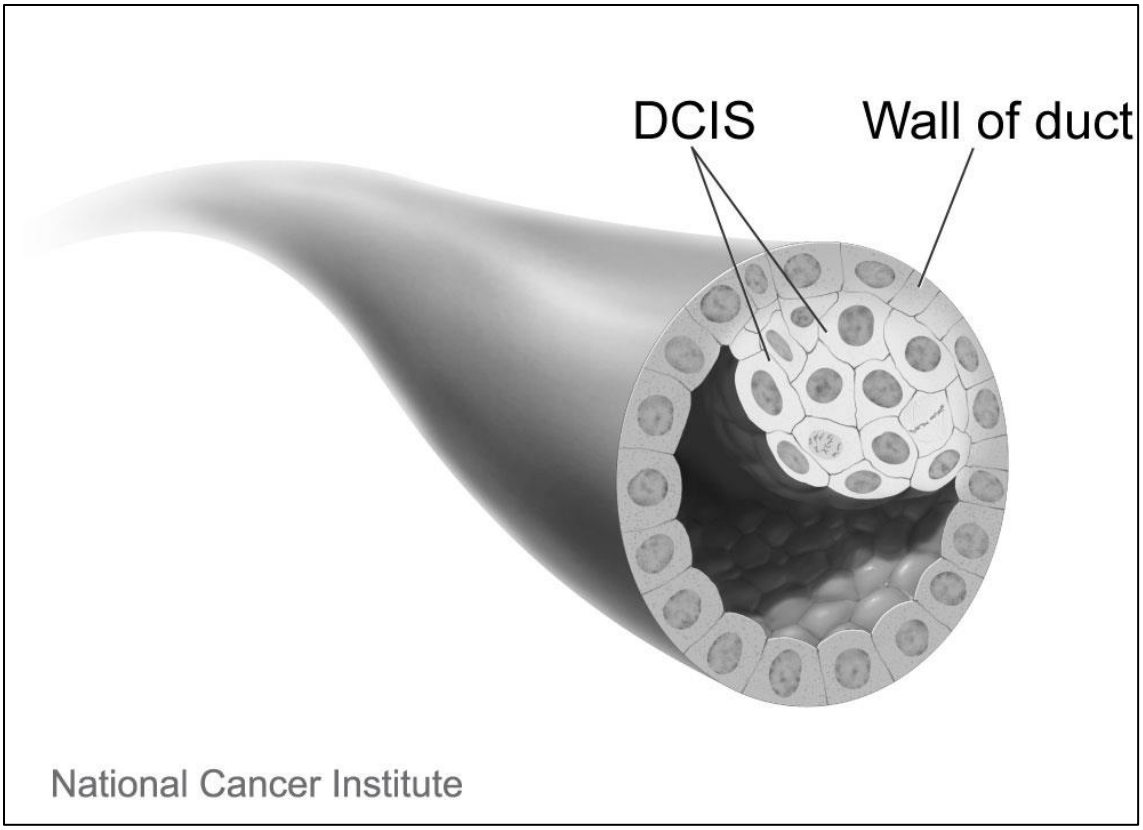

Figure 4: Ductal carcinoma in situ

Reproduced from https://visualsonline.cancer.gov/details.cfm?imageid=4353

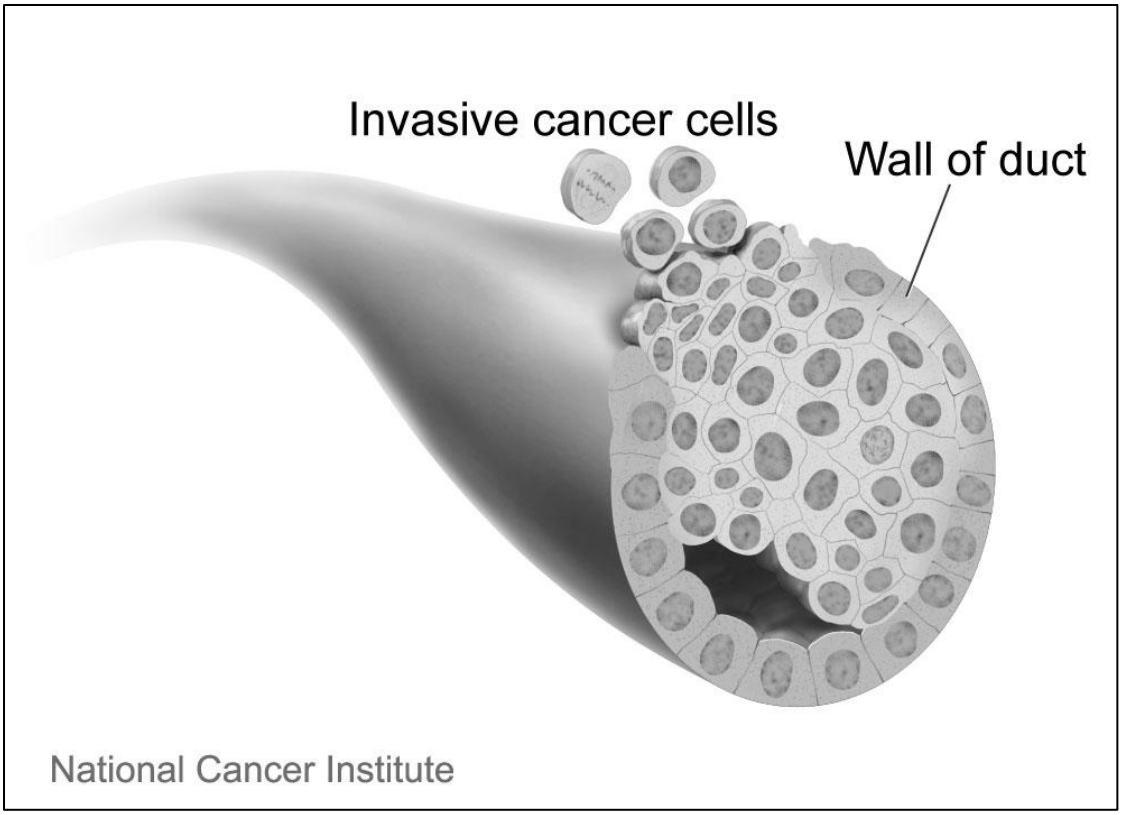

Figure 5: Invasive breast cancer

Reproduced from https://commons.wikimedia.org/wiki/File:Invasive_breast_cancer.jpg

Molecular subtypes of breast cancer

Breast cancer is also classified based on immunohistochemical expression of ER (estrogen receptor) PR (progesterone receptor), HER2 (human epidermal growth factor 2 receptor) and Ki67. [33, 34] The four main types are:

1. Luminal A (ER^+ or PR^+, $HER\text{-}2^-$)
2. Luminal B (ER^+ or PR^+, $HER\text{-}2^+$)
3. HER2 (ER^- or PR^-, $HER\text{-}2^+$)
4. Triple Negative (ER^- or PR^-, $HER\text{-}2^-$)

1. Luminal A breast cancer

Based on the molecular profile, majority of infiltrating lobular carcinomas belong to Luminal A subtype. This accounts for 50-60% of all cases of breast cancer[35]. The expression of estrogen receptors is similar between Luminal A breast cancers has low expression of cell cycle related genes (eg: MK167 and AURKA), and higher expression of luminal related proteins such as progesterone receptor and FOX 1. Luminal A tumor subtype also show a lower number of mutations across the genome. The patients with this type of cancer have better prognosis compared to Luminal B subtypes, but is associated higher incidence of bone metastasis in patients with tumor relapse. [35] The treatment options include aromatase inhibitors, selective estrogen receptor modulators and selective regulators like tamoxifen and fulvestrant respectively. [36, 37]

2. Luminal B breast cancer

This subtype represents 10-20% of all breast cancer cases. Luminal B subtype is more aggressive and has poor prognosis [33] compared to luminal A type. The main factor that distinguishes this subtype from luminal A type is the increased expression of proliferation genes such as MK167 and cyclin B1, and expression of HER2 and EGFR. The luminal B subtype has tumors with $ER^{+}/HER\text{-}2^{+}$ with high Ki67 expression. The treatment is challenging because of the poor prognosis. The luminal B type responds better to neoadjuvant chemotherapy achieving complete response in 17% of cases. [33, 37] Studies are underway to determine the mechanisms of metastasis vis-a-vis effective treatment approaches for this subtype. [37]

3. HER-2 positive breast cancer

The human epidermal growth factor receptor 2 (HER-2) gene encodes a transmembrane tyrosine kinase receptor protein that is a member of epidermal growth factor receptor (EGFR).[38] An increased expression of HER-2 gene/protein expression constitutes 10-34% of all invasive breast cancers.[39] This tumor subtype is characterized by higher expression of HER-2 related and proliferation related genes and proteins. At the DNA level, this shows the highest number of mutations across the genome. This type of tumor constitutes 15-20 % of all cases of breast cancer cases and has a poor prognosis.[39] However in the last decade anti-HER2 therapy has significantly improved the survival of patients with HER2 positive breast cancer.[40]

4. Triple negative/basal-like breast cancer

The basal like tumors represents 10-20% of all breast cancers. The term basal like is used because of the similarities in the expression of genes (CK5 and CK 17, EGFR. CD 44 etc.) in normal myoepithelial cells and luminal epithelium[33] (CK8/18, Kit etc.), but at significantly lower levels than luminal subtypes. These tumors show a high response rate to chemotherapy; however, have a higher rate of relapse within the first three years and a worse prognosis than luminal types. One of the key features of this subtype is the absence of ER, PGR and HER-2. These tumor subtypes tend to be infiltrating carcinomas with aggressive metastasis visceral organs, mainly lungs, CNS and lymph nodes. [36] The standard systemic treatment for triple negative cancer follows the same principle as other types of breast cancer. [41] One of the most promising therapies to treat these tumors is poly-ADPribose-polymerase-1 (PARP-1) inhibitors, which is associated with a higher response rate and clinical benefit. [42] The advance of multiomics have led to the discovery of targeted therapies which can be particularly beneficial for this subtype.

C.THERAPEUTIC APPROACHES FOR BREAST CANCER

Breast cancer treatment regimens depends upon several factors like the extent of tumor lymph node metastasis, grade of the tumor, hormone receptor status and HER2 overexpression, age and menopausal status of the patient. The most common treatment modalities currently used are described below.

1. Surgery
2. Radiotherapy
3. Chemotherapy
4. Hormone Therapy

5. Targeted Therapy

1. Surgery

Currently most of the early stage tumors are removed by surgical approaches. [43] However, the major drawback is that the chance of tumor relapse is unpredictable. Adjuvant chemotherapy is recommended along with surgery, which results in unwanted side effects. [44] In case of patients with larger tumor size and high nodal involvement at diagnosis, neoadjuvant therapy is recommended with the goal being to shrink the tumor to aid surgery. Earlier, the standard treatment for breast cancer was limited to mastectomy, which is the complete removal of breast tissue along with the underlying muscle tissue and the associated lymph nodes. [45] This procedure significantly impairs the quality of life of patients and several studies [46] show increased risk of depression and body image issues in these patients. However, improvements in mammographic screening techniques lead to early diagnosis and a reduction in mastectomy. [47] As a result, local resection of the tumor followed by radiotherapy with chemotherapy is favored for patients diagnosed with breast cancer. [48]

Breast conservation surgery (Lumpectomy) is an established procedure for women diagnosed with early stage breast cancer. It involves the surgical resection of tumor, axillary node dissection followed by radiotherapy of the affected breast.[49] Almost two thirds of patients are eligible for breast conservation surgery, with an average presentation of tumor size at less than 2 cm. However lumpectomy does not completely eliminate the chances of tumor relapse in the conserved breast. The major factors that determine the local

recurrence within the conserved breast are the margin status and an extensive *in situ* component. Other factors include age (< 35 years) and nodal status, large tumor size (>2 cm), and higher histological grade at the time of surgery.

The choice of adjuvant chemotherapy depends on several factors ranging from the extent of spread of tumor locally or to the axillary lymph nodes. Depending upon the stage of cancer, sentinel lymph node technique allows for the removal of axillary lymph nodes bypassing the need for axillary curettage if these nodes are not invaded.[50] Axillary lymph node dissection is associated with edema, numbness, pain and decreased mobility of the affected arm. As a general procedure in breast conservation therapy, radiation therapy accompanies the treatment and the affected breast is irradiated with additional dose of radiation to the tumor excision region and to the lymph node regions.

2. Radiotherapy

Different types of radiation therapies such as external beam radiation therapy, brachytherapy and systemic radioisotope therapy and fractionation regimens are employed in many types of cancer including breast cancer. [51] Radiotherapy is also used to reduce the size of the tumor before lumpectomy and is also as a way to reduce the treatment burden to the patient undergoing chemotherapy. [52] With technological advancements, image-guided treatment devices enabled more precise delivery of high intensity beams of radiation to tumor site with decreased damage to healthy surrounding tissue. However, the overall benefit from radiotherapy is unpredictable as some of the tumor cells resist radiation damage giving rise to recurrent tumors for which there are limited treatment options

available.[53] Also, radiation therapy is expensive and time consuming and hence shorter treatment options are preferred by patients.[54]

3. Chemotherapy

The potential for the development of chemotherapeutic drugs dates back to the First World War when soldiers who underwent treatment after exposure to sulfur mustard gas developed lymphoid aplasia. Later, nitrogen mustards became the first chemical agents to be tested in clinic and showed remarkable results in lymphoma patients.[55] Most of chemotherapy drugs reduce the rate of cell growth either by interacting with the DNA or by interfering with cell division. [56]

These drugs lack the ability to distinguish between normal and cancer cells and this non-specificity result in serious side effects. They are used either as single agents or in combination to reduce the chances of cancer resistance towards a single agent. The drugs and drug combinations approved by USFDA to treat breast cancer are listed in Tables 2 and 3. If the cancer is diagnosed at later stages, the goal of chemotherapy is palliative and treat the symptoms to improve quality of life.[55] The common prognostic indicators for breast cancer include the size of tumor, grade, lymph node evasion and age. The presence of hormone receptors (estrogens and progesterone), overexpression of epithelial growth factor receptor 2 (HER2) and Ki67 index which quantifies the cellular proliferation levels have been included as prognostic indicators in the recent years.[52] Administration of chemotherapy after surgery has improved the rates of disease free and overall survival rates is contingent upon the above mentioned prognostic markers. [57, 58] Anthracyclines and taxanes (paclitaxel and docetaxel) are considered to be most beneficial for adjuvant

chemotherapy. A randomized study showed improved survival upon administration of four cycles of doxorubicin/cyclophosphamide (AC) followed by four cycles of paclitaxel.[59] In a larger randomized trial, patients were administered four cycles of AC followed by paclitaxel once in three weeks or weekly, docetaxel once in three weeks or weekly docetaxel. Improved survival rates were observed with four cycles of AC followed by a single dose of paclitaxel every week for 12 weeks.

Table 2: USFDA Approved chemotherapeutic agents for breast cancer

Drug	Route of Administration
Paclitaxel Albumin- stabilized Nanoparticle Formulation	IV
Pamidronate Disodium	IV
Capecitabin	Tablet
Cyclophosphamide	IV, tablet, capsule
Docetaxel	IV
Doxorubicin Hydrochloride	IV, liposomal
Epirubicin Hydrochloride	IV
Eribulin Mesylate	IV
Everolimus	Tablet
Exemestane	Tablet
5-FU(Flurouracil)	IV
Gemcitabine Hydrochloride	IV
Methotrexate	IV, Tablet
Paclitaxel	IV
Thiotepa	IV
Vinblastine Sulfate	IV

IV – Intravenous, 5FU- 5 Fluorouracil

Source: National Cancer institute (https://www.cancer.gov/about-cancer/treatment/drugs/breast)

Table 3: USFDA approved combination chemotherapy for breast cancer treatment

Code	Drugs used in combination
AC	Doxorubicin Hydrochloride, Cyclophosphamide
AC-T	Doxorubicin Hydrochloride, Cyclophosphamide, Paclitaxel
CAF	Cyclophosphamide, Doxorubicin Hydrochloride, Fluorouracil
CMF	Cyclophosphamide, Methotrexate, Fluorouracil
FEC	Fluorouracil, Epirubicin Hydrochloride, Cyclophosphamide
TAC	Docetaxel, Doxorubicin Hydrochloride, Cyclophosphamide

Source: National Cancer institute (https://www.cancer.gov/about-cancer/treatment/drugs/breast)

Limitations of chemotherapy

The process governing cell division (mitosis and apoptosis) are common to tumor cells and normal cells and chemotherapy affects both cell populations. The goal of treatment is to attain sufficient tumor cell killing while limiting toxicity towards normal cells. However, the therapeutic index for most conventional chemotherapy drugs is close to one and toxicity to the normal cells is dose limiting. [56] During the treatment period, the rapidly dividing cells of the GI tract, hair follicles, bone marrow and gonads are predominantly affected by these drugs. The common side effects include hair loss, nausea and vomiting, myelosuppression and reduced fertility. [56] Also, majority of these drugs can cause teratogenicity effects and hence harmful to the fetus. Long term effects of chemotherapy include the potential for development of cardiomyopathy caused by doxorubicin and pulmonary fibrosis due to treatment with bleomycin. [60] Some of the common side effects of chemotherapy associated with chemotherapy agents are listed in table 4.

Table 4: Common adverse effects of cytotoxic chemotherapy [55]

Tissue	Manifestations	Agents likely to cause toxicity
Reticuloendothelial	Neutropenia Anaemia Thrombocytopenia	Alkylating agents, anthracyclines, taxanes, Topoisomerase inhibitors
Gastrointestinal	Diarrhoea Oral mucositis Nausea and vomiting	Antifolates, fluoropyrimidines Various
Neurological	Peripheral sensory neuropathy Ototoxicity	Vinca alkaloids, taxanes Cisplatin, oxaliplatin
Renal	Acute renal failure	Cisplatin
Hepatic	Transaminitis	Raltitrexed
Cardiac	Acute or chronic cardiomyopathy Cardiac ischaemic events	Anthracyclines Fluoropyrimidines
Respiratory	Pulmonary fibrosis	Bleomycin
Bladder	Haemorrhagic cystitis	Cyclophosphamide

Others	Hand-foot syndrome Vesicant Anaphylaxis Alopecia, fatigue, lethargy Subfertility/infertility Increased risk of second malignancy	5FU infusion, capecitabine Doxorubicin, vincristine Taxanes Combination chemotherapy containing alkylating agents

Reproduced from Corrie, P.G., 2008. Cytotoxic chemotherapy: clinical aspects. *Medicine*, *36*(1), pp.24-28.

4. Endocrine/Hormone Therapy

Hormone receptor positive (estrogen and progesterone) breast cancer constitutes 65-75% of all breast cancers. [61] In this subtype, the tumor cells are largely dependent on female hormones for their growth and survival. The serum concentrations of the major hormones estrogen and progesterone are regulated through hypothalamic-pituitary-gonadal axis. In pre-menopausal women, estradiol is synthesized by ovaries whereas in post-menopausal women, estradiol is produced from adrenal androgens in the peripheral tissues mainly adipose tissues. [62]

The two main classes of drugs used for endocrine therapy are i) selective estrogen receptor modulators (SERM's) and ii) aromatase inhibitors (AI's). SERM's binds competitively to the estrogen receptors and interfere with the DNA synthesis and eventually inhibit G0 to G1 cell cycle progression. [63] AI's inhibit the enzyme aromatase which converts circulating testosterone and androstenedione to estradiol and estrone respectively by aromatization. [64] Hence AI's is proven to be beneficial in post-menopausal women, where the primary source of estrogen is depleted. The most commonly reported side effects of hormone therapy are hot flashes, weakness and tendency towards weight gain and depression. [52]. Although rare, but serious, these agents also cause thrombo-embolic events and endometrial cancer. [52] There are also reports of reduced bone density resulting in increased fracture rate and an increase in the coronary artery events with these agents. [65] The USFDA approved endocrine therapy agents to treat breast cancer listed in Table 5.

1. SERM's

Estrogen is a steroid hormone that plays a major role in growth and function of breast, uterus and ovaries. It also plays a key role in maintaining bone density and lowering the cholesterol levels in the body. In case of ER+ cancers, it stimulates the growth of cancer cells in the breast and uterus. Estrogen mediates its action through estrogen binding receptors (ERα and Erβ) that function as transcription factors which regulates the expression of estrogen responsive genes[61, 66].

SERM's act as agonist to maintain the cholesterol levels and bone density, and has antagonistic effects in the breast tissue[67]. Tamoxifen is a widely used anticancer drug in post-menopausal women with axillary lymph node positive and in pre and post-menopausal women with lymph node negative ER+ cancers. It has also been used as a chemopreventive agent to reduce the risk of breast cancer in high risk and in pre and post-menopausal women with breast cancer[68].

2. Aromatase inhibitors

Aromatase inhibitors are another class of drugs that are of significance in adjuvant therapy for breast cancer. In post-menopausal women in which the ovaries are dysfunctional, estrogen is produced peripherally by the conversion of androgens by the enzyme aromatase[69, 70]. Aromatase belongs to the family of CYP450 enzymes and it catalyzes the final step of estrogen biosynthesis. Three of the approved AI's (Table 5) for treating breast cancers show better activity than tamoxifen, however the long-term safety of these agents is still under investigation. AI's are considered to be standard treatment for postmenopausal women. The American Society of Clinical Oncology states that the adjuvant chemotherapy

should include an aromatase inhibitor as an initial therapy or after tamoxifen therapy for 2-5 years[71].

Table 5: USFDA approved hormone therapy drugs for breast cancer

Drug	Target
Tamoxifen	SERM
Tamoxifen Citrate	SERM
Raloxifene	SERM
Toremefine	SERM
Fulvestrant	EA
Anastrozole	AI
Exemestane	AI
Letrozole	AI

AI – Aromatase inhibitor, SERM-Selective estrogen receptor modulator, EA estrogen antagonist

5. Targeted therapy

A greater understanding of the biological factors that play a role in breast cancer has identified new molecular targets. Breast cancer cells sustain and proliferate by several growth factor receptors driven signaling pathways. Of note are the epidermal growth factor receptor (EGFR) family of tyrosine kinase receptors which includes four different types: EGFR (ErbB-1), ErbB-2 (HER2), ErbB-3 and ErbB-4.[72] Each of these receptors possess a ligand binding domain in the extracellular space, a transmembrane domain and a tyrosine kinase containing domain in the cytoplasm inside the cell. Upon the binding of peptide growth factors to these receptors dimerizes, which in turn activates kinase enzyme which then phosphorylates tyrosine residues[73]. Some of the known targets for tyrosine kinase inhibitors (TKI's) include HER1, HER2, HER3, Insulin growth factor receptor (IGFR), hepatocyte growth factor receptor (C-MET), fibroblast growth factor receptor (FGF) and intracellular targets which includes Phosphoinositide 3-kinase (PI3K), protein kinase B (PKB/AKT), mammalian target of rapamycin (mTOR), extracellular signal-regulated kinase (ERK).[74]

Human epidermal receptor (HER) family of receptors is classified into HER1, HER2, HER3 and HER4. Amongst these HER2 amplification is present in 10-34% of breast cancers [39] and is linked to poor prognosis. [75] In one of the trials, trastuzumab, a monoclonal antibody directed against HER 2-receptor showed early survival benefit in patients with HER 2 positive early stage breast cancer. In this study, trastuzumab was administered concurrently with anthracyclines (AC) based chemotherapy (AC followed by paclitaxel/trastuzumab) followed by 52 weeks of trastuzumab. Lapatinib is another small

molecule tyrosine kinase inhibitor directed against epidermal growth factor and HER2. A combination of Lapatinib and capecitabine improved the survival rates in patients with metastatic breast cancer. [76] Pertuzumab is another monoclonal antibody that binds to a different domain of HER 2 protein. A combination of trastuzumab and pertuzumab showed synergistic action in preclinical studies. [77] Overexpression of insulin-like growth factor 1 receptor (IGF-IR) is associated with poor prognosis as well as resistant towards several drugs. [78] Activation of signaling pathways triggered by binding of ligands to these growth factor receptors are well characterized in breast cancer cell lines. Of significance are mitogen-activated protein kinase (MAPK) and PI3K/Akt/mTOR pathways and clinical trials are underway to test several inhibitor molecules targeting various aspects of these pathways. [78] (Table 6)

Table 6: Biological targeted therapy in development for the treatment of breast cancer[79]

Agent	**Target**	**Current Phase of Clinical Development**
Pertuzumab	HER2	III
TDM1	HER2	III
Erlotinib	EGFR	II
Afatinib	EGFR, HER2	III
Neratinib	EGFR, HER2	III
Aflibercept	VEGF	II
Sunitinib	PDGFR, VEGFR-1, VEGFR-2,c-KIT, FLT3	III
Sorafenib	PDGFR, VEGFR-2, RAF	II
Axitinib	PDGFR, all VEGFR, c-KIT	II
Vandetanib	VEGFR, EGFR	II
Pazopanib	PDGFR, all VEGFR, c-KIT	III
Temsirolimus	mTOR	II
Everolimus	mTOR	III
Ridaforolimus	mTOR	II
Cixutumumab	IGF-1R	II
AMG 479	IGF-1R	II
Dasatinib	Src	II
Bortezomib	Proteasome	II

Tanespimycin	Hsp90	II
Rataspimycin	Hsp90	II
Vorinostat	HDAC	II
Iniparib	PARP1	III
Olaparib	PARP1	II

D. LOCALIZED CHEMOTHERAPY

The chemotherapy drugs approved for breast cancer are associated with short-term and long-term side effects. With the goal to minimize these side effects, localized delivery approaches have been explored. These approaches include transdermal, transpapillary (topical application on the nipple) and intraductal drug delivery.

1. Transdermal delivery

As the largest organ in the human body, skin provides convenient site for drug administration. However, the skin has naturally evolved to protect the entry of foreign molecules and to minimize the water loss from the body. The human skin is made up of epidermis, dermis and subcutaneous tissue (Figure 6). The skin's barrier function is entirely accomplished by the outermost layer of the epidermis of the skin – *stratum corneum* (10-15 µm thick*)*. This layer is composed of compressed keratin filled corneocytes (terminally differentiated keratinocytes) embedded in a lipid rich matrix.[80-83] The lipids in SC are different from phospholipids in cell membranes in the following aspects. [83]

a) Continuous phase and diffusion path from the surface to the base of the stratum corneum
b) Unique in its composition which consists of ceramides, free fatty acids and cholesterol and absence of phospholipids
c) Exists as multilamellar sheets
d) Presence of saturated long chain hydrocarbons which facilitates highly ordered configuration

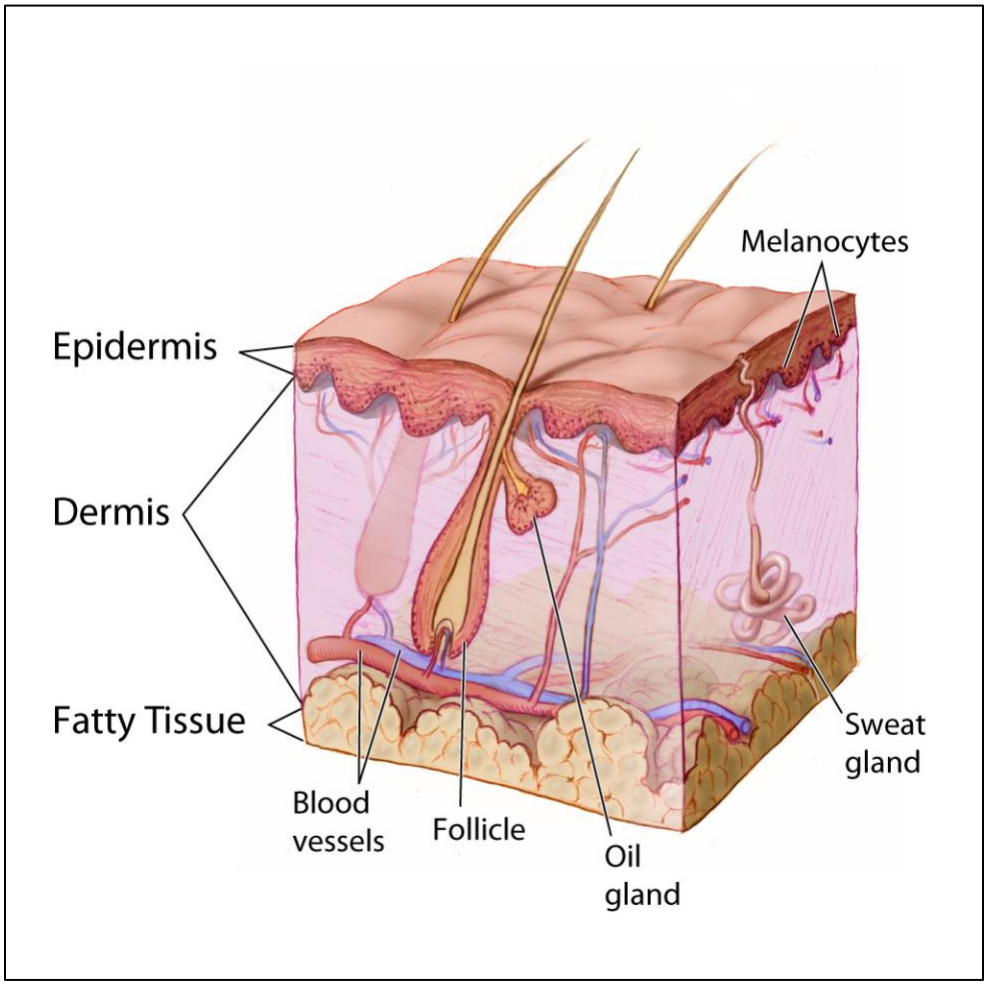

Figure 6: Skin structure.

Image reproduced from https://visualsonline.cancer.gov/details.cfm?imageid=4604

Due to the presence of this formidable barrier, an ideal molecule for transdermal delivery should possess the following properties to cross the skin. These include molecular weight < 500 Da, Log P 1-3, aqueous solubility >1 mg/ml, dose < 1 mg per day and a low melting point[81]. Candidates that are currently approved have molecular weight of only up to a few hundred Daltons, partition coefficient predominantly favors lipids and the dose requirements of 1 mg or less per day.[84] There are three major routes of drug absorption pathways after transdermal delivery.[85, 86]

i) Transcellular route: The drug traverses through alternating layers of cells and extracellular matrix. This involves a series of partitioning between alternating hydrophobic and hydrophilic domains. Lipophilic molecules tend to follow this route of drug permeations.

ii) Paracellular route: In this the drug molecules takes a tortuous path within the extracellular matrix without traversing through the cells. Hydrophilic molecules tend to favor this route of permeation.

iii) Transappendgeal route: The drug molecules permeate through the hair follicles or sweat ducts and are also known as shunt pathway or transfollicular pathway.

The simplest approach to enhance permeation involves formulation approaches ranging from modifications of partition coefficient ($K_{sc/veh}$) [83] and using different vehicles as well as using supersaturated drug solutions[87] to other formulations like microemulsion [88] and liposomal systems.[89] The most extensively researched enhancement method involves chemical enhancers that can reversibly compromise the skin barrier to allow molecules to

pass through the membrane. These includes alcohols, fatty acids, sulfoxides, esters, terpenes, surfactants and phospholipids to mention a few.[90]

Due to its unique features of skin in the breast, the human breast has been explored for transdermal delivery. [91-94] These features include embryological origin of the breast as a skin appendage, lymphatic circulation and presence of fatty envelope (subcutaneous and retromammary). [95] Topical application of 4-hydroxytamoxifen resulted in higher local drug levels and minimal systemic exposure.[91] Topical gel formulations of 4-hydroxy tamoxifen and endoxifen to the mammary glands achieved higher drug levels in the mammary glands. But, this approach resulted in systemic exposure of the drug, as the levels were similar for topical gel and systemically treated groups.[95] In a preclinical study, topical toremifene was able to achieve higher breast concentrations in baboon model with undetectable serum concentrations.[96] In another study, transdermal delivery of SERM's were investigated for its permeation across porcine skin. Results showed significant enhancement in the permeation of SERM's via breast skin.[97] However, further studies are required to validate the drug localization in the breast ducts and its retention in the ducts.

2. Transpapillary delivery

Transpapillary delivery involves drug delivery through the ductal openings at the nipple. [98, 99]

Despite being a disease of the ducts, delivery of drugs through the mammary papillae has not received considerable attention until recently. For the very first time Heard et al [98] demonstrated the transpapillary delivery of tamoxifen and two other test compounds *in vitro*. In another study[99], the effect of lipophilicity of molecules via transpapillary route

was investigated. The study found that hydrophilic molecules are better candidates for drug delivery via this route. In a follow up study[100], delivery of macromolecules ranging from 5 to 67 KDa was demonstrated *in vitro*. The study showed a decrease in the permeability of macromolecules with increasing molecular weight and higher permeation achieved through the nipple compared to breast skin. In an attempt to enhance the permeation of hydrophobic molecules through this route, influence of hydro alcoholic vehicles on the permeation of 4-hydroxtamoxifen was investigated. The study showed that an increase in the alcohol concentration resulted in increased permeation of 4-hydroxytamoxifen to the mammary papilla serving as a depot releasing the drug after treatment.[101] In a more recent study, the transport pathway through this route was characterized using model dyes. The results showed that hydrophilic molecule was mainly transported through transepidermal pathway whereas lipophilic via transductal route. In another study[102] by the same group, nanoemulsions with higher water content enhanced the penetration of hydrophobic dye into the nipple. In a follow up study[103], the same group used liposomes to skew the permeation through the ducts. This route has been explored for the therapeutic potential of a natural chemopreventive agent α-santalol. Results showed that transdermal delivery of the compound through the breast and mammary papilla enhanced local drug concentrations with undetectable levels in the plasma. Also, transdermal delivery of α-santalol reduced the tumor incidence and tumor multiplicity in rats. [104]

Despite the advantages of this route, further studies are needed to validate the amount drugs reaching the mammary ducts where 95% of breast cancers originate and also the localization of the penetrated drug molecules within the ductal network. Retention of drug

molecules in the mammary ducts is poor and despite an increased permeation through the nipple, the retention of these compounds in the mammary gland needs to be further investigated. Another limiting factor is the inability of this approach to distinguish the diseased duct vs healthy duct. Moreover, the limited surface area of the nipple restricts the delivery of only potent compounds for drug absorption via this route.

3. Intraductal Delivery

Intraductal delivery involves delivering therapeutic agents to the breast ducts by cannulating the diseased duct through the nipple. This allows for the delivery of therapeutic agents directly to the tumor forming ducts thereby enhancing drug levels at the tumor site.

This approach has precedence and the first study dates back to as early as 1842 by Ashley Cooper.[105] In this study, Cooper intraductally injected colored waxes into the breast and described the human breast as separate lobes comprising of a central duct, its peripheral branches and associated glandular tissues. Subsequently this route has been explored for therapeutic and preventive options for breast cancer (Table 7). Earlier studies have also investigated the potential for mammary tumorigenesis in rat models after intraductal delivery of activated Raf.[106] Results showed efficient expression of the protein and tumor induction in a small fraction of mammary epithelial cells *in situ*. Another study explored the delivery of adenoviral vectors carrying thymidine kinase gene[107], followed by ip administration of ganciclovir. Results showed efficient transduction and ablation of proliferating cells (>90%) but the tumor incidence in treatment group was found to be higher compared to control. The first chemopreventive study was performed by Yasuo Kamiyama[108] and colleagues using a microtubule inhibitor, paclitaxel. Paclitaxel significantly reduced tumor burden at the end of 36 weeks in N-Methyl-N-nitrosourea (MNU) induced mouse model compared to ip injection. Moreover, intraductal paclitaxel did not produce any toxic side effects such as weight loss or local duct damage. Also, the cytotoxic effects were confined only to the developed tumor.[108]

In a study by Sukumar et al[109], 4-Hydroxytamoxifen and PEGylated liposomal doxorubicin (PLD) were investigated for chemoprevention and therapy in MNU-induced murine models. Intraductal 4HT showed chemopreventive effects comparable to subcutaneously administered tamoxifen group. However, no metabolites were reported to be produced in the mammary glands. Intraductal PLD once a week for 2 weeks resulted in complete

regression of tumors and the animals remained tumor free for 3 months. Pharmacokinetic studies showed that intraductal doxorubicin rapidly diffused out of the ducts into systemic circulation and peak plasma levels in was observed at 4 hours. However, PLD delayed the T_{max} of doxorubicin to 24 hours due to delayed release of doxorubicin from liposomal formulations. In a clinical study conducted subsequently [110], the same group tested the feasibility and safety of PLD in females awaiting mastectomy. Intraductal delivery resulted in only a mild breast discomfort during drug delivery and mastectomy specimens showed a wide distribution of formulations in the duct reaching the terminal lobular units. This was one of the first clinical study which established the feasibility of intraductal delivery in human subjects. In the same study, other anticancer drugs (carboplatin, nanoparticle albumin-bound paclitaxel and methotrexate) along with 5-FU were tested for efficacy in MNU induced mammary tumors in rat. Amongst the agents tested, intraductal 5-FU showed significant protective effects against development of lesions as well as complete regression of established tumors. In this study, it is important to note that 5-FU showed efficacy in treated and untreated mammary glands bearing tumor indicating systemic exposure from the intraductally treated mammary glands.

Sinko et al tested the influence of polymer molecular weight and architecture on intraductal retention. The breast $t_{½}$ of fluorescein disodium was increased up to 21.5 ± 2.7 hrs when conjugated with 40 KDa PEG compared to free dye which exhibited a $t_{½}$ of only 14.5 ± 1.4 minutes. In a subsequent study[22] by the same group, doxorubicin conjugated to higher molecular weight PEG carriers enhanced ductal retention (10-12 hours). Nanoemulsions In a more recent study, nanoemulsions containing ceramide was retained in the mammary

glands for 6 days. [111] The improved retention of ceramide in the mammary glands was attributed to the increased lipophilicity of ceramide (Log P > 6) suggesting improved retention of hydrophobic compounds in the mammary glands. Despite advancements in the field, the major challenge of poor intraductal retention remains to be further investigated. Additional studies are required to understand the formulation factors that influence the retention of drugs in the ducts for designing optimal formulations for intraductal delivery. This includes devising a formulation strategy to minimize the frequency of intraductal injections. To this end, the major goal of this study is to develop long-acting intraductal delivery systems which will sustain drug levels in the breast and reduce the frequency of injections.

Table 7: Summary of intraductal delivery studies

Drug	Year	Preclinical/ Clinical	Findings
Paclitaxel	2005	Rats	Intraductal paclitaxel significantly reduced the tumor burden. No toxic effects on normal cells[108]
4-HT, PLD	2006	rats, mice	4-HT and PLD caused regression of established tumors and prevented tumorogenesis. No long term changes in histopathology of mammary glands[109]
5-FU, Carboplatin, paclitaxel nanoparticles, PLD, methotrexate	2011	rats, humans	5-FU showed greatest antitumor effects amongst 5 agents in rats. Carboplatin showed beneficial effects in early and established tumors in rats. PLD well tolerated in humans with only mild discomfort[110].
PLD	2012	Mice	Alteration in structure of mammary glands and tumor formation upon long term studies (80 weeks)[112]
Curcumin	2012	Rats	Able to lower the administered dose by 20 fold

			Significantly lowered mammary tumor incidence with significant reduction in nuclear factor κβ[113]
PEG	2012	Rats	Intraductal retention increased with increase in molecular weight, retention decreased with increase in branching for same molecular weight, nanocarriers delayed the t_{max}
PLD, Carboplatin	2014	Humans	PLD showed mild erythema and swelling of breast at 50mg dose, carboplatin showed mild nausea and vomiting at 300mg dose, both drugs rapidly diffused out of ducts to systemic circulation[114]
siRNA	2014	Mice	Suppressed cell proliferation and reduced mammary tumor incidence by 75%[115]
^{225}Ac-trastuzumab	2016	Mice	Therapeutic efficacy of radioimmunoconjugate reduced the dose from 120 nCi per mouse (IV) to 30-120 nCi per mouse (ID), No renal toxicity or loss of body weight upon intraductal administration[116]
Cisplatin combined with PARP1 inhibitor	2017	Mice	Ablation of mammary epithelial cells, delayed tumor onset from 153 to 239 days, long term toxicity studies demonstrated tumor formation by 6.3% due to systemic exposure to cisplatin[117]

Ceramide nanoemulsions	2018	Rats	Prolonged drug localization by more than 120 hours, no histological changes in the mammary glands[111]
PEG-Doxorubicin	2018	Rats	Intraductal retention is influenced by architecture of nanocarriers[22]
Piplartine nanoemulsions	2019	Rats	Charge of bio adhesive polymer does not have an impact on intraductal retention, mammary retention upto 120 days with no tissue damage[118]
Fulvestrant	2019	Rats	Intraductal fulvestrant showed comparable or better therapeutic efficacy in two preclinical animal models through degradation of ERα, inhibition of angiogenesis, ↓c-Myc and Cyclin D1, ↑ERβ [119]

4-HT- 4-hydroxytamoxifen, PLD – Pegylated liposomal doxorubicin, 5-FU – 5- Fluorouracil, PEG – Polyethylene glycol, Ac – Actinium, PARP - Poly ADP ribose polymerase, ER is estrogen receptor

E. SCOPE AND GOAL OF THIS STUDY

About 1 in 8 U.S. women will develop invasive breast cancer over the course of her lifetime. Ductal carcinoma in situ (DCIS) is pre-invasive breast cancer and accounts for 20% cases of all diagnosed case of breast cancer. [120] DCIS is characterized by the proliferation of epithelial cells of milk ducts and terminal lobular units that have not breached the basement membrane and become invasive. [120] Although the precise pathways of tumor incidence and progression are poorly understood, majority of invasive carcinomas arise from DCIS. The standard treatment for DCIS is normally a combination of breast conservation surgery followed by radiotherapy with adjuvant chemotherapy depending on the stage of cancer. [31]

Systemic chemotherapy results in significant short-term and long-term side effects. [55, 121, 122] Therefore, there is a need to develop localized delivery systems that can enhance drug concentration in the breast and minimize adverse effects. DCIS being confined to the breast, intraductal delivery enhanced drug concentration in the breast and minimized systemic exposure. [110, 123] Moreover, this approach showed improved efficacy in pre-clinical and clinical studies. [114] [108, 110, 119] However, the major drawback of this approach is the rapid diffusion of drugs into systemic circulation, warranting repeated intraductal injections to sustain drug levels in the ducts. [22, 124] To this end, the main goal of the present study is to develop long acting intraductal delivery systems to minimize the frequency of injections and to sustain drug levels in the breast.

Recent studies [22, 111] have used polymer drug conjugates and emulsions to sustain drug retention in the ducts. However, the critical determinants of developing long- acting delivery systems including the formulation matrix and particle size and its influence on intraductal retention is yet to be studied. Poly (lactic-co-glycolic acid) [PLGA] is a widely used polymer for developing sustained release formulations. [125-129] Several PLGA long-acting formulations including microspheres and *in situ* gel systems are used for wide ranging applications. [125, 130, 131] However, these are yet to be explored for drug delivery via this route. In order to develop effective intraductal drug delivery systems, several critical parameters like particle size and formulation matrix needs to be investigated. To this end, the major goal of this dissertation is to study the major formulation factors influencing drug retention vis-a-vis use the findings to develop optimal long-acting intraductal delivery system for breast cancer.

The specific aims of the dissertation are:

1) To investigate the effect of particle size and formulation on intraductal and lymph node retention

2) To develop and optimize poly (lactic-co-glycolic acid) formulations of tamoxifen and determine its pharmacokinetics in rats.

3) To develop and test the pharmacokinetics of long-acting PLGA formulations of 4-hydroxytamoxifen

CHAPTER I

INFLUENCE OF PARTICLE SIZE AND FORMULATION ON BREAST AND LYMPH NODE RETENTION

1.1. BACKGROUND

Localized delivery to the breast through intraductal injections enhanced drug levels in the breast and reduced systemic exposure. Intraductal delivery (ID) has been effective in preclinical and clinical studies. [109, 110, 119, 123] Several anticancer drugs (carboplatin, methotrexate, 5FU, 4-hydroxytamoxifen, paclitaxel) delivered by this route have been shown to be effective in chemoprevention as well as chemotherapy in both chemical carcinogenesis as well as transgenic tumor models of breast cancer. [108-110] However, the major challenge of this approach is the rapid diffusion of drugs out of the ducts into systemic circulation. In a preclinical study, intraductal doxorubicin exhibited retention half-life of only 2 hours.[22] In another study[110], intraductal 5-FU showed superior efficacy in treated and untreated mammary gland which was attributed to the diffusion of 5-FU into systemic circulation. In a clinical study [132], carboplatin rapidly distributed into the systemic circulation after intraductal injection, with a T_{max} of ~30 minutes. The systemic and ID levels were similar in comparison, suggesting that small molecules diffuse rapidly out of the ducts. In another study, ID administration of PEGylated doxorubicin (liposome) showed superior efficacy than IV administration.[110] The blood level of doxorubicin was fivefold lower than IV, with no systemic toxicity. However, doxorubicin released from these liposomes caused local toxicity and edema.

Taken together, there is a need to develop formulations that can prolong and sustain drug levels in the breast, minimizing systemic side-effects. There have been some recent attempts to develop approaches to prolong drug retention in the breast. Singh et al investigated the influence of molecular weight and polymer architecture (Linear 12, 20, 30,

40 KDa and Two-arm 60 KDa, Four-arm 20, 40 KDa and Eight-arm 20 KDa) to prolong drug retention in the ducts. [124] The results showed that fluorescent labelled PEG showed ductal half-life in the range of 7-22 hours, while the half-life of free fluorescein was only 15 minutes. The duct retention half-life increased with an increase in molecular weight (12 – 60 KDa) and the particle sizes of the investigated polymers were in the range of 5-10 nm. Pharmacokinetic analysis showed a delayed the t_{max} to 32 ± 13.8 hours with two-arm 60KDa carriers compared to free fluorescein which showed t_{max} of 0.5 hours. In a subsequent study[22], doxorubicin labelled PEG nanocarriers of higher molecular weight and branching (40KDa, 4 arm) delayed the $t_{1/2}$ to 13.1± 3.4 hours compared to free doxorubicin which exhibited $t_{1/2}$ of 2.0± 0.4 hours. Histopathological studies showed that PEG conjugated doxorubicin induced only transient inflammation compared to free intraductal doxorubicin. Intraductal administration of nanoemulsions[111] (<100 nm) were retained in the rat breast ducts for 120 hours. These nanoemulsions encapsulated a highly hydrophobic compound ceramide. In vivo whole-body images showed retention of formulations for 120 hours. The improved retention of ceramide in the mammary glands was attributed to the increased lipophilicity of ceramide (Log P > 6) suggesting improved retention of hydrophobic compounds in the mammary glands. However, additional studies are required to investigate the retention of particles of larger size for designing formulations that can prolong and sustain drug levels in the breast.

The main goal of this study is to investigate the influence of polymeric particles ≥ 100nm and formulation on intraductal and lymph node retention using fluorescent probes. Fluorescent labeled polystyrene particles (100-1000nm) were used to study the influence

of particle size on breast duct retention. To translate the findings to clinical application, poly lactic-co-glycolic acid (PLGA), a US-FDA approved polymer was used for preparing nanoparticles (NP), microspheres (MS) and in-situ gel (ISG) formulations. PLGA has been extensively studied as a drug delivery system due to its biodegradability, tunable physicochemical properties and the ability to form different delivery systems.[15] Furthermore, there are several PLGA based long-acting parenteral formulations in clinical use.[16] The breast retention and lymph node distribution after ID delivery of different formulations were studied using in-vitro and in-vivo imaging techniques in rats and pig.

The specific aims of this study are:

1. To investigate the influence of particle size on ductal retention and biodistribution using polystyrene carriers of different particle size

2. To investigate the influence of PLGA formulations (microparticles, nanoparticles and in-situ gel) on ductal retention and biodistribution.

1.2. MATERIALS AND METHODS

Poly (lactic-co-glycolic acid) (LA:GA = 75:25, 65-75 KDa and 25 KDa, LA:GA = 50:50, 5-10 KDa) was purchased from Akina, Inc. (West Lafayette, IN). Cyanine 5.5 carboxylic acid (Cy 5.5) was procured from Lumiprobe (Hallandale Beach, FL, USA). The isoflurane was obtained from VetOne, Boise, ID and Veet hair removing cream was obtained from Reckitt Benckiser North America (Parsippany, NJ). Polystyrene particles (NIRexTM) labeled with Near IR dye was obtained from Phosphorex (St. Hopkinton, MA). All other reagents were purchased from Sigma-Aldrich (St. Louis, MO).

1.2.1. Animals

Female Sprague Dawley Rats (3-4 weeks old) were obtained from USD animal facility and housed in South Dakota State Animal Resource Wing. The animals were maintained on a 12-hour light/dark cycle in a temperature-controlled environment with food and water were given ad libitum. The animals were acclimatized for 1 week before starting the study.

For the pig study, 5-6-month-old gilt was procured from South Dakota State University Swine Education and Research Facility. The animal was maintained on a 12-hour light/dark cycle in a temperature-controlled environment and fed a standard finisher diet and was acclimatized for 1 week prior to initiating the study. All animal experiments were performed with approval from the Institutional Animal Care and Use Committee (IACUC) at South Dakota State University.

1.2.2. METHODS

1.2.2.1 Preparation of PLGA microparticles

Microparticles were prepared by oil-in-water (O/W) emulsion method reported in the literature. [133] Briefly, PLGA polymer (500mg) and Cy5.5 (1mg) were dissolved in 5 ml methylene chloride (DCM). The organic phase was added dropwise into an aqueous phase containing 1% PVA. The mixture was then emulsified by homogenized at 10,000 rpm for 1 minute to form o/w emulsion. The resulting emulsion was then stirred at 300-400 rpm for 3 hours to allow the solvent to evaporate. The microparticles were then separated by centrifugation at 4000 rpm for 20 minutes. The pellet was washed with distilled water, a total of three times and freeze-dried. The formulation was stored at 4°C for further studies.

1.2.2.2. Preparation of PLGA nanoparticles

PLGA nanoparticles were prepared by reported emulsion solvent evaporation method.[134] Briefly, 100 mg of PLGA was dissolved in 4ml methylene chloride containing Cy5.5 (1mg). The organic phase was added dropwise into an aqueous phase containing 1% PVA. This was then sonicated using a probe sonicator set at 50W of energy output for 1 minute to form oil-in-water (o/w) emulsion. The resulting emulsion was then stirred at 300-400 rpm for 2-3 hours to remove the organic solvent. The nanoparticles were separated by ultracentrifugation (20,000 rpm) for 20 minutes, washed with distilled water three times. The pellet was lyophilized and was stored at 4°C for further use.

1.2.2.3. Preparation of PLGA in-situ gel

PLGA in situ gel was formed by phase inversion process, where the polymer in organic solvent undergoes sol to gel transition on contact with an aqueous medium.[135] In situ gel was prepared by mixing PLGA of different copolymer ratios and molecular weights in N-methyl-2-pyrrolidone (NMP) using a previously reported method with slight modification.

[136, 137] PLGA with different copolymer ratios of LA: GA and molecular weights (50:50 and 75:25 of molecular weights 5-10 KDa and 10-15 KDa respectively) were used to prepare 15 wt% in-situ gel to achieve the desired syringeability and sustained release characteristics for intraductal injection. For forming 15 wt% gel, 75 mg of PLGA 75:25 (10-15 KDa) and 75 mg PLGA 50:50 (5-10 KDa) was weighed into glass vials and dissolved in 1 ml of NMP by placing on a continuous shaker and kept overnight to completely dissolve the polymer. Cy5.5 was dissolved in NMP and added into polymer solution and used for in vitro release studies. For intraductal injection, the polymer was dissolved in NMP overnight and Cy5.5 was dissolved in the polymer solution 30-60 minutes prior to the injection.

1.2.2.4. Characterization of PLGA formulations

The particle size and zeta potential of nanoparticles were measured by DLS on a Malvern Zetasizer Nano ZS (Malvern Instruments Inc., Southborough, MA). The morphology of PLGA formulations was characterized using Scanning Electron Microscopy (SEM). The particle size of microparticles was measured using SEM by measuring the size of 50 particles with Smart Tiff V3 (Carl Zeiss, MA). The ex vivo fluorescence intensity of formulations was measured using spectrofluorimetry (SpectromaxM2, Molecular Devices, Sunnyvale, CA) using 690 and 750 nm as the excitation and emission wavelengths. Encapsulation and loading efficiency of microparticles and nanoparticles were calculated using the following equation:

$$\text{Encapsulation Efficiency (\%)} = \frac{\text{Weight of Cy 5.5 in the formulation}}{\text{Weight of Cy 5.5 initially added}} \times 100$$

$$\text{Loading Percent (\%)} = \frac{\text{Weight of Cy 5.5 in the formulation}}{\text{Total Weight of the formulation}} \times 100$$

1.2.2.5. In vitro release study

In vitro release of Cy 5.5. from the formulations were studied using a reported method with slight modifications.[138-140] Briefly, 5-10 mg of microparticles and nanoparticles were dispersed in 1 ml of release medium (PBS, pH 7.4 containing 1% w/v Tween 80) in an Eppendorf tube and was placed in an orbital shaker water bath (shaken at 120 per minute) at 370C. At each time point, the tubes were centrifuged at 10,621 x g for 10 minutes and 1 ml of the supernatant was removed for analysis. The pellet was redispersed in 1 ml of fresh release medium to maintain the sink conditions. The supernatant was analyzed using fluorescence spectroscopy to determine the dye concentration in the release medium. For in-situ gel, 10µg equivalent of the gel was injected into 1 ml release medium using 27 G needle to form the gel and the release study was carried out as described above.

1.2.2.6. In vivo studies

Intraductal injections were performed using a previously established method. [109] One day prior to starting the study, rats were anesthetized and hair around the nipple region was removed using a depilatory cream. Female SD rat was anesthetized using isoflurane and placed under a surgical microscope. Keratin plug from the mammary gland was removed by gently holding the nipple using a tweezer and wiping with 70% alcohol. The formulations were injected using 27-31 G needle into one pair of the inguinal mammary glands. For lymph node retention studies, thoracic mammary glands were used for introduction injection, since it drains into the axillary lymph node. This is consistent with the breast to axillary lymph node drainage in humans. The amount of Cy5.5 (1.5 mcg) injected was kept constant for all the formulations. For microparticles and nanoparticles,

0.5 to1.5 mg particles were dispersed in 150 µl of PBS containing 0.05% w/v Tween 80 and vortexed for 30-60 seconds before injection. For in-situ gel, 100 µl of the formulation was used for intraductal injection. Free Cy5.5 was dissolved in a minimal amount of NMP followed by dilution with PBS containing 0.05% w/v Tween 80. Similarly, fluorescent labeled polystyrene particles (1% w/v) were injected into the inguinal mammary gland and an equivalent amount of the free dye was used for comparison. The animals were anesthetized and imaged at different time points after injecting the particles using Bruker In Vivo Extreme II optical system. The animals were then allowed to recover back in their cages.

For the pig study, the animal was anesthetized by intramuscular injection of TKX (Telazol and Xylazine at 50mg/ml each and ketamine at 100mg/ml; 2.5m/50kg body weight). The hair around the nipple region was removed using hair removing cream one day before starting the study. Before starting the study, alcohol swab (70% ethanol) was used to remove the keratin plug. The PLGA formulations were dispersed in 500-1000µl of PBS containing 0.05% w/v Tween 80 and injected into the mammary glands using 27G blunt needle. Consistent with the 3R (replacement, reduction, and refinement) principles related to animal use in research, we used one pig to test all the formulations. All seven pairs of the mammary gland were utilized for the study (Figure S1). Since the mammary glands are not connected, the chance of spill-over from one mammary gland to another is very limited. We used 2-3 teats for each formulation and the breast distribution was studied at different time points (2 hrs and 4 days). At the end of the treatment, the animal was euthanized using an IV injection of pentobarbital (1ml/10 lb). The mammary glands were excised and imaged using in vivo imager.

1.2.2.7. Ex-vivo and In-vivo imaging

The distribution of fluorescently labeled polystyrene particles (0 - 3 days), PLGA formulations (0 - 4 days) and the free dyes was measured by whole-body imaging using Bruker In Vivo Xtreme II optical imaging system. In a separate set of experiments, to study the lymph node retention, the rat was euthanized by CO_2 asphyxiation at 2, 24 and 48 hours to excise the breast and axillary lymph nodes and imaged using in-vivo imager. For polystyrene particles, the ex vivo and in vivo fluorescence intensity was measured using the following instrument settings: Excitation/Emission 730/790nm, Bin 1x1 and f stop 1.1. For in vivo and ex vivo imaging studies of PLGA formulations, the fluorescence intensity was measured using the following instrument settings: excitation/emission: 690/750nm; Bin: 1x1 pixels; Exposure time: 20 seconds, f-stop of 1.2, FOV: 19. To compare the different treatment groups, the data was plotted as percentage of the initial fluorescence signal against time and the pharmacokinetic parameters (elimination rate constant and retention half-life) were determined by non-compartmental analysis using PK solutions software.[124] The elimination rate constant (k) was determined from the regression analysis of semi-logarithmic plot of fluorescence intensity vs time. Retention half-life ($t_{1/2}$) is defined as the time at which the fluorescence intensity becomes 50% of the initial value.

1.2.2.8. Mammary whole mount

At the end of the treatment, the rat was euthanized and mammary whole mounts were prepared using a literature reported method with slight modifications.[124] Briefly, mammary glands were dissected and mounted onto a glass slide and fixed in chloroform/isopropanol/acetic acid (6:3:1) for 6 hours. The glands were then defatted using

acetone for 2-3 hours. The slides were then stored in methyl salicylate and the images were captured using a confocal microscope with 10X objective.

1.2.2.9. Fluorescence microscopy

To visualize the distribution of PLGA formulations in the breast, the rat was euthanized, and the mammary gland was excised. The tissue was snap-frozen in optimum cutting temperature (OCT, Tissue Tek, Torrance, CA) medium placed in hexane under liquid nitrogen. The OCT block was sliced to 8-10 µm thick sections in a cryostat (UV800, Leica Microsystems, Bannockburn, IL) at -25ºC. The section was dried for 6 hours at 37 ºC and the coverslip was sealed using CytoSeal (Vector laboratories, Burlingame, CA). The tissue sections were then observed under an Olympus FluoView 1200 (Center Valley, PA) confocal laser scanning microscope (excitation/emission wavelength: 682/703 nm) at 20X magnification.

1.2.2.10. Histology

To test the local tissue toxicity of the formulations, in a separate set of experiments, the rats were euthanized seven days after intraductal administration of PLGA formulations. The mammary glands were excised, and the tissue was fixed in 10% buffered neutral formalin for 24 hours at room temperature. The tissue was embedded in paraffin and 6 µm sections were prepared using a microtome (Olympus CUT 4060E, Center Valley, PA). The sections were stained with hematoxylin-eosin and examined under a light microscope (Olympus AX70, Center Valley, PA) for histological changes at 40X magnification.

1.2.2.11. Statistical analysis

All the experiments were conducted in triplicates. The data is represented as a mean ± standard deviation. The groups were compared by Students t-test and One-way analysis of variance (ANOVA) using Minitab® statistical software (Minitab Inc., State College, PA) at a significance level of $p<0.05$.

1.3. RESULTS AND DISCUSSION

DCIS is confined to the breast and current systemic therapies are associated with significant physical and emotional distress, impacting the quality of life in women with preneoplasia, who are otherwise healthy.[120, 141, 142] Alternatively, intraductal delivery of anti-cancer agents through cannulation of the diseased ducts is an effective and safe 'chemical mastectomy' approach for eradicating premalignant lesions with reduced systemic toxicity.[108-110, 113, 123] Poor retention of drugs is a major challenge and it is important to understand the factors that influence drug retention in the breast to develop effective formulation strategies for intraductal drug delivery. The main objective of this preliminary study is to understand the influence of particle size and formulation on retention and distribution in the breast and regional lymph nodes.

1.3.1. Effect of particle size on breast retention and distribution

To understand the influence of particle size, fluorescent-labeled polystyrene particles in three size ranges (100, 500 and 1000 nm) were tested. The commercially available polystyrene particles were used due to their uniform size (Table 8) and its reported use for in-vitro and in-vivo imaging studies.[143] As shown in Figure 7, after intraductal injection in rats, the nanoparticles and microparticles showed higher retention compared to the free dye. The fluorescence from the nanoparticles (100 and 500 nm) and microparticles was observed till 2 and 3 days respectively. On the other hand, there was hardly any fluorescence observed for the free dye after 6 hours (Figure 7). The results were also supported by whole-mount imaging studies. The whole-mount images of the

breast showed intense fluorescence for the microspheres and there was hardly any fluorescence seen for the free dye (Figure 8

Table 8: Characteristics of Polystyrene particles

Particles	Particle Size (nm)	PDI	Zeta Potential (mV)
PS 100 nm	99.21 ± 2.37	0.10 ± 0.03	-53 .3 ± 0.90
PS 500 nm	502.5 ± 4.85	0.18 ± 0.04	-51.26 ± 0.56
PS 1000 nm	1006 ± 3.05	0.32± 0.13	-48.3 ± 0.50

Data is Mean ± S.D (n=3); PS is polystyrene; PDI is polydispersity index

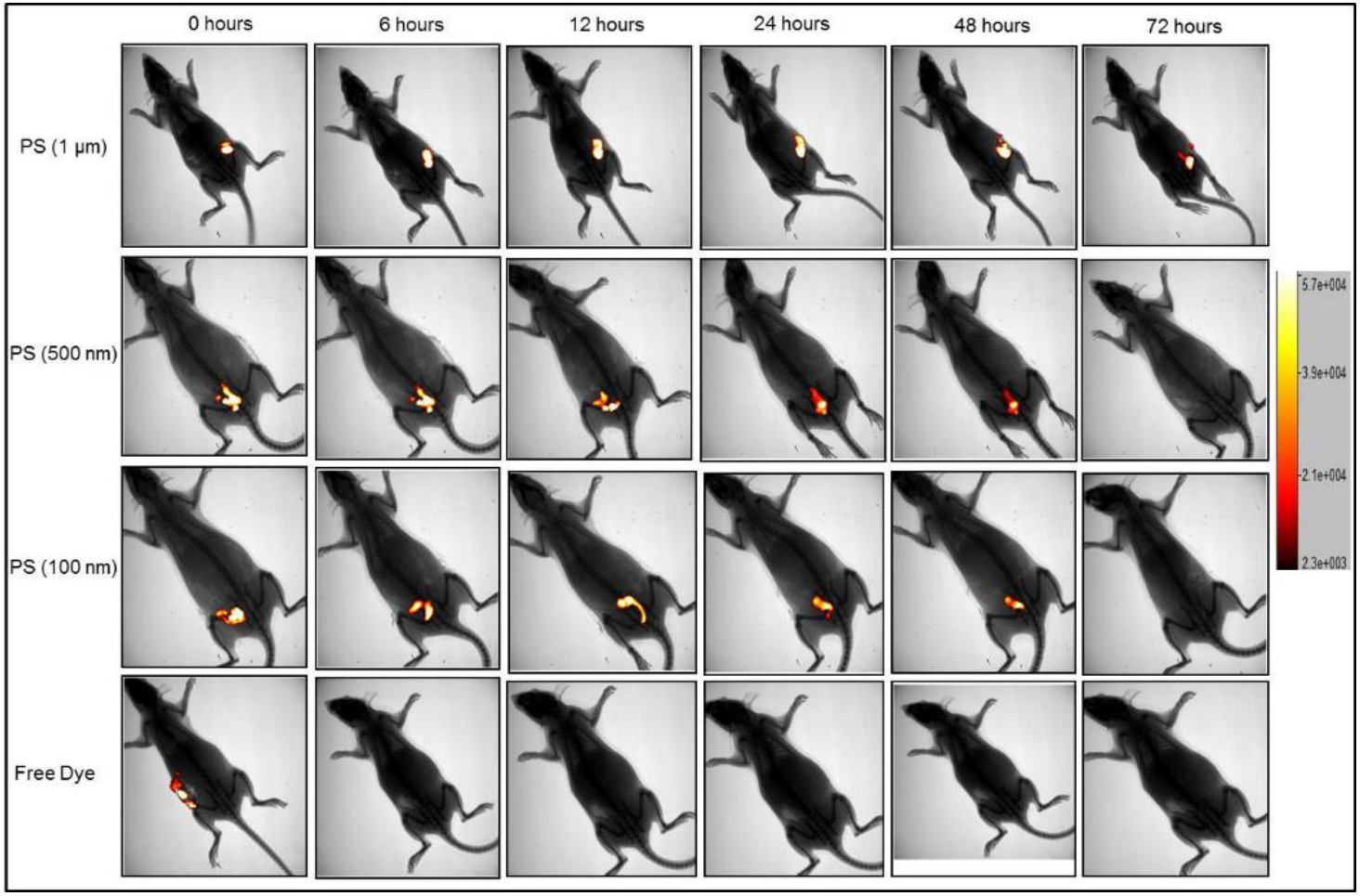

Figure 7: Representative images (n=3) showing distribution of polystyrene (PS) particles of different particle sizes (100nm, 500nm and 1 µm) in the breast. Free Dye was used as a control. The images were captured using in-vivo imager from 0-72 hours.

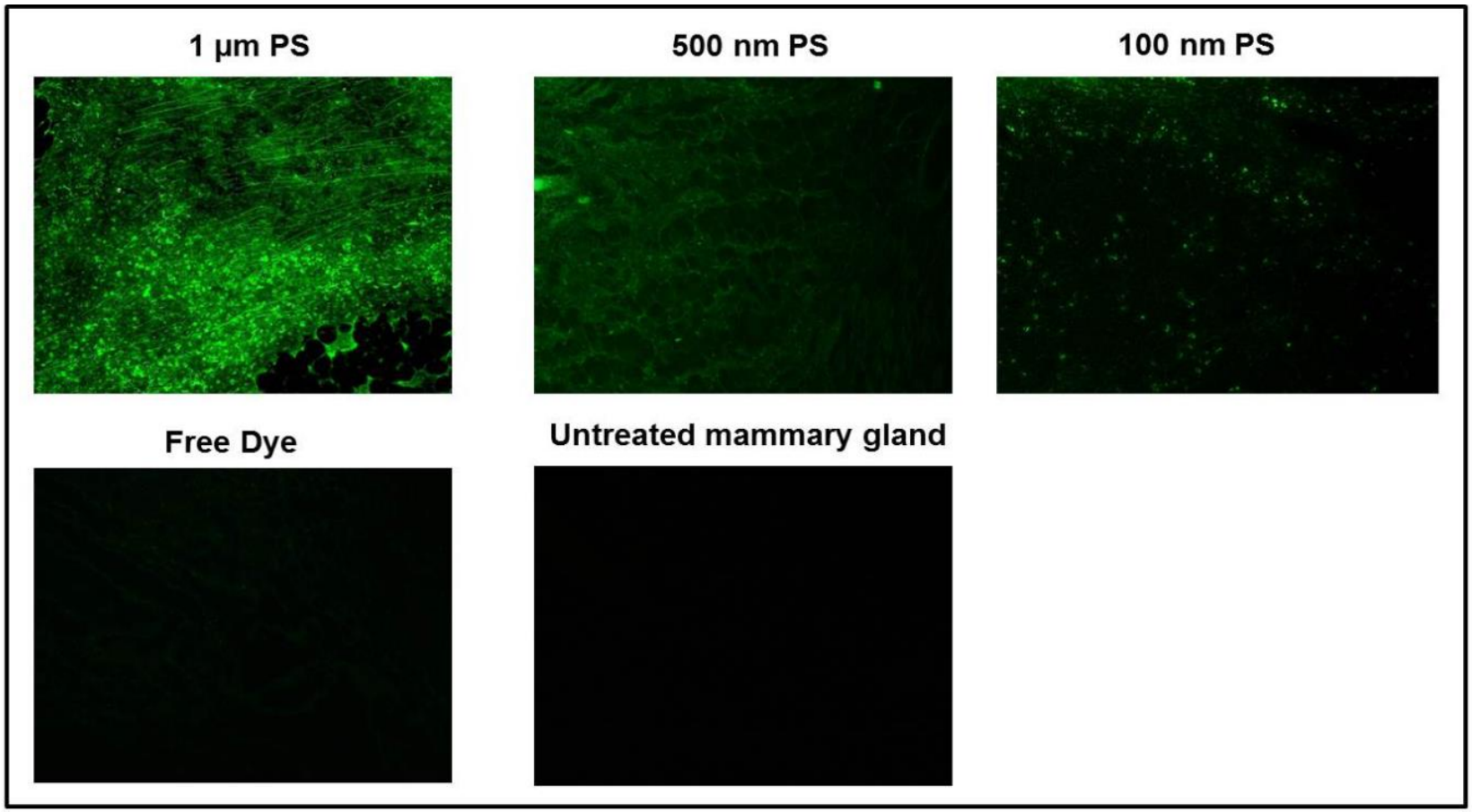

Figure 8: Representative mammary gland whole mount images of rat after treatment with polystyrene (PS) particles and free dye after 72 hours. The whole mount was imaged under 10X using a confocal microscope.

The elimination of the particles from the breast decreased with time (Figure 9). The 100 to 500 nm PS particles showed similar retention half-life, but an increase in the particle size from 500 nm to 1000 nm increased the half-life by five-fold (Table 9). The fluorescence from the free dye declined rapidly. Based on qualitative analysis, the fluorescence in the various organs was high with the free dye followed by the 100 nm and 500nm. On the other hand, relatively lesser fluorescence was observed in the organs for 1000 nm particles (Figure 10).

Table 9: Kinetic parameters of Polystyrene particles

Formulation	k (h^{-1})	$t_{½}$ (hrs)
Polystyrene 1µm	0.007 ± 0.0005 ^{ab}	94.87 ± 4.12 ^{abc}
Polystyrene 500nm	0.029 ± 0.002 ^{a}	24.15 ± 3.16 ^{a}
Polystyrene 100nm	0.033 ± 0.11 ^{a}	22.35 ± 4.72 ^{a}
Free Dye	0.662 ± 0.06	1.06 ± 0.16

The data represents mean ± S.D (n = 3). 'k' is the elimination rate constant; $t_{1/2}$ is the retention half-life, i.e. time at which the fluorescence intensity is 50% of the initial value. 'a' is significant in comparison to Free Dye; 'b' is significant to Polystyrene 100 nm; 'c' is significant to Polystyrene 500nm. The values are significant at $p < 0.05$.

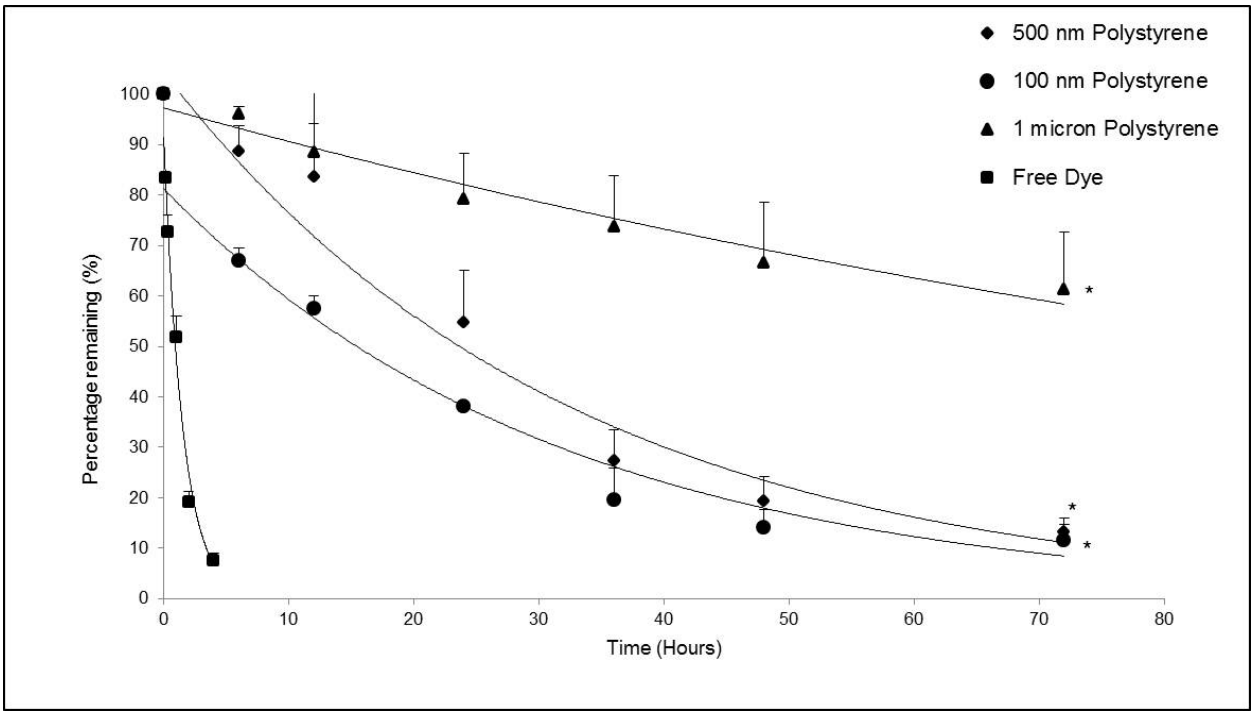

Figure 9: Fluorescence intensity profiles of polystyrene particles (100nm, 500nm and 1µm) expressed as percentage of initial fluorescence. Free dye was used as control. Each value represents mean ± S.D (n = 3). * is significant compared to free dye ($p < 0.05$).

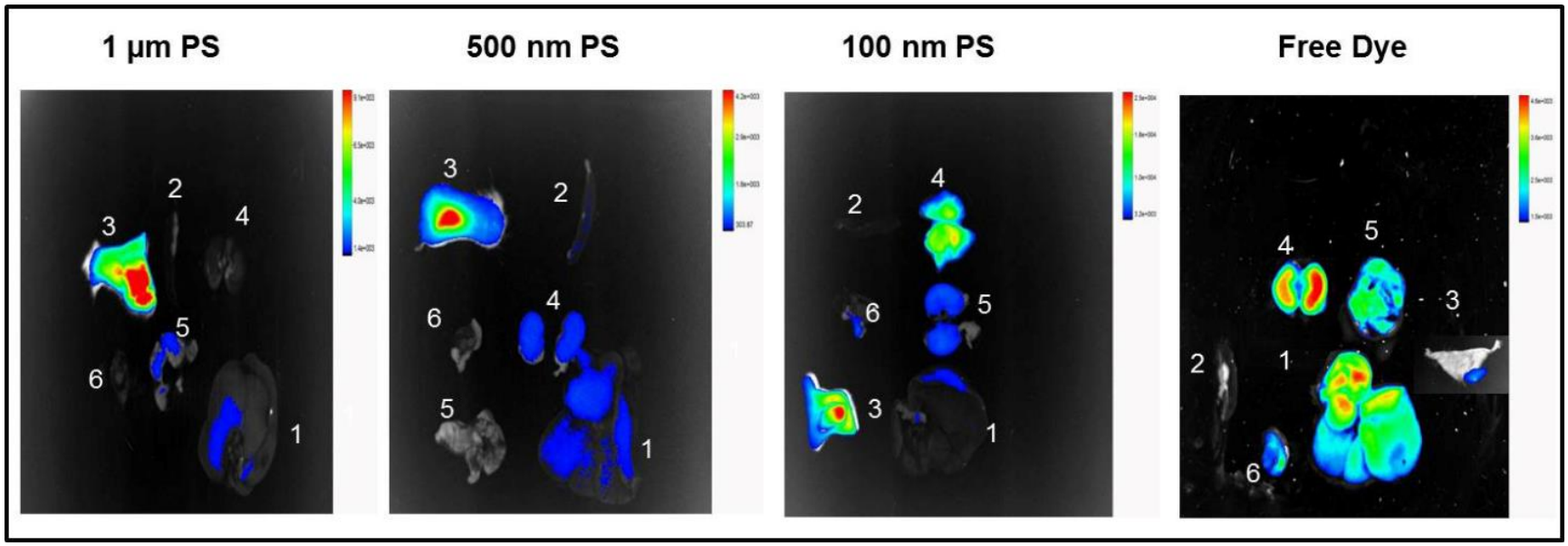

Figure 10: Representative ex-vivo fluorescence images of different organs after intraductal injection of polystyrene (PS) particles (1µm, 500nm and 100nm). The organs and mammary glands were excised and imaged at 72 hours. 1 – liver, 2- spleen, 3- mammary gland, 4- kidneys, 5- lungs, 6- heart)

Earlier studies have shown that size and polymer architecture influence the formulation retention in the breast.[22, 124] Gu et al showed that the retention half-life of doxorubicin increased linearly with increase in molecular weight of PEG from 5-40 kDa (hydrodynamic radius of 3-7 nm).[22] The retention half-life ranged from 2 to 13 hours. Similarly, the retention half-life of fluorescein-conjugated PEG (12-40 KDa; 5-10nm) showed a retention half-life of 7-22 hours.[124] On the other hand, the retention half-life of free dye and doxorubicin was 15 minutes and 2 hours respectively. [22, 124] Multi-arm (two, four and eight-arm) PEG polymers showed similar or lower retention half-life than the linear PEG. [22, 124] Carvalho et al studied the breast retention nanoemulsions (<100nm) in rats.[111, 118] The nanoemulsions were retained in the breast for up to 5 days with an elimination half-life of 20-30 hours, which is consistent with the half-life observed for 100 and 500 nm particles in our study. The half-life for the free dye (Alex Fluor) was around 2-3 hours. [118] On the other hand, the free ceramide was found to be retained in the breast for 48 hours.[111] The authors did not find any significant difference in the retention between negative and positively charged nanoemulsions. However, as is evident from these studies, the physicochemical properties of the molecule including Log P and molecular weight influence ductal retention in the breast.

Results from our study and the earlier studies suggest that an increase in molecular weight and particle size limits diffusion through the ducts. Furthermore, hydrophilic molecules are cleared rapidly from the breast compared to hydrophobic molecules.[22, 111, 118, 124] The slower clearance of hydrophobic molecules can be attributed to the binding to the breast tissue.[111] On the other hand, an increase in molecular weight and particle size can limit the diffusion

through the ducts. Taken together, the results from this study for the first time demonstrate the retention of particles ≥ 100 nm in the breast.

1.3.2. Preparation and characterization of PLGA formulations.

To develop clinically relevant formulations, we used PLGA, a US-FDA approved polymer. PLGA is biodegradable which under physiological conditions undergoes hydrolysis through the labile ester groups. The degradation time can be customized from weeks to years based on the route and delivery application by adjusting the lactic acid/glycolic acid ratio and molecular weight.[144] Given the versatility of PLGA, it is widely used for sustained release applications by various routes of administration. [144] In this study, we used Cy 5.5 loaded PLGA microspheres, nanoparticles and in-situ gel for studying the influence of formulation on breast duct retention.

PLGA microspheres and nanoparticles showed a spherical morphology (Figure 11). PLGA microspheres and nanoparticles had an average particle size of 8.66 ± 3.25µm and 200 ± 17.08 nm with a low PDI value. (Table 10)

Table 10: Properties of Cy 5.5 loaded PLGA formulations.

Formulation	Particle size	Zeta potential (mV)	PDI	Encapsulation Efficiency (%)	Loading Percent (%)
PLGA Microparticles	8.66 ± 3.25µm*	-31.75 ± 1.12*	0.121 ± 0.045*	63.47 ± 2.92*	0.15 ± 0.04*
PLGA Nanoparticles	200 ± 17.08 nm	-21.12 ± 2.73	0.229 ± 0.089	36.02 ± 3.07	0.11 ± 0.08

(PDI) polydispersity index; Each value represents mean ± S.D (n = 3); (PDI)

polydispersity index; * is significant compared to PLGA Nanoparticles

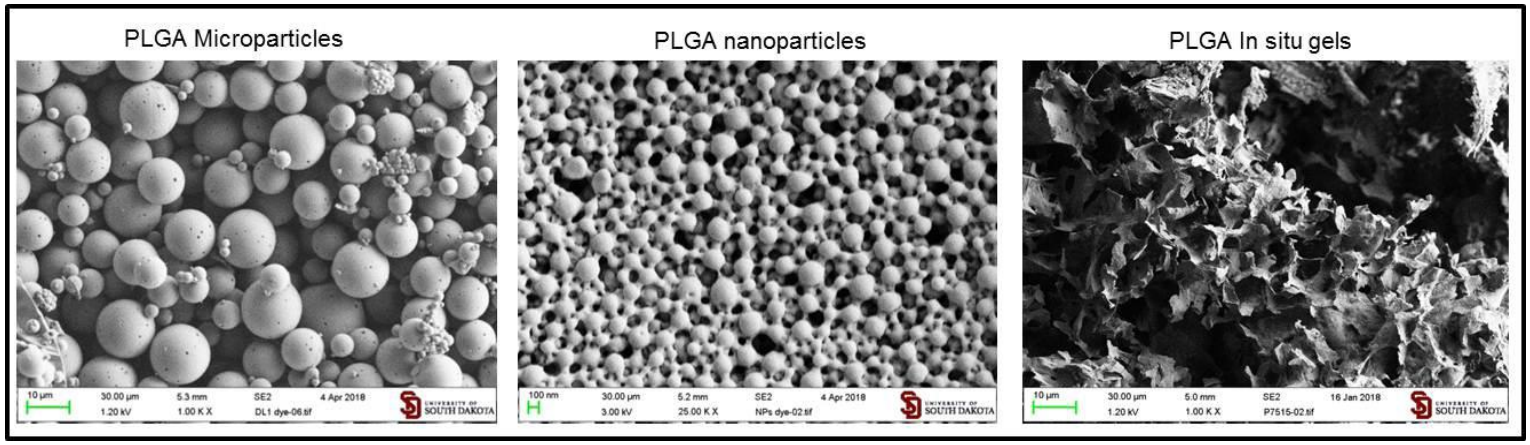

Figure 11: Scanning electron microscopy (SEM) images of PLGA formulations

In-situ PLGA gel was prepared by the phase inversion method using NMP as the organic solvent. When the PLGA suspension in NMP comes in contact with the aqueous fluid in the injection site precipitates to form a gel.[135] NMP is the most commonly used solvent for in-situ PLGA gels, because of its solvating ability and its safety profile.[136] The SEM image shows the porous structure of the PLGA gel (Figure 11), which is consistent with the literature.[145]

One of the goals for developing intraductal formulations is to minimize the frequency of injections is by sustaining drug release for prolonged periods in the breast. As can be seen from the *in vitro* release studies (Figure 12), all the three formulations sustained the release of Cy 5.5. A biphasic release profile was observed for all the three formulations and the release profile is consistent with sustained release characteristics of PLGA formulations.[146, 147] A higher burst release was seen with the nanoparticles compared to the other two formulations. The higher release can be attributed to the larger surface area of the nanoparticles compared to microparticles.[148] On the other hand, there was no significant difference in the release profile between the microparticles and in-situ gel. Around 40% of the dye was released in 96 hours from the nanoparticles, while only 8% and 11% of the dye was released from in-situ gel and microparticles respectively (Figure 12). The slower release in addition to maintaining the drug levels in the breast can also reduce the local tissue toxicity of chemotherapeutic agents such as doxorubicin.[12]

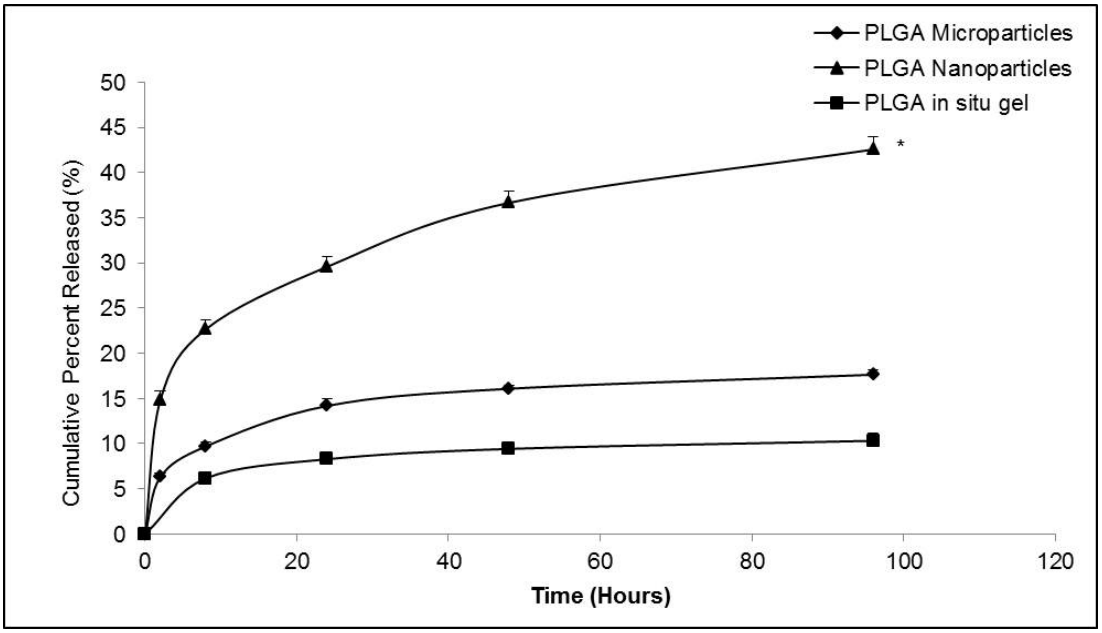

Figure 12: In vitro release profile of Cy5.5 from PLGA microspheres, nanoparticles and in-situ gel. The data represents mean ± S.D (n = 3). * is significant in comparison to ISG ($p < 0.05$)

1.3.3. Effect of PLGA formulations on retention and distribution in the breast

The next goal was to test the retention and distribution of the PLGA formulations in rat breast after intraductal injection. Similar to the results from polystyrene particles, the free dye was cleared rapidly from the breast, while the PLGA nanoparticles were found to be retained in the breast up to 48 hours (Figure 13). On the other hand, PLGA microparticles and in-situ gel were retained in the breast for up to 4 days. This was also confirmed from ex-vivo imaging study of the mammary gland fluorescence from the tissue sections of excised breast tissue (Figure 14). Unlike the results from the polystyrene study, there was no detectable fluorescence in the organs for any of the treatment groups at the end of 96 hours (Figure 15). This is not surprising considering the half-life of plasma half-life of Cy 5.5 (2.2 hours).[149]

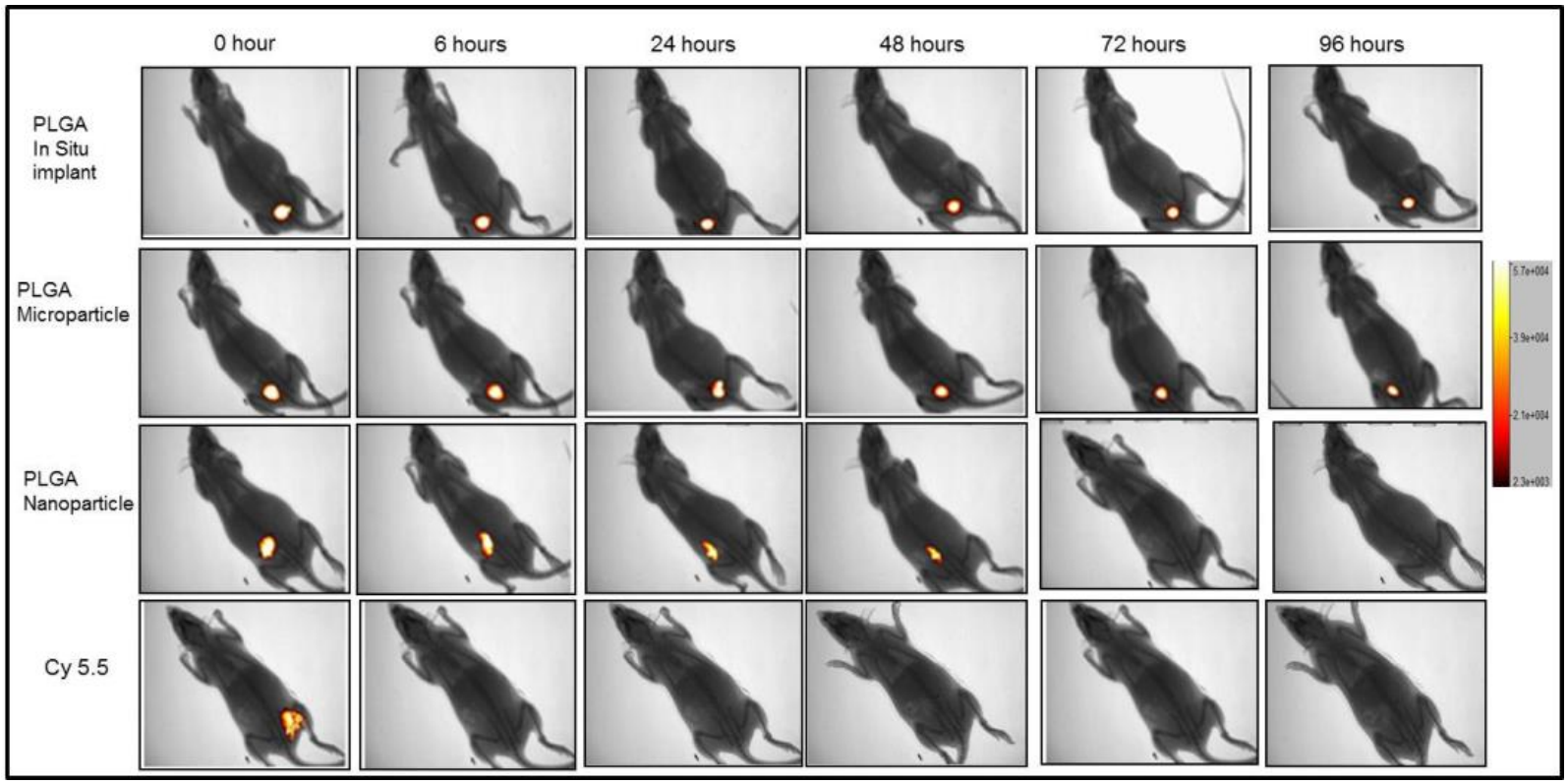

Figure 13: Representative fluorescence images (n=3) depicting intraductal retention of PLGA in-situ gel, microparticles, nanoparticles and free dye (Cy5.5) at different time points from 0-96 hours. The images were captured using in-vivo imager.

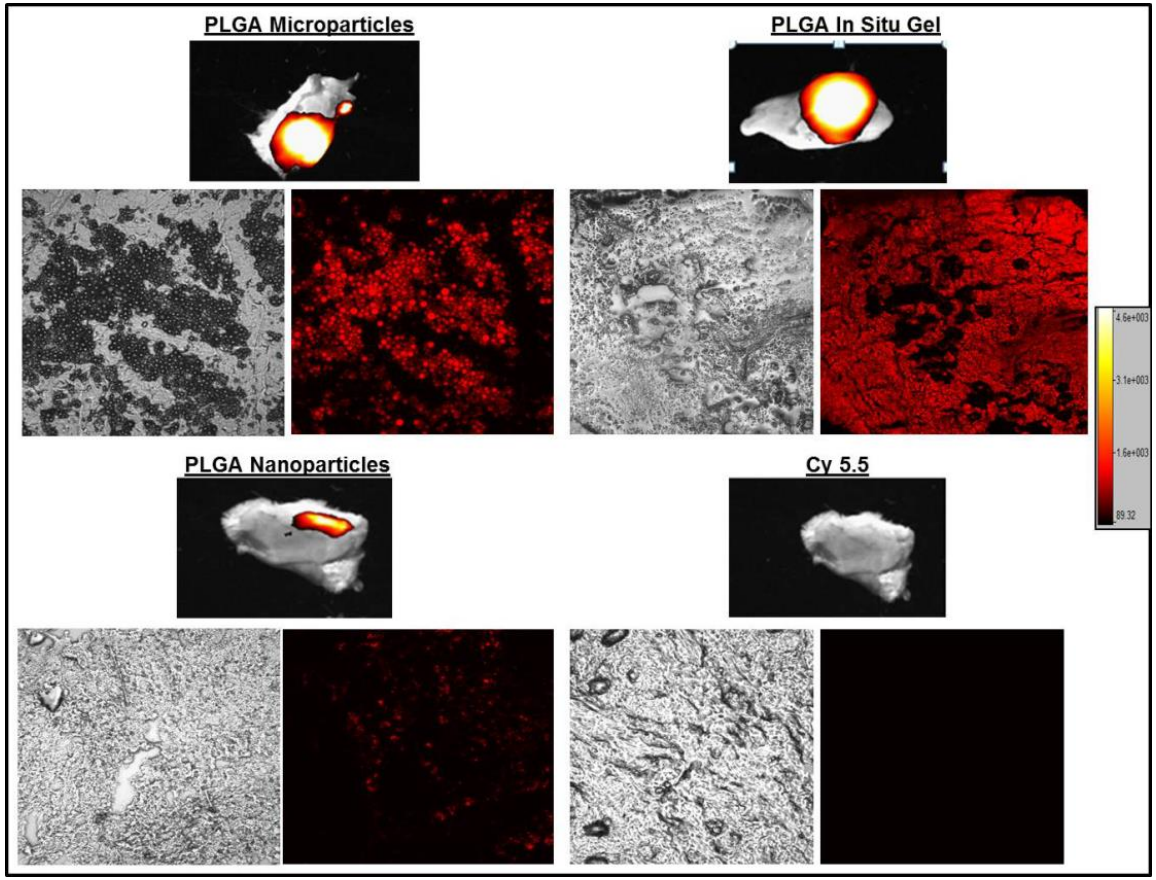

Figure 14: Representative fluorescence images of PLGA formulations and free dye at the end of study. Ex-vivo images of the mammary glands were recorded using in-vivo imager. Mammary glands were cryosectioned (8-10 µm) and viewed under 20X using confocal microscope. The terminal time points were 4 hours for control, 48 hours for PLGA nanoparticles and 96 hours for PLGA in situ gel and microparticles.

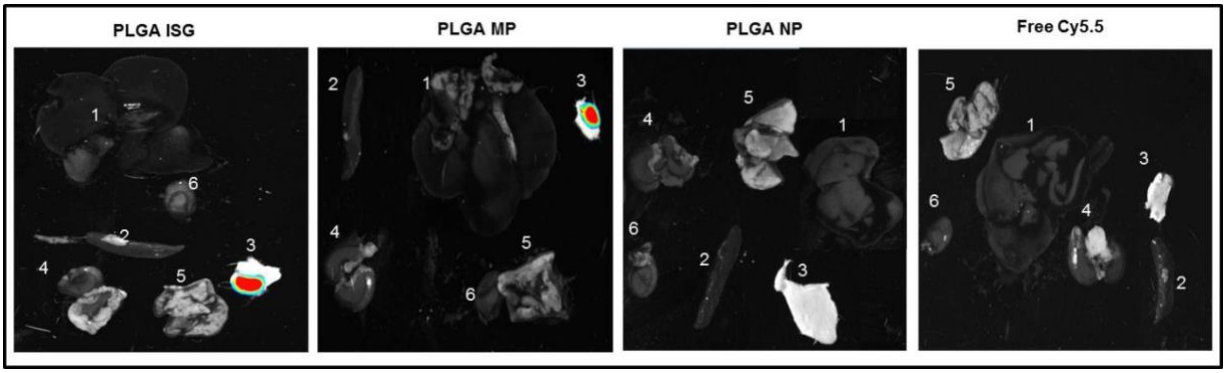

Figure 15: Representative fluorescence images showing in organ biodistribution of PLGA in situ gel (ISG), microspheres (MS), nanoparticles (NP) and free Cy5.5 after intraductal injection in rat. Organs (liver, kidney, lungs, spleen and heart) and mammary glands were excised and imaged at 60 hours for PLGA nanoparticles, 96 hours for PLGA in situ gel and microparticles and 4 hours for free Cy5.5.

The fluorescence in the breast rapidly declined with time for both the free dye and the nanoparticles, while the decline was slower with microspheres and in-situ gel (Figure 15). The retention half-life was highest for in-situ gel, which was two-fold higher than PLGA microparticles (Table 11). The dye diffusion is limited by the higher viscosity of the gel and increases retention in the duct. The PLGA nanoparticles showed a similar half-life (20-24 hrs) compared to polystyrene particles. The half-life for the nanoparticles is comparable to the half-life observed with nanoemulsions (<100nm).[118] Based on our results and results from earlier studies, some general conclusions can be drawn regarding the effect of particle size on ductal retention in the breast. [22, 111, 118, 124] The ductal retention half-life of particles in the size range of 10-500 nm is in the range of 20-24 hrs, while the retention half-life of microspheres in the size range of 1-9 µm is in the range of 88-95 hrs. As the particle size increases, the particles undergo hindered diffusion through the ducts. However, further studies with additional size ranges in the nanometer and micron range are required to confirm these findings. The higher size range will be limited by the diameter of the ductal opening (0.5-2 mm) to prevent particles from blocking the duct.[118]

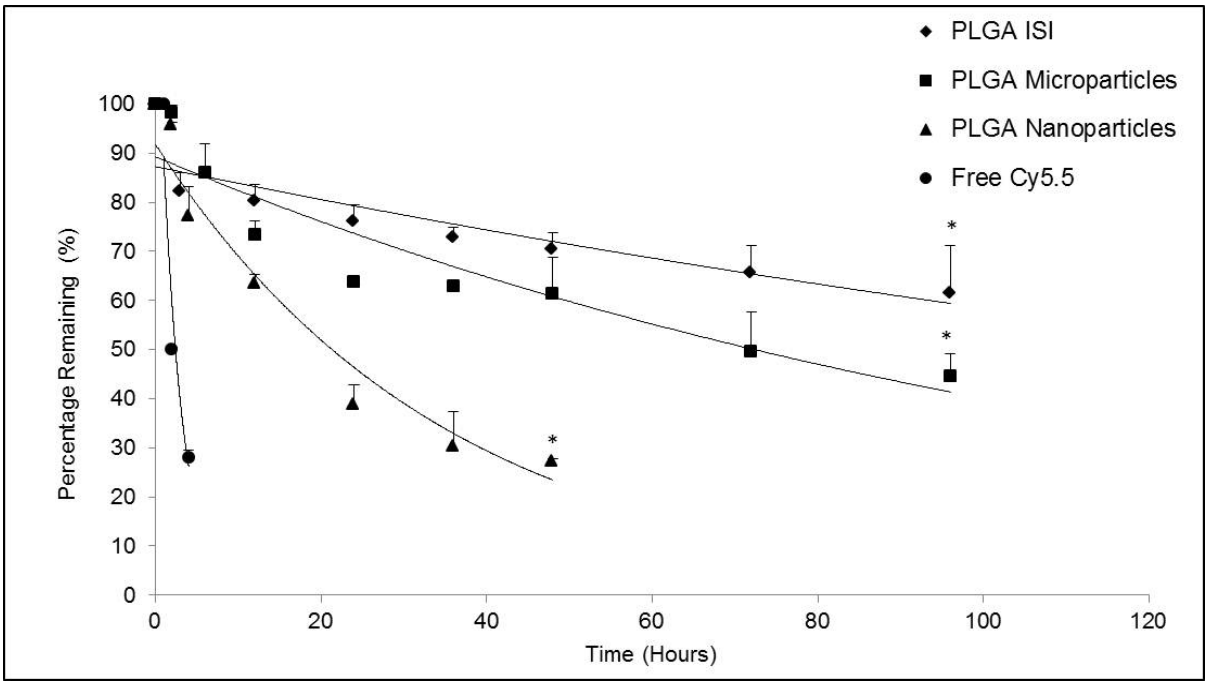

Figure 16: Fluorescence intensity profiles of PLGA in-situ gel, microparticles, nanoparticles expressed as percentage of initial fluorescence. Free Cy5.5 was used as a control. The data represents mean ± S.D (n = 3). * indicates statistical significance from free Cy5.5 using students t-test at ($p < 0.05$)

Table 11: Kinetic parameters of Cy 5.5 loaded PLGA formulations.

Formulation	k (h^{-1})	$t_{½}$ (hrs)
PLGA In situ gel	0.004 ± 0.002 ab	192.5 ± 11.11 ab
PLGA Microparticles	0.008 ± 0.002 ab	88.35 ± 8.76 ab
PLGA Nanoparticles	0.02 ± 0.001 a	24.23 ± 1.12
Cy 5.5	0.40 ± 0.03	1.70 ± 0.16

Each value represents mean ± S.D (n = 3). 'k' is the elimination rate constant; $t_{1/2}$ is the retention half-life, i.e. time at which the fluorescence intensity is 50% of the initial value. 'a' is significant in comparison to Cy 5.5; 'b' is significant in comparison to PLGA nanoparticles. The values are significant at $p<0.05$.

The whole mount showed that the formulations were distributed throughout the ductal tree (Figure 17). To further confirm that the formulations did not block the duct, we injected crystal violet along with the three formulations. The formulations did not affect the crystal violet distribution in the ductal tree, suggesting that the formulations do not block the ducts in the breast (Figure 18).

Histopathological assessments were performed on H&E stained breast tissue sections to determine the effect of the formulations on the tissue morphology. Similar to the untreated mammary gland, ductal architecture was maintained in all the formulations group; there was no damage to epithelial lining, nor any cellular detachment was observed (Figure 19). However, scattered inflammatory cells in the surrounding stromal tissue were observed in the in-situ gel group. Notably, this inflammatory influx was also observed in NMP-treated group indicating that this minor inflammatory reaction could be possibly attributed to the solvent (NMP) used for the gel formulation and warrants the need for testing other alternative solvent-based gel formulations including aqueous-based gels for overcoming the inflammatory response.

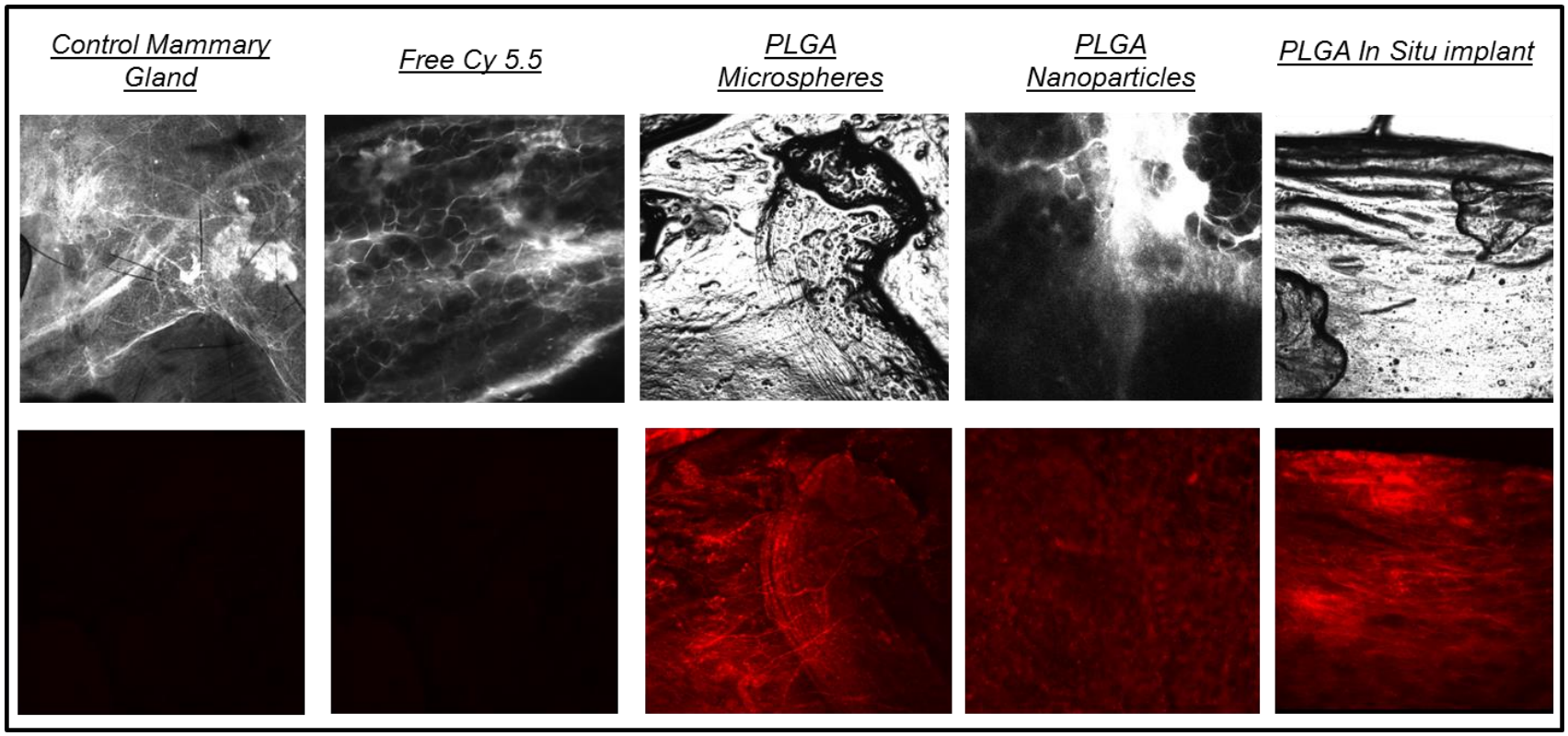

Figure 17: Mammary whole mount 30 minutes after intraductal injection of free dye and PLGA formulations. The images were viewed under 20X using confocal microscope.

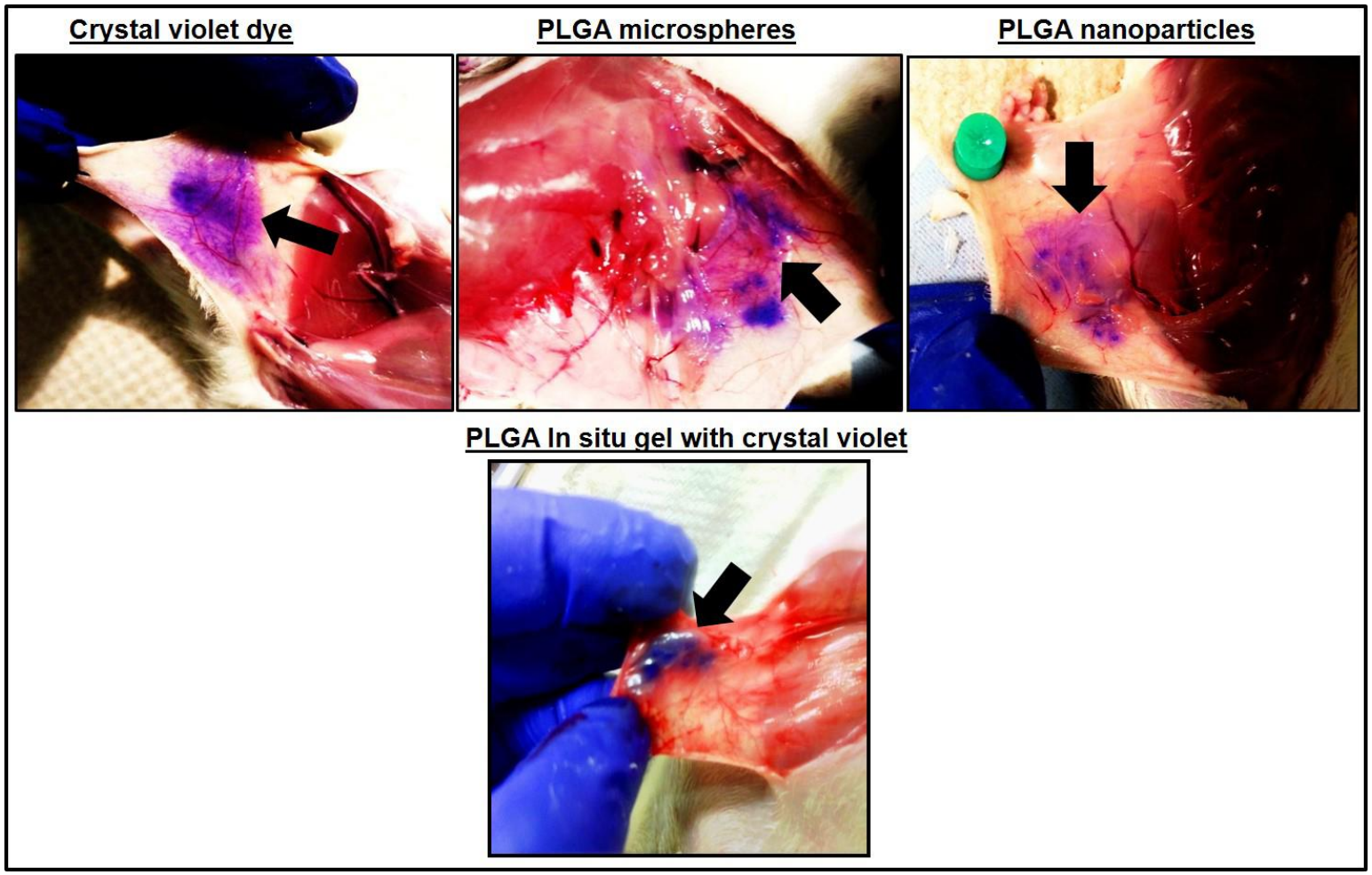

Figure 18: Intraductal distribution of crystal violet after mixing with PLGA formulations

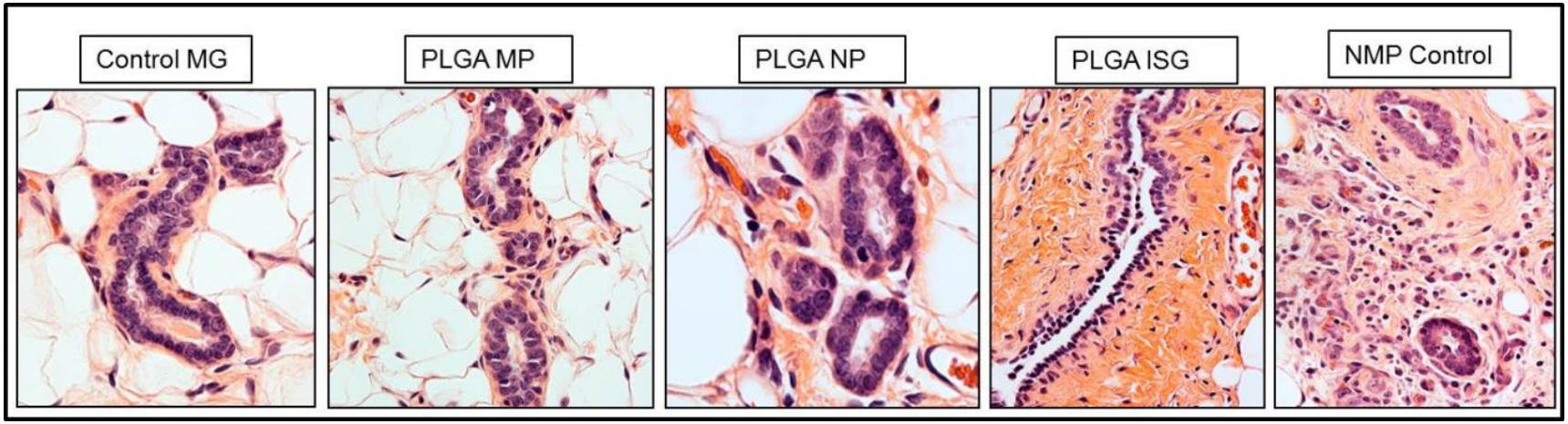

Figure 19: H&E stained sections (5µm) of mammary glands after treatment with PLGA formulations. Images were viewed in a light microscope under 10X. MS- microspheres; NP- nanoparticles; MG is mammary gland; ISG- in-situ gel; NMP- N-methyl pyrrolidone.

Typically, DCIS is localized to a single duct, and therefore it is important to ensure that the drug distributes to the entire ductal tree including the terminal buds, where the majority of pre-cancerous lesions begin.[120] The diffusion of the formulation can be influenced by the ductal permeability. Gu et al in a recent study showed that the ductal retention of PEG-doxorubicin conjugate was not significantly different between normal duct and tumor in the duct in a DCIS rat model.[150] However, the ductal permeability can vary with the stage of the disease.[109, 124] The ductal permeability in early stages of DCIS is similar to the normal ducts but is significantly altered during later stages of tumor development. [109, 124] To this end, the localized intraductal delivery may be more suited as a chemoprevention strategy for treating preneoplasia and early-stage DCIS.

The extrapolation of these results to humans should take into consideration the differences between the rodent and human breast. Rodents have a single duct, unlike multiple ducts in the human breast. To confirm that the results can be extrapolated to humans, we conducted a pilot study in pig, which has a much closer mammary gland structure to humans.[151] The distribution and retention of PLGA formulations in the pig followed a similar trend as observed with the rat breast (Figure 20). Taken together, the results firmly establish that ductal retention in the breast can be prolonged by optimizing physicochemical properties of the formulation.

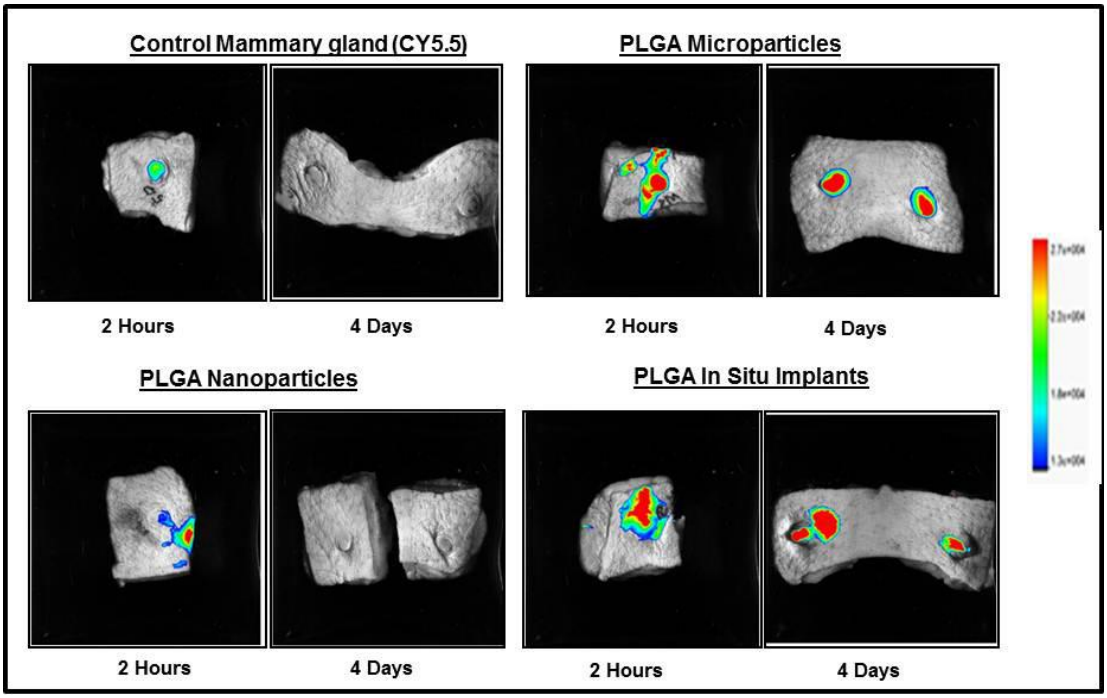

Figure 20: Representative fluorescence images (ex-vivo) of porcine mammary glands. Mammary glands were excised and imaged using in-vivo imager.

1.3.4. Effect of PLGA formulations on retention and distribution in the regional lymph node

Breast cancer spreads from the primary tumor to the regional lymph node in the axilla prior to systemic dissemination.[152] Axillary lymph node, which is the main lymphatic basin for the breast, serves as a reservoir for cancer cells. [152] Therefore, we tested the lymph node distribution of PLGA formulations after ID injection in rats. Within 1 hour of ID injection, the PLGA microspheres were found in the axillary lymph node and the fluorescence was seen up to 2 days (Figure 21). On the other hand, the fluorescence signal from nanoparticles was detected only up to 24 hours. There was no detectable fluorescence in the in-situ gel and free dye treatment groups (Figure 21).

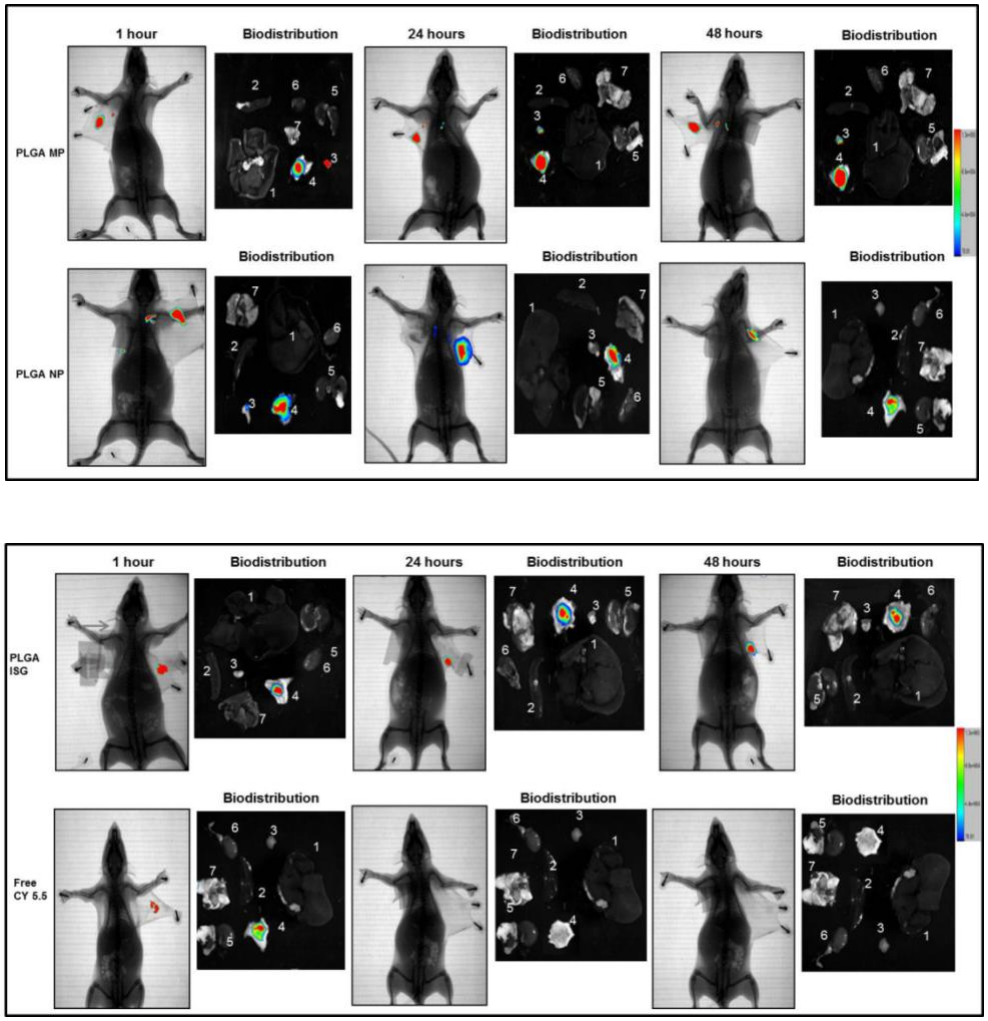

Figure 21: Representative fluorescence images (n=3) of mammary gland, axillary lymph node and organ distribution of PLGA microparticles (MP), nanoparticles (NP), in-situ gel (ISG) and free Cy5.5 (top to bottom) from 1-48 hours. Images were captured using in-vivo imager. 1 – liver, 2-spleen, 3- lymph node, 4- mammary gland, 5- kidneys. 6-heart, 7-lungs.

The lymph node uptake is dependent on the physicochemical properties of the molecule, vehicle and the route of administration.[153] Lymphatic capillaries play an important role in the uptake of particles and macromolecules through the fenestrations and pores in the lymphatic capillary walls. [153] Particles in the size range of 100-1000 nm are taken up by the lymph nodes by pinocytosis.[154] However, unlike the microparticles, the nanoparticles may be washed out relatively faster than from the lymph node. [155] In contrast to the particulate systems, the in-situ gel is primarily retained in the mammary gland and only the released dye is transported to the lymph node. Therefore, it is not surprising that there is no measurable fluorescence in the lymph node with the gel formulation, similar to the free dye treatment group.

Chemotherapy given through systemic routes does not achieve sufficient concentration in the lymph nodes.[153] Hence, in advanced breast cancer, the regional lymph nodes are surgically removed and/or subjected to radiation therapy. This is associated with painful lymphedema.[156] The results from this study demonstrate that intraductal delivery of particulate formulations offers the additional advantage of targeting the lymph node to prevent metastasis. However, the lymph node uptake can vary with the stage of cancer.[153] Further studies are required to understand the different factors which influence lymph node distribution after ID injection. Nevertheless, the results serve as a proof of concept to guide future formulation development for optimizing drug retention in the breast and regional lymph nodes.

1.4. CONCLUSIONS

Results from the study demonstrate the effect of formulation on retention in the breast and lymph node. Microparticles showed longer retention than nanoparticles in the breast and lymph node. PLGA in situ gel formulation showed the highest retention in the duct among the formulations tested. Taken together, the results demonstrate the proof-of-concept for locoregional targeting of breast and lymph nodes by optimal formulation design. Findings from this study can be used to develop safe and effective localized therapeutic strategies for breast cancer.

CHAPTER 2

INTRADUCTAL DELIVERY OF PLGA FORMULATIONS OF TAMOXIFEN

2.1. BACKGROUND

DCIS accounts for nearly 25% of all the breast cancers diagnosed in the U.S. and affects nearly 60,000 women each year. [157] Studies suggest that about 20-30% of DCIS will become invasive cancer even though there are no accurate biomarkers to predict its potential to progress to the invasive form. [119, 120, 157] Estrogen receptors (ERα) are overexpressed in 70% diagnosed DCIS cases. Estrogen is a steroid hormone that plays a major role in the growth and function of the breast and mediates its action through estrogen receptors (ERα and Erβ). [61, 66]

Tamoxifen (TMX) is a selective estrogen receptor modulator (SERM's), which is widely used for the treatment of ERα-positive DCIS and invasive cancers. [158, 159] It is also the first SERM that has been successfully used in the clinic to prevent and treat breast cancer. [159 68, 159] Tamoxifen is estimated to have saved the lives of over 400,000 women with breast cancer. [160] TMX is a prodrug which requires cytochrome P450 (CYP 450) to convert to its active metabolites 4-hydroxytamoxifen (4HT) and N-desmethyl-4-hydroxytamoxifen (Endoxifen) (Figure 22). These metabolites of TMX are 30-100 times more potent than tamoxifen. [161] One of the seminal chemopreventive trials with TMX in humans was the National Surgical Adjunctive Breast and Bowel project study (NSABP) chemoprevention study in the 1970's. In this study, 13,388 high risk pre- and post-menopausal women were randomized and treated with TMX or placebo for five years. The results showed a 50% reduction in invasive cancer and DCIS and a non-significant decrease in bone fractures in volunteers treated with TMX. [160]

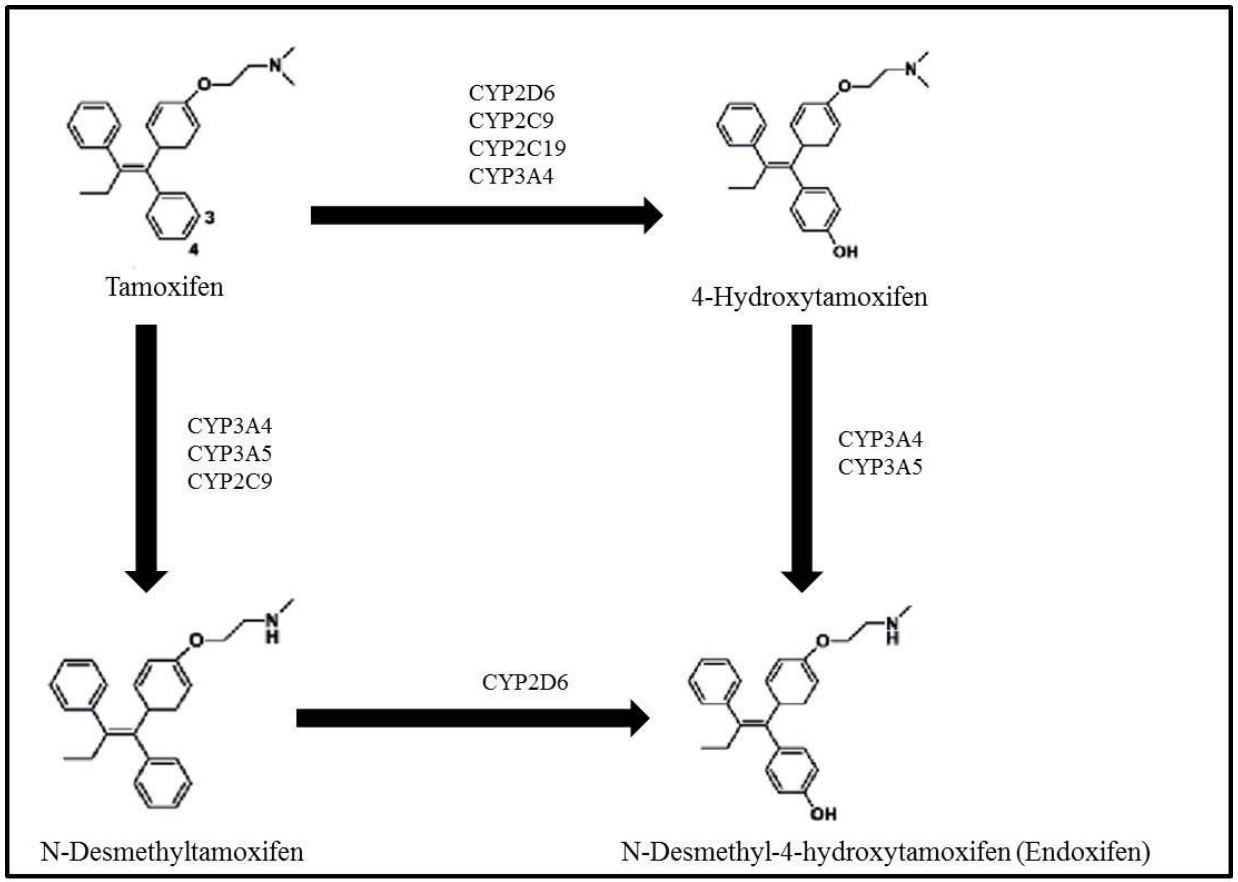

Figure 22: Metabolism of Tamoxifen

Modified from Mürdter, T.E., et al. Clinical Pharmacology & Therapeutics, 89(5), pp.708-717.

However, oral TMX therapy (20 mg daily for 5 years) is associated with side-effects such as thromboembolic events and endometrial cancer limiting its use for prevention and therapy.[158] TMX therapy is also linked to drug resistance as they are substrates of P-glycoprotein, breast cancer resistance protein (BCRP) and multidrug resistance associated protein (MRP) [161-164]. TMX has low oral bioavailability and low specificity towards tumor cells.[161] Localized administration of TMX showed reduction in systemic side effects of TMX. [164, 165] In the present study, we hypothesize that long-acting intraductal TMX formulations will not only provide a therapeutic advantage by sustaining drug levels in the breast, but also reduce the side-effects associated with oral TMX.

As described in the previous chapter, PLGA MS and ISG were retained in the mammary glands for 4 days with reduced systemic exposure compared to PLGA NP and free dye. Also, we found that PLGA MS and NP was transported and retained in the regional lymph nodes for 24 and 48 hours respectively. Building on these findings, the main objective of the present study is to develop intraductal PLGA formulations of TMX and to test the biodistribution in rats.

The specific aims of the study are:

i) Development and optimization of TMX loaded PLGA formulations

ii) In-vitro characterization and release of TMX from PLGA formulations

iii) Determine the biodistribution of TMX loaded PLGA formulations in rat

2.2. Materials and Methods

Poly (lactic-co-glycolic acid) (LA:GA = 75:25, 75-85 KDa and 10-15 KDa, LA:GA = 50:50, 5-10 KDa) were purchased from Akina, Inc. (West Lafayette, IN). The isoflurane was obtained from VetOne, Boise, ID and Veet hair removing cream was obtained from Reckitt Benckiser (Parsippany, NJ). All other reagents were purchased from Sigma-Aldrich (St. Louis, MO).

2.2.1. Formulation of PLGA microspheres

Microspheres were prepared by oil-in-water (O/W) emulsion method as described in the earlier chapter (section 1.2.2.1). To prepare particles of different sizes, homogenization[133] (10,000 rpm for 1 minute) and overhead stirring[166] (1000 rpm for 10 minutes) were used. 50 mg TMX was used in all the formulations.

2.2.2. Formulation of nanoparticles

PLGA nanoparticles were prepared by emulsion solvent evaporation and sonication method[134] as described in section 1.2.2.2. Tamoxifen was used in different amounts ranging from 10-50 mg and 100-200 mg PLGA 75:25 (10-15 KDa) were used in the formulations.

2.2.3 Formulation of *In situ* gel

PLGA *in situ* gel was prepared using a previously reported method. [137] PLGA *in situ* gel (25% w/w) was prepared using PLGA 50:50 (5-10KDa) and PLGA 75:25 (10-15 KDa), either alone or mixed at 1:1 w/w ratio as described in section 1.2.2.3.

2.2.4 HPLC

The HPLC analysis of TMX was performed on a Waters system (Milford, MA) equipped with an isocratic pump, degasser, and autosampler. The compound was separated using a waters symmetry C18 column (Waters Corporation, Milford, USA) (4.6 mm × 150 mm, ID 5 μm). The mobile phase for TMX was a mixture of acetonitrile, methanol and water (7:3:3 v/v) containing 0.1 % v/v acetic acid and 0.01% v/v triethanolamine. The mobile phase was pumped at a flow rate of 0.8 ml/min and was monitored at 243 nm. The calibration curve of tamoxifen in acetonitrile (peak area versus drug concentration) was linear (R_2 = 0.999) in the concentration range of 25 to 360 μg/mL for TMX. The data was analyzed using in built software (Breeze version 3.30 SPA).

2.2.5 Determination of encapsulation and loading efficiency

For determining encapsulation and loading efficiencies, 3 mg of MS and NP was dissolved in 1 ml of methylene chloride (DCM). The sample was then vortex mixed and sonicated for 1-2 minutes and the solvent was evaporated to dryness using gentle stream of Argon. The sample was then reconstituted using 1 ml acetonitrile and 10 μl was injected to RP-HPLC determine drug concentrations using conditions as described in section 2.1.4. The encapsulation and loading efficiencies were calculated using the equation in section 1.2.2.4

2.2.6 *In vitro* release study

The release study was performed as described in 1.2.2.5. Briefly 10 mg of PLGA microspheres and nanoparticles were dispersed in 2 ml of release medium (PBS, pH 7.4

containing 0.5 % w/v SLS) in an eppendorf tube. At each time point, tubes were centrifuged at 10,000 rpm for 10 minutes. The supernatant was collected (1.8ml) and replaced with fresh release medium to maintain sink conditions. For, PLGA ISG, 500 µl of formulation was injected into 4 ml release medium using a 27G needle. At each time point, 2 ml of the medium was collected and replaced with same volume of fresh release medium to maintain sink conditions. The supernatant was then analyzed using HPLC as described in section 2.1.4 to determine the TMX concentrations.

2.2.7 *In vivo* studies

For pharmacokinetic studies, Female Sprague Dawley rats 4-6 weeks old, 150-200 g were used for the study. All animal studies were performed after getting approval from IACUC at South Dakota State University. TMX formulations were injected (1 mg x 2 teat) into the inguinal mammary glands (n=3) for breast retention studies and axillary mammary glands for lymph node localization studies. Blood samples were (0.5 -0.1µl) were collected from tail vein at time points (0-14 days). The plasma was separated by centrifuging the tubes were then centrifuged at 10,000 rpm for 10 minutes. For lymph node localization study, lymph nodes were excised at time points (0 -14 days). Pharmacokinetics was performed using PK solutions using non compartmental analysis.

2.2.8 Tissue preparation

Before collecting the organs, the tissues were perfused with saline to remove blood from the organs. The tissues were weighed and mixed with 0.1mM Tris HCl (0.1 g/ml). The tissue was homogenized using tissue homogenizer at 10, 000 rpm for 2-3 minutes with

sample kept under ice. The lymph nodes were homogenized using probe sonicator at 40W amplitude (2 minutes) in an eppendorf tube kept under ice. Around 100µl of the tissue homogenate was mixed with 400 µl of acetonitrile (1:4 w/v) to precipitate proteins. The mixture was vortex mixed for 30 to 60 seconds and further sonicated for 1-2 minutes. The sample was then centrifuged at 10,000 rpm for 10 minutes. The supernatant was collected and evaporated to dryness under stream of Argon. The samples were then reconstituted using 100 µl of 7:3 v/v of ammonium formate and acetonitrile and analyzed using LC-MS. The same procedure was followed for determining drug concentrations in the plasma.

2.2.9 LC-MS

Tamoxifen and two major active metabolites 4-hydroxytamoxifen and endoxifen were quantified by Liquid Chromatography Tandem Mass Spectrometry (LCMS) using a previously reported method.[167] Plasma and tissue samples were analyzed using an Agilent 1260 infinity LCMS system (Agilent, Santa Clara, CA, USA). The mobile phase (Table 11) (Mobile phase A was 3.5mM ammonium formate, pH adjusted to 3.5 using formic acid and mobile phase B was acetonitrile) was pumped through reversed-phase HPLC column (Agilent Poroshell 120 SB-C18 column (2.1 x 100 mm, I.D 2.7µm) attached to a guard column (Agilent SB-C18, 2.1 x 5mm, I.D 2.7µm) at a flow rate 0.5 ml/min using gradient elution method (Table 12) at 30° C. The volume of injection was 15µl and the needle was washed using a mixture of acetonitrile methanol and water (7:3:3) before and after each injection. Detection of TMX and metabolites (4HT and EDX) was performed in positive ion mode using a single quadrupole mass analyzer. The most intensive signal in the spectrum was from quasi-molecular ion [M + H]+ and hence the selected monitored ion

(m/z) was set to 372, 374 and 388 for tamoxifen, endoxifen and 4-hydroxytamoxifen respectively. The standard curve range for tamoxifen was 1 ng/ml (LLOQ) to 25 ng/mL; the range for 4-hydroxytamoxifen was 2.5 ng/ml (LLOQ) to 25 ng/mL; and the range for endoxifen was 2.5 ng/ml (LLOQ) to 50 ng/ml.

2.2.10 Statistical analysis

All the experiments were conducted in triplicate using three independent batches of formulations unless noted otherwise. The data is represented as mean ± standard deviation. One-way ANOVA was performed to determine statistical significance followed by Bonferroni post hoc analysis at $p<0.05$.

Table 12: Gradient elution method for TMX, 4HT and EDX

Time	Mobile phase A (Ammonium Formate 3.5mM, pH 3.5 adjusted with Formic acid)	Mobile phase B 100%Acetonitrile	Flow Rate (ml/min)
0	70	30	0.250
4	30	70	0.250
4.10	20	80	0.250
8	20	80	0.250
8.10	0	100	0.250
12	0	100	0.250
12.10	30	70	0.250
16	70	30	0.250
16.10	70	30	0.250
22	70	30	0.250

2.3. RESULTS AND DISCUSSION

The use of systemic therapy is TMX is limited due to its bothersome side- effects.[158, 159] Localized delivery of TMX is an effective way to minimize systemic toxicity associated with TMX. [165] Intraductal delivery has showed enhanced drug levels in the breast in several preclinical and clinical studies [109, 110, 119], but poor retention of drugs remains a major barrier for translation of this approach to clinic. [22] A more recent study showed improved efficacy of fulvestrant in treating ER + breast cancer in two preclinical animal models. [119] However, the drug was dosed 3-4 times at biweekly intervals to sustain therapeutic levels in the ducts. Previously, intraductal TMX did not result in chemopreventive effects as no major metabolites was detected in the mammary glands. However, enhanced retention time of TMX in the mammary glands and its biotransformation into active forms is not very well understood. To this end, the major goal of the study is to develop PLGA formulations of TMX and determine the *in vivo* biodistribution. This will aid in the development of an intraductal delivery system that can enhance drug levels in the breast, minimize systemic exposure and reduce the frequency of intraductal injections.

2.3.1. Preparation and characterization of PLGA microspheres

Poly (lactic-co-glycolic acid) [PLGA] microspheres (MS) were formulated using emulsion solvent evaporation [168] by homogenization [148] and overhead stirring methods. [166] We chose PLGA as the delivery system because of its extensive application in drug delivery and is approved by USFDA. [125] To prepare MS of different particle sizes, PLGA of copolymer (LA: GA) ratio of 75:25 and molecular weights 10-15 KDa (low) and 75-85 KDa (high) and two methods, homogenization and overhead stirring were used. With lower molecular

weight PLGA, homogenization and overhead stirring resulted in the formation of MS with particle sizes 3.36 ± 1.19 µm and 54.36 ± 12.93µm respectively (Table 13). This was consistent with previous finding that homogenization results in increased shear and thus breaks down the emulsion droplets to form particles of smaller size. [169] The drug content in the MS increased with increase in particle size consistent with previous findings [148]. But when a higher molecular weight PLGA was used, homogenization resulted in lower particle size of 9.12 ± 3.77 µm and higher drug content [170] Higher molecular weight polymer has increased viscosity and hence a larger shear is required to breakdown the droplets to produce smaller particles. PLGA MS with particle size 9.12 ± 3.77 µm showed a spherical morphology (Figure 24) with higher encapsulation and loading efficiencies (Table 13). With high molecular weight PLGA, overhead stirring resulted in particles with particle size was >100 µm, which was deemed not feasible for intraductal injection (data not shown). Despite variabilities in the duct diameter, it is found that the diameter of the duct ranges from 0 - 0.2 mm. Previous studies with PLGA microspheres showed that particle size of 1-10 µm exhibited similar duct retention times. In this study, the goal was to prepare PLGA MS with particle size ~10µm that can sustain TMX release for 2 weeks.

Table 13: Characteristics of TMX loaded PLGA microspheres

Formulation	Particle size (µm)	Zeta Potential (mV)	PDI	EE (%)	LE (%)
PLGA 75:25 (10-15 KDa, H)	3.36 ± 1.19	-31.36 ± 0.92	0.44 ± 0.09	55.43 ± 1.95	6.23 ± 0.14
PLGA 75:25 (10-15 KDa, OH)	54.36 ± 12.93	-30.48 ± 0.52	0.44 ± 0.09	73.01 ± 3.14	8.89 ± 0.26
PLGA 75:25 (75-85 KDa, H)	9.12 ± 3.77	-28.36 ± 0.74	0.44 ± 0.09	95.35 ± 2.01	10.22 ± 0.12

PLGA is poly (lactic-co-glycolic acid), LA is lactic acid, GA is Glycolic acid, H is homogenization, OH is overhead stirring. Data is Mean ± SD. Particle size calculated as an average of 30-50 microspheres using Smart Tiff software. EE is encapsulation efficiency, LE is loading efficiency, PDI is poly dispersity index

In vitro release studies were performed for all the three MS formulations described in the earlier. It is known that smaller particle size tends to release the contents faster because of the increased surface area. In the present study, PLGA MS with three different particle sizes (Table 13) were chosen to determine the *in vitro* release. PLGA MS with particle size 3.36 ± 1.19 µm released TMX in 7 days (Figure 28). PLGA MS of particle size 54.36 ± 12.93 µm sustained the release of TMX >7 days, but the particle size was beyond the size range for this study. This trend in drug release is because of the larger surface area of smaller microspheres and shorter diffusion path lengths. [166, 171] However, when a higher molecular weight of PLGA (75-85 KDa) was prepared using homogenization, the particle size was determined to be 9.12 ± 3.77 µm. This formulation sustained TMX release for >20 days and was chosen for in vivo studies (Figure 23). This is due to the slower hydrolytic degradation of high molecular weight polymer resulting in sustained release of TMX. [172]

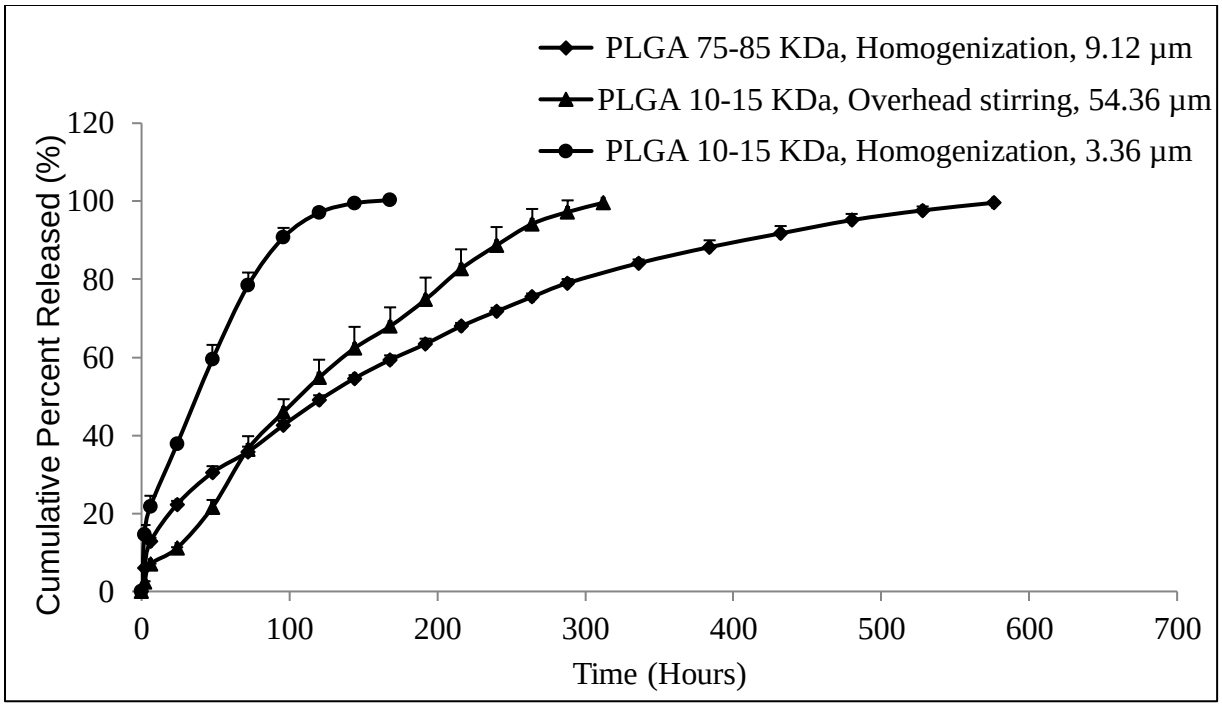

Figure 23: *In vitro* release of tamoxifen from PLGA microspheres of different particle sizes. Data is Mean ± SD (n=3)

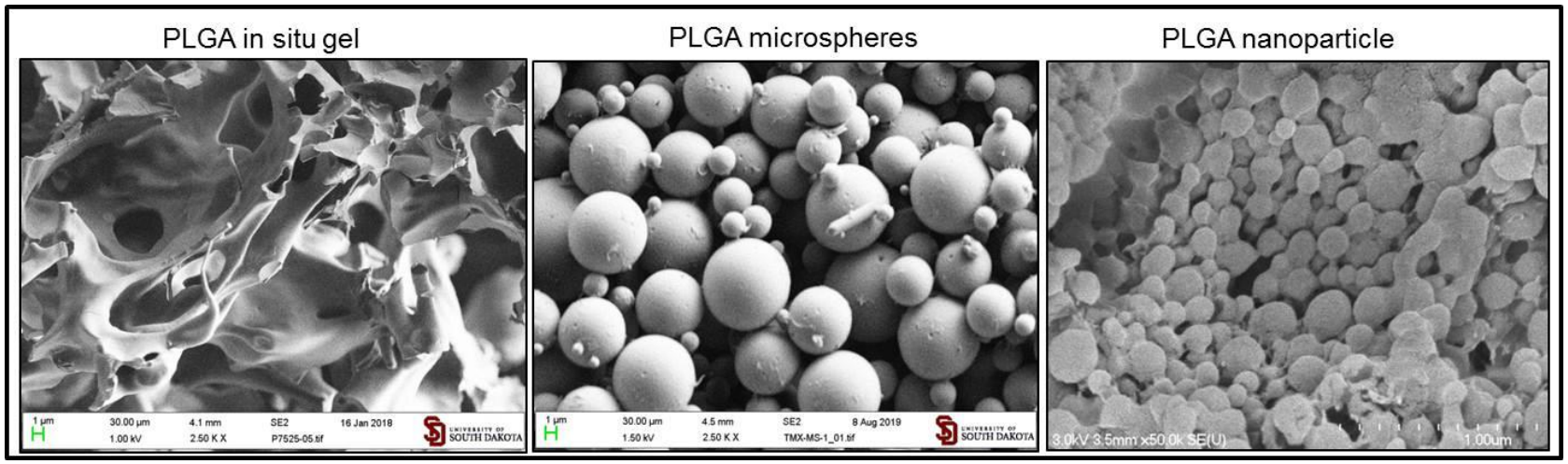

Figure 24: Representative SEM images of PLGA formulations

2.3.1 Preparation and characterization of PLGA nanoparticles

PLGA nanoparticles (NP) were prepared by emulsion solvent evaporation and sonication method. [134] Previous studies with polystyrene particles showed that particle size of 100-500 nm exhibited similar retention $t_{1/2}$ in the ducts. So, the goal of the present study was to formulate PLGA NP of particle size 200-300 nm that can sustain drug release for at least 14 days. Initial optimization studies focused on optimizing the PLGA amounts and sonication parameters to prepare PLGA NP of this particle size range (data not shown). By keeping PLGA amount (100mg) and other parameters constant, increasing TMX amount resulted in increase in the particle size (Table 14). However, by increasing the polymer amount to 200 mg with 10 mg of TMX resulted in the formation of PLGA NP with particle size 274.1 ± 6.07 with encapsulation and loading efficiencies of 91.28 ± 2.17 and 6.19 ± 0.17 %. This was consistent with previous findings where an increase in the polymer amount increased the viscosity of the polymer solution (increased particle size) and resulted in higher drug encapsulation. [173]

The next goal was to determine the formulation that can sustain TMX release for ~14 days which was the duration of our *in vivo* study. PLGA NP has higher surface area and higher drug amounts results in burst release resulting in drug loss. [174] *In vitro* release of PLGA NP was performed for 48 hours to optimize the amount of TMX that can be loaded to PLGA NP (Figure 25). With 50 mg TMX, 80% of TMX was released in 48 hours. By reducing TMX to 15mg, the TMX release was reduced to ~60%. This was consistent with previous findings with PLGA nanoparticles[134] where higher amounts of drug resulted in a faster drug

release. However, with 10mg TMX, TMX release was sustained for 2 weeks and was chosen for further studies (Figure 26). This formulation also exhibited a spherical morphology (Figure 24) with higher encapsulation and loading efficiencies of 91.28 ± 2.17 and 6.19 ± 0.17 % respectively (Table 14). This formulation was chosen for *in vivo* study.

Table 14: Characteristics of TMX loaded PLGA nanoparticles

Amount of Tamoxifen (mg)	Particle size (nm)	Zeta Potential (mV)	Encapsulation Efficiency (%)	Loading Percentage (%)
50	252.2 ± 4.02	-22.14 ± 2.05	77.85 ± 3.78	35.60 ± 6.17
25	234.1 ± 2.01	-20.12 ± 0.09	61.25 ± 4.75	16.78 ± 5.09
15	228.1 ± 9.12	-22.14 ± 1.79	58.04 ± 2.14	7.66 ± 2.45
10*	274.1 ± 6.07	-19.17 ± 3.77	91.28 ± 2.17	6.19 ± 0.17

Data is Mean ± SD, (n=3), PLGA 75:25 (10-15 KDa) amount 100 mg; * indicates PLGA amount of 200mg; PVA was 1%

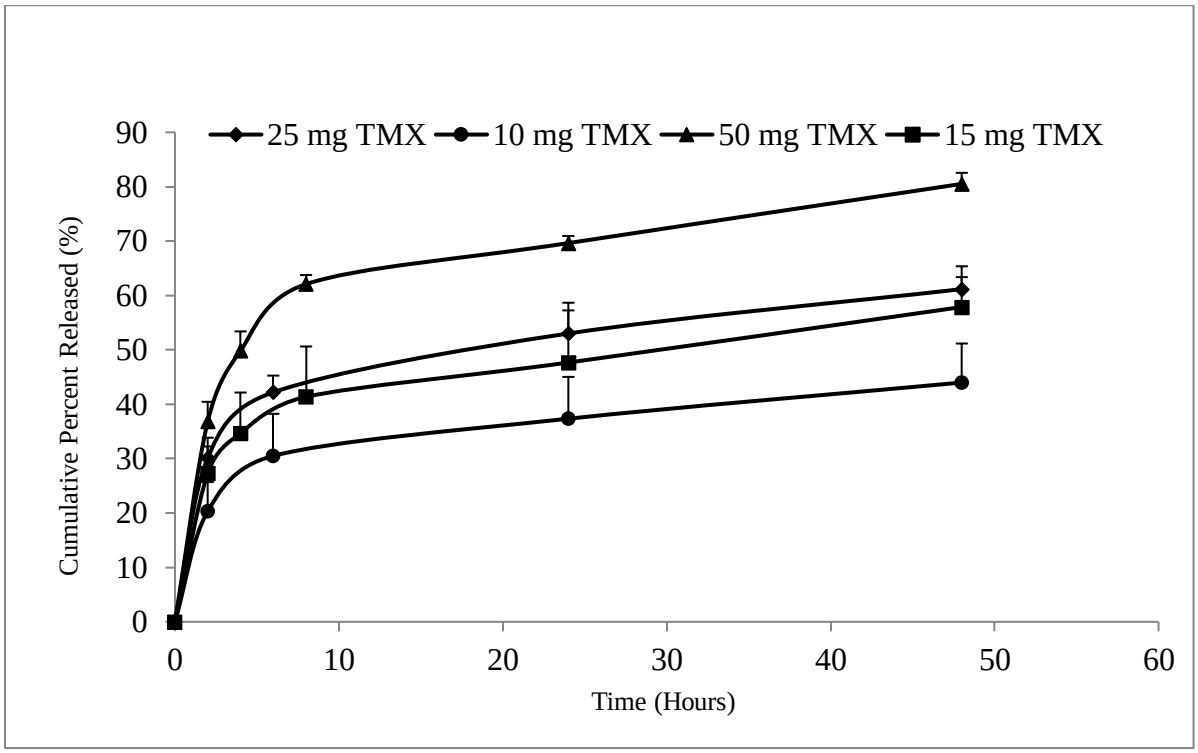

Figure 25: Effect of tamoxifen loading on the burst release of tamoxifen from PLGA nanoparticles. Data is Mean ± SD, (n=3)

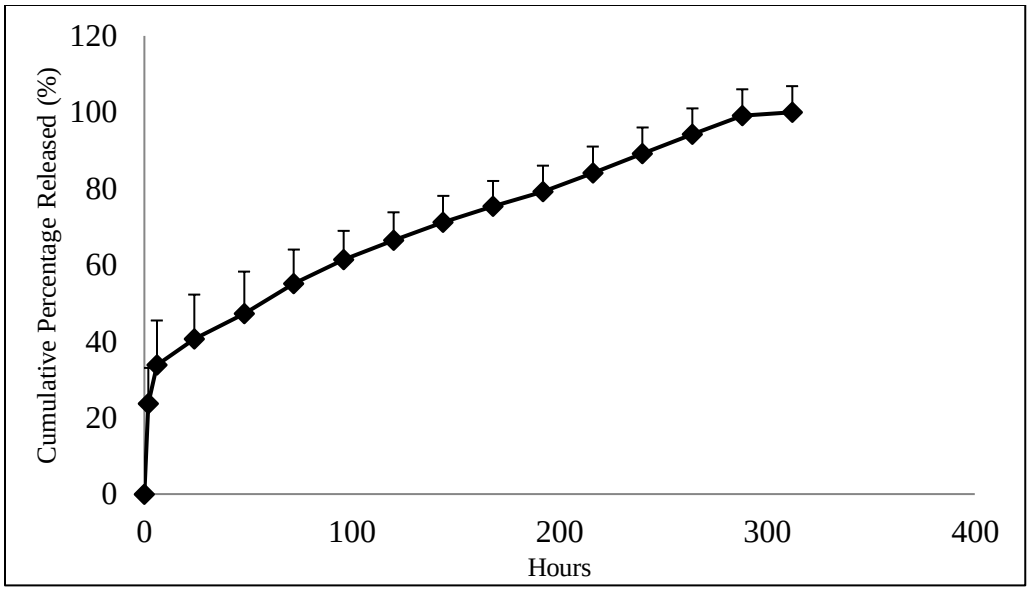

Figure 26: *In vitro* release profile of tamoxifen from optimized PLGA nanoparticles Data is Mean ± SD, n=3.

2.3.2 Preparation and characterization of PLGA in situ gel

PLGA *in situ* gel (ISG) was formulated using NMP as the solvent. NMP was chosen as the solvent because of its extensive use in the preparation of *in situ* forming systems and because of its pharmaceutical precedence. [175] The contact of PLGA ISG with aqueous medium results in phase inversion and eventually the precipitation of the polymer. [135] Initial studies focused on optimizing PLGA ISG with desired viscosity for intraductal injections. Reducing the polymer concentration decreased the viscosity (Table 15), but resulted in faster drug release[175] (data not shown). Viscosity of PLGA is directly related to its molecular weight[125] and hence PLGA with molecular weights 5-10 KDa and 10-15 KDa were chosen for the present study.

In vitro release study showed that 20wt% of PLGA 5-10 KDa sustained release for ~10 days (Figure 27). Blending of PLGA of different molecular weights is an effective method to modulate drug release [137, 146] . In the present study a blend of PLGA 5-10 KDa 10-15 KDa were blended at 1:1 ratio as used to formulate 25 wt% PLGA ISG. This formulation showed viscosity of 25cP (Table 15) and sustained TMX release for > 20 days and was chosen for in vivo experiments (Figure 27).

Table 15: Viscosity of PLGA *in situ* gel formulations

Formulation	**Viscosity (cP)**
10 wt% PLGA 50:50 (5-10 KDa)	<12.5
20wt% PLGA 50:50 (5-10 KDa)	25
20wt% PLGA 75:25 (10-15 KDa)	37.5
25 wt% ISG blend PLGA 50:50 (5-10 KDa) & PLGA 75:25 (10-15 KDa)	25

cP is centipoise. Each value is Mean ± S.D, n=3

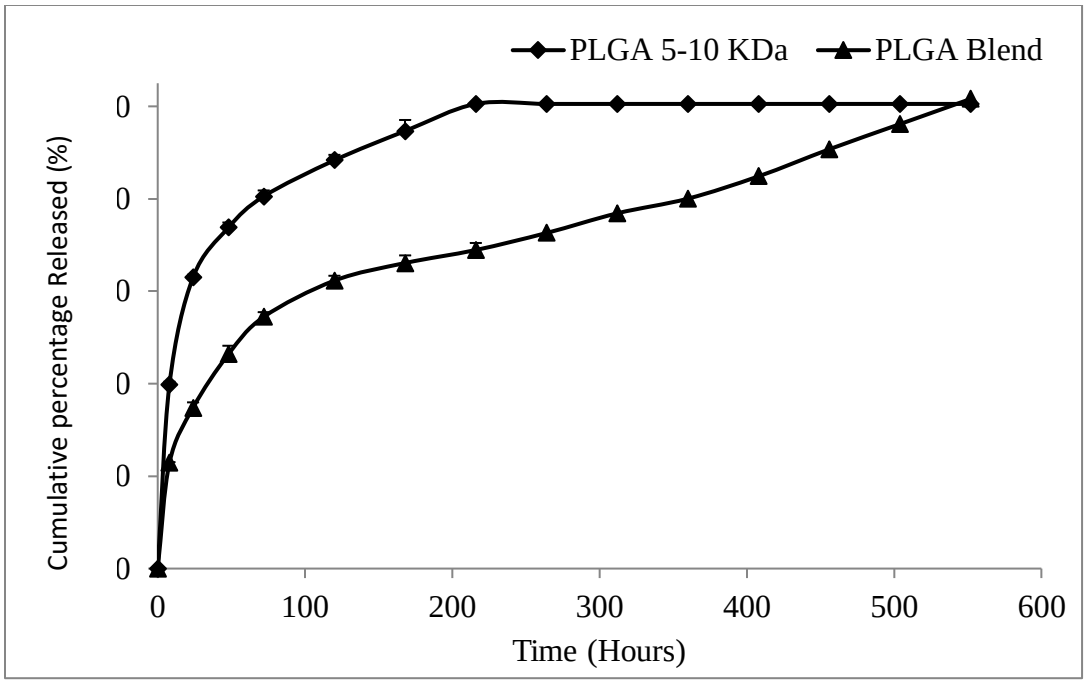

Figure 27*: In vitro* release profile of tamoxifen from 25 wt% PLGA ISG; PLGA blend is (5-10 KDa) and (10-15 KDa) at 1:1 wt%. Each Value is Mean ± SD, n=3.

2.3.4 Effect of PLGA formulations on breast retention and distribution

To study the distribution of PLGA formulations in the breast, we used Poly (lactic-co-glycolic acid) PLGA microspheres (MS) and nanoparticles (NP) and in situ gel (ISG). The formulations were injected into the 2 inguinal mammary glands (1 mg X 2 teats) and the concentrations of TMX and metabolites in the mammary glands were determined at days 0.5, 1, 2, 4, 6, 7, 10 and 14.

PLGA MS was retained in the mammary gland for 14 days compared to PLGA NP which was retained for 6 days (Figure 28). This was in accordance with our previous findings where particle size was found to impact drug retention in the breast. PLGA NP showed significantly ($p<0.05$) higher k_e ($0.0105 \pm .002$ hrs $^{-1}$) compared to PLGA MS (0.0012 ± 0.0003 hrs $^{-1}$) suggesting faster diffusion of PLGA NP from the breast (Table 16). The diffusion of PLGA MS from the mammary ducts was slower because the larger particle size offered hindrance to diffusion from the mammary ducts. [22] At day 6, TMX level in mammary glands treated with PLGA MS were 4-fold and 6-fold higher than PLGA NP and free TMX respectively (Figure 28). Moreover, the $t_{1/2}$ and MRT of PLGA MS was ~100-fold higher compared to PLGA NP and free TMX (Table 15)

PLGA ISG was retained in the mammary glands for 14 days and the levels were significantly higher than PLGA NP and free TMX (Figure 28). The $t_{½}$ for PLGA ISG was significantly higher than PLGA NP and free TMX (Table 16). The amount of TMX in the breast for PLGA MS and ISG were found to be 1.05μg/mg and 2.20 μg/mg respectively

after 2 weeks following single intraductal injection. PLGA ISG showed longer retention times in the breast and was found to have k_e of 0.0007 hrs $^{-1}$ which was lower than PLGA MS. The MRT of PLGA ISG was found to be 2-fold higher than PLGA MS (Table 16).

Tamoxifen is a prodrug that is metabolically converted to 4-hydroxy tamoxifen[176] or can undergo metabolic conversion to 4-hydroxy N- desmethyl tamoxifen (endoxifen)[177] by cytochrome P450 enzymes [161] (Figure 22). Interestingly, we observed 4-hydroxytamoxifen in the mammary glands treated with PLGA MS and ISG (Figure 29). The 4HT levels in the breast was significantly higher ($p<0.05$) with PLGA MS and ISG compared to free TMX (Figure 34). The 4HT T_{max} for PLGA MS and ISG of were 144 and 168 hours respectively. Compared to free TMX, the C_{12hr} was ~ 6-fold lower with PLGA MS and ISG. At day 14, the amount of 4HT in the breast was 1.5 and 3.3-fold higher than free TMX group for PLGA MS and PLGA ISG respectively (Table 17). No 4HT was detected in free TMX group and PLGA NP after 48 and 168 hours respectively. In comparison to PLGA nanoparticles, the level of 4HT for PLGA MS and ISG was significantly higher at 168 hours. Free TMX showed much lower levels of 4HT till 48 hours and was below detection at later time points. PLGA NP showed 4HT levels till 7 days and was undetectable afterwards. At day 6, the levels of 4HT in mammary glands treated with PLGA MS were 5-fold and 2-fold higher than PLGA NP and PLGA ISG. The 4HT level of PLGA ISG peaked at day 7 with 4-fold higher levels than PLGA MS. At day 14, the 4HT levels in the mammary glands were 1.5-fold and 3.5-fold higher than free TMX.

Previously (Figure 7), we found that particle size plays a major role in ductal retention. Also, it is known that hydrophobic drugs are cleared slowly from the breast than hydrophilic drugs[111]. Tamoxifen is an extremely lipophilic molecule with Log P value around 6. The fatty envelope of the breast tissue may serve as a drug reservoir aided by intra-mammary lymphatic circulation can enhance the drug retention and distribution in the breast.[95] Previously, intraductal TMX did not show chemopreventive effects in MNU induced rat carcinogenic model. [109] It is fair to conclude that shorter retention time of TMX in the mammary glands did not facilitate the metabolism of TMX by resident CYP enzymes in the breast.[178] However, in this study PLGA MS and ISG showed retention t ½ >200-fold higher in the mammary glands compared to free TMX. The CYP 3A4 enzyme is found to be expressed in the normal breast tissue and in breast tumors and this facilitates the conversion of TMX in the breast to 4 hydroxy tamoxifen. [178] From our studies, we conclude that retention of formulation is important determinant for this conversion of TMX in the breast tissue and PLGA MS and ISG with longer retention times aids in the formation of 4HT in the breast. The role of TMX as an inducer of CYP enzymes in the breast needs also needs to be considered. [179] The reported IC50 value of TMX in MCF-7 cells is 3.34 – 3.71 μg/ml and clinically relevant concentration in breast cancer patients is 1.85 μg/ml. [180, 181] Results from this study suggests that TMX concentrations were maintained above the therapeutic levels following single dose of intraductal injection. Moreover, 4HT levels were maintained above the therapeutic levels of 4HT (IC50 – 1.52 – 6.97 ng/ml) [182] in mammary glands treated with PLGA ISG and MS for 14 days.

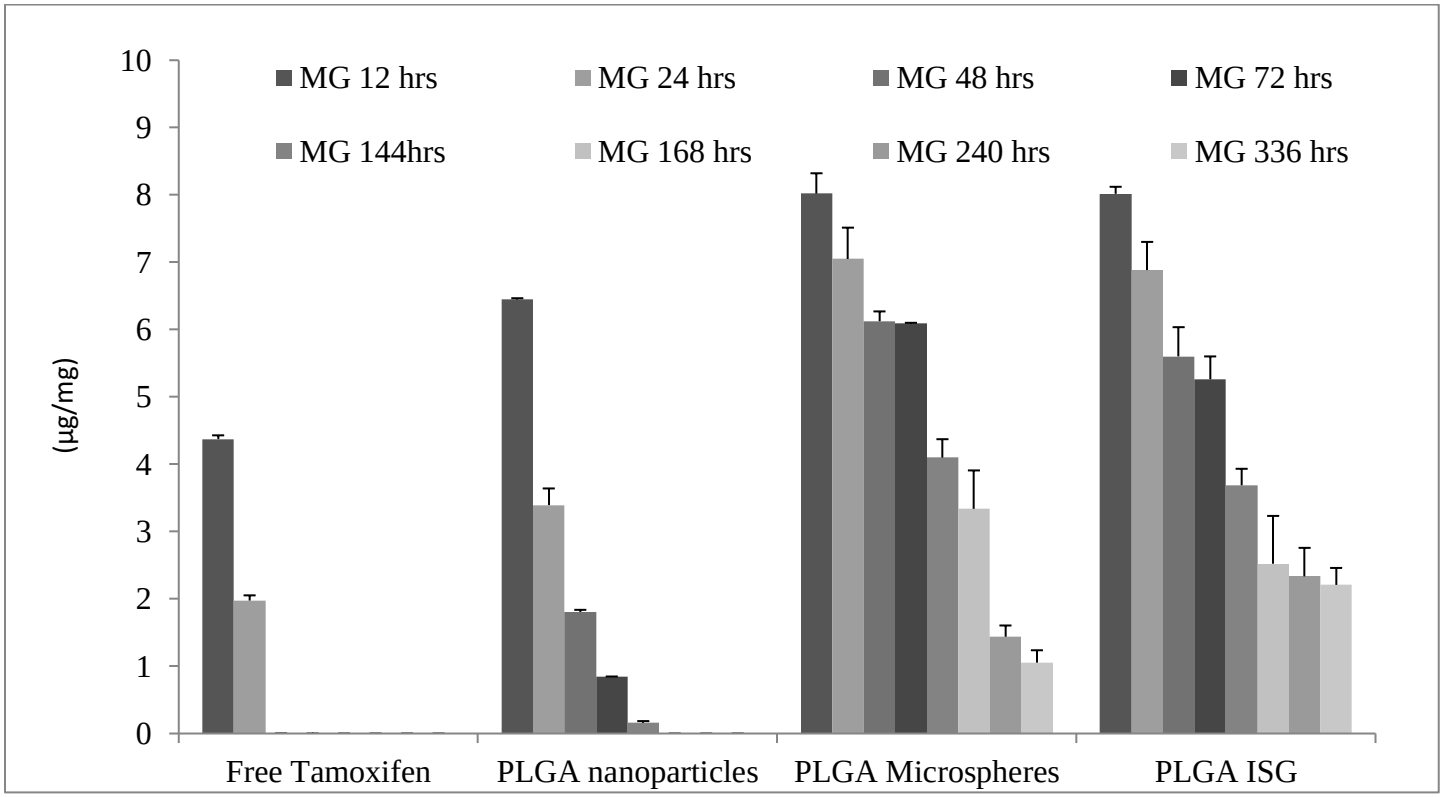

Figure 28: Concentration of tamoxifen in the mammary glands from 12-336 hours. ISG is in-situ gel. Each value is Mean ± SD, n=3. * is significant in comparison to free tamoxifen treatment group

Table 16: Pharmacokinetic parameters of tamoxifen in breast

	$t_{½}$ (hrs)	**k_e (hrs^{-1})**	**AUC (ng. hr/ml)**	**AUMC ($ng. hr^2/ml$)**	**MRT (hrs)**
Free TMX	14.87 ± 0.04	0.020 ± 0.0005	125355.4 ± 3692.96	3654696 ± 120023.3	26.5 ± 4.3
PLGA NP	28.61± 5.74	0.0105± 0.002 a	235444.4± 2744.84	9360274.65± 874274.5	39.7± 3.25
PLGA MS	204.80±17.33 ab	0.00125± 0.0003 ab	1493077.05± 33219.38 ab	325087882.4± 28461186 ab	217.55± 14.21ab
PLGA ISG	557.13± 52.93 abc	0.0007± 0.0003 ab	2916866.333±197615.3 abc	2116349830±354466261.3 abc	755±108.64 abc

$t_{½}$- plasma half-life; k_e - elimination rate constant; AUC – area under the curve; AUMC- area under the first moment curve; ; MRT- mean residence time. TMX- is tamoxifen; NP is nanoparticle; MS is microsphere; ISG is PLGA in-situ gel. a is significant to Free TMX, b is significant to PLGA NP, c is significant to PLGA MS by One-way Anova followed by Bonferroni post-hoc test

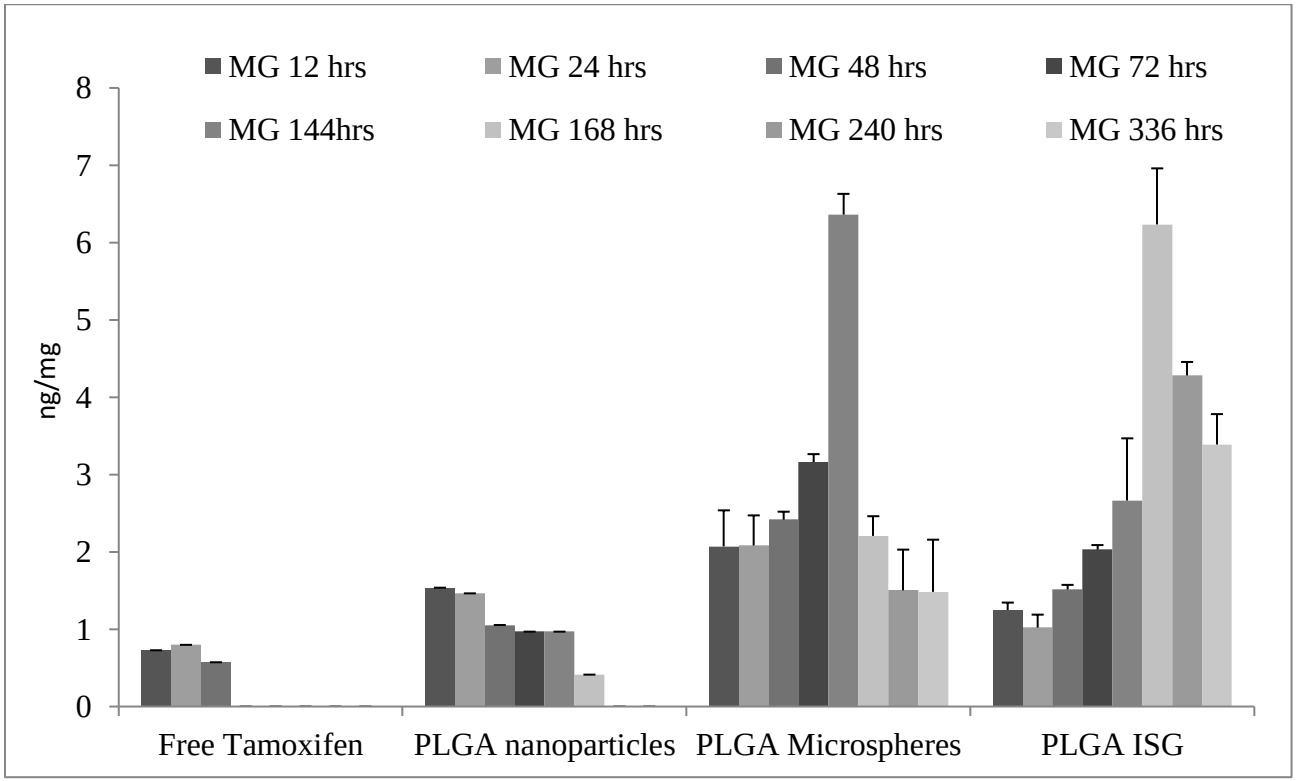

Figure 29: Concentration of 4-hydroxytamoxifen in the mammary glands from 12-336 hours. PLGA NP is nanoparticles; PLGA MS is microspheres; PLGA ISG is in situ gel. Each value is Mean ± SD, n=3. * is significant in comparison to Free tamoxifen treatment group by One-way Anova followed by Bonferroni post hoc analysis

Table 17: Pharmacokinetic parameters of 4-hydroxytamoxifen in breast

	$t_{½}$ (hrs)	**k_e (hrs^{-1})**	**AUC (ng. hr/ml)**	**AUMC ($ng. hr^2/ml$)**	**MRT (hrs)**
Free TMX	49.06 ± 12.37	0.0064±0.001	88.33±7.07	7689.96±1836.07	86.53±15.83
PLGA NP	59.12 ±23.84	0.005±0.002	365.15±171.19	61320.1±47356.5	154.5±57.27
PLGA MS	116.62±5.64 ^{a}	0.002^{a}	1118.35±214.04 ^{ab}	239585.9±18355.8 ^{ab}	216.6±25.03 ^{a}
PLGA ISG	319.34±29.35^{abc}	0.0009±0.0001 ^{a}	1959.73±840.76 ^{ab}	1365242.6±485313 ^{abc}	528.3±67.64 ^{abc}

$t_{½}$- plasma half-life; k_e - elimination rate constant; AUC – area under the curve; AUMC- area under the first moment curve; ; MRT- mean residence time. TMX- is tamoxifen; NP is nanoparticle; MS is microsphere; ISG is PLGA in-situ gel. a is significant to Free TMX, b is significant to PLGA NP, c is significant to PLGA MS by One-way Anova followed by Bonferroni post-hoc test.

2.3.5 Lymph node localization of PLGA formulations

Regional lymph nodes serve as the primary site for lymphatic drainage from the breast. Axillary mammary glands were treated with PLGA formulations to test the role of regional lymph nodes in the clearance of PLGA formulations from the breast. The regional lymph nodes were excised and analyzed for TMX and metabolites at time points 12, 48, 168 and 336 hours. Results showed that PLGA MS and NP drained to the lymph node and was retained for 336 hours and 48 hours respectively (Figure 30). At 12 hours, TMX was detected with the free TMX and PLGA ISG groups and the amounts were not significant, but no TMX was detected at later time points. At 12 hours, the amount of TMX at regional lymph nodes was 3-fold higher for PLGA NP and MS respectively compared to the free TMX. Based on the time points chosen for the present study, PLGA NP was retained for 48 hours and showed 12-fold higher levels at lymph nodes compared to free TMX. The TMX levels were highest for PLGA MS at 48 hours and this was 5-fold higher than PLGA NP at 12 hours. The results were in accordance with our observations in the previous chapter where PLGA MS and NP drained to the axillary lymph node. The presence of metabolites in the lymphatic system can possibly due to the recirculation metabolites from the plasma to the lymph nodes (Figures 31 and 32). [183] However, the levels of metabolites observed were much lower than TMX. Subcutaneous administration of carboplatin microspheres was found to sustain drug levels in the lymph nodes. [184]. In another study, a combination therapy of long acting injectable antiretroviral drugs was found to enhance drug levels in the lymph nodes. The particles are preferentially taken up by more permeable lymphatic capillaries and can be retained in the lymphatic vessels and transported throughout the lymphatic system. The microspheres (<10μm) from the breast are

predominantly phagocytosed and transported to the regional lymph nodes. Lymphatic capillaries play crucial role in uptake of particles (100-1000nm) through pinocytosis.[154] The transport mechanism also dictates the lymph node kinetics of microspheres and nanoparticles. Particles >200nm are exclusively transported to the lymph node by the dendritic cells.[155] Unlike microspheres nanoparticles are washed out much quicker from the lymph nodes. [155]

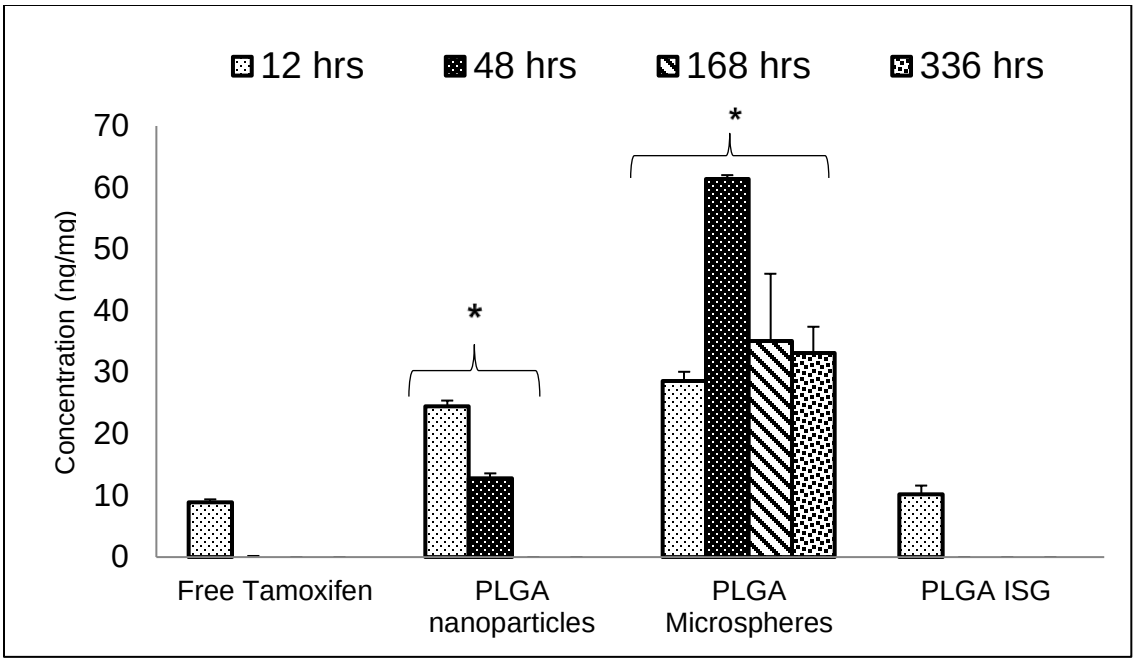

Figure 30: Lymph node concentration of Tamoxifen at different time points (12-336 hrs). Each Value is Mean ± SD, n=3. * is significant in comparison to free tamoxifen treatment group by One-way Anova followed by Bonferroni post hoc analysis. * indicates significance compared to free TMX.

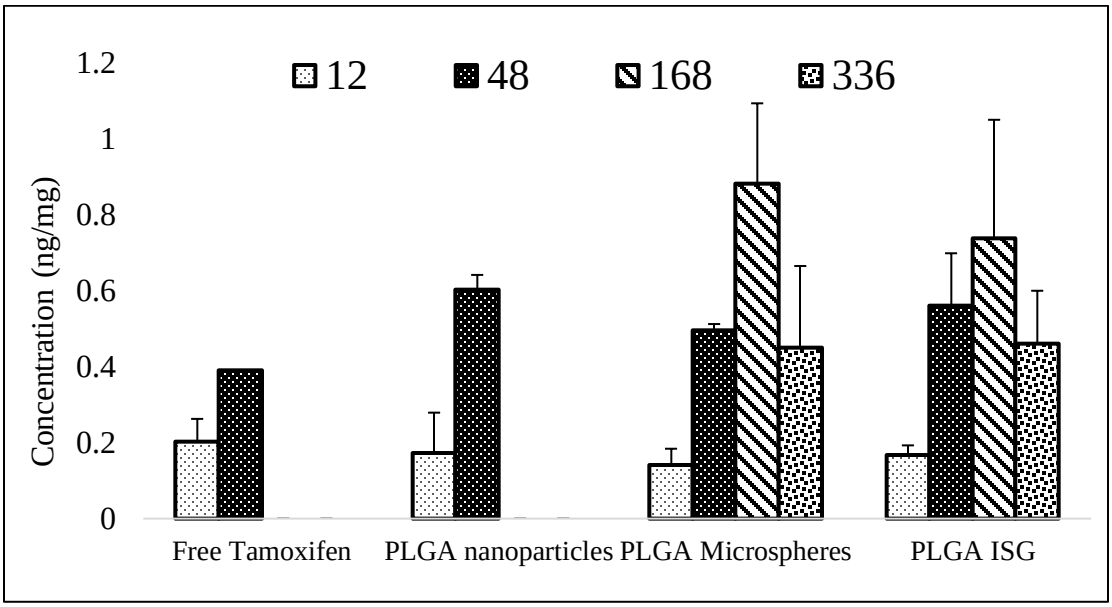

Figure 31: Lymph node concentration of Endoxifen at different time points (12-336 hrs).

Each Value is Mean ± SD, n=3

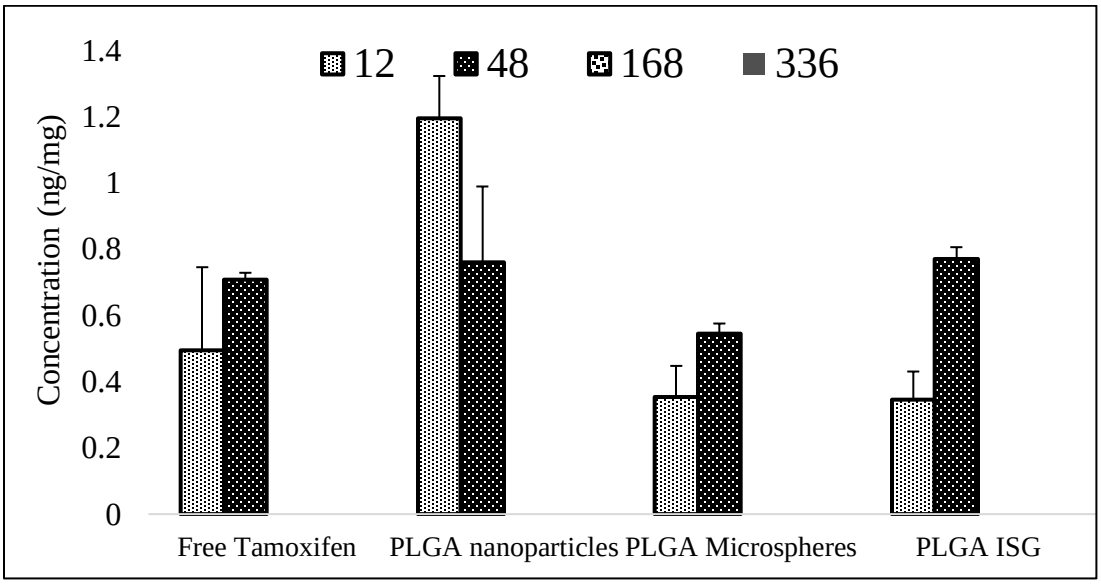

Figure 32: Lymph node concentration of 4-Hydroxytamoxifen at different time points (12-336 hrs).. Each Value is Mean ± SD, n=3

2.3.6 Systemic distribution

To determine the pharmacokinetics of intraductal TMX, the plasma levels of TMX, EDX and 4HT were measured from 0-14 days. The plasma level of TMX was lower compared to 4HT and EDX (Figure 33). Free TMX showed shorter $t_{1/2}$ of 19.51 ± 4.24 hrs for TMX and was significantly lower than PLGA MS and ISG (Table 18). Also, the C_{max} of TMX for free TMX was found to be 8.9 ± 1.55ng/ml which was significantly higher ($p<0.05$) than PLGA MS and PLGA ISG which was ~3-fold higher than PLGA MS and ISG (Table 18). These results suggest higher systemic exposure of free TMX compared to PLGA MS and ISG. The plasma $t_{1/2}$ of PLGA MS and ISG ~ 5- fold higher than free TMX which is due to the higher retention of TMX in the breast resulting in lower amounts of TMX reaching the systemic circulation. This was consistent with previous observations where subcutaneously administered tamoxifen loaded MS showed delayed $t_{1/2}$ with PLGA microspheres compared to subcutaneous TMX suspensions. [164] Moreover, the T_{max} for TMX was in the decreasing order PLGA ISG<PLGA MS<PLGA NP<free TMX (Table 18). The levels of TMX was sustained for 14 days with PLGA MS and ISG with significantly ($p<0.05$) higher MRT of 147.73 ± 59.28 and 230.2 ± 0.68 hrs for PLGA MS and ISG respectively.

The plasma levels of TMX and two major metabolites, EDX and 4HT were in the following rank order, TMX<4HT<EDX following intraductal administration of TMX. TMX is converted to metabolites predominantly by the CYP enzymes in the liver and the delayed $t_{1/2}$ of EDX (Table 20) and 4HT (Table 18) with PLGA MS and ISG suggests a slower

diffusion of TMX from the breast. PLGA NP showed higher plasma levels of 4HT and EDX compared to PLGA MS and ISG and was below detection limit after day 5 suggesting the lower amounts of TMX biotransformed to the metabolites. This was consistent with our observations in the breast levels of TMX where PLGA NP was retained only for 7 days with much lower levels than PLGA MS and ISG. EDX is the major metabolite of TMX[185] and in the present study TMX levels were found to be lower than metabolites which is consistent with previous findings. [186] It is not very well understood whether the endoxifen concentrations accounts for toxicity or treatment outcome in patients taking tamoxifen. [181] In comparison to free TMX, PLGA MS and ISG showed minimal systemic distribution of TMX and metabolite with highest levels found in the liver. The levels of TMX, EDX and 4HT remained undetectable in the uterus for rats treated with PLGA MS and PLGA ISG.

The TMX metabolic profile in rats resembles to that of humans. [187] However, some differences have been reported in the metabolic profile of rats and humans. In biodistribution studies, rat tissues showed equal or higher level of 4HT than endoxifen, whereas the levels of endoxifen were found to be the most abundant in human tissues. The apparent volume of distribution for tamoxifen is about 50-60 liters/kg in humans suggesting extensive tissue binding of tamoxifen [177]. In another study, the plasma levels of tamoxifen and its two metabolites (N- desmethyl tamoxifen and 4-hydroxytamoxifen) was studied in rat and mouse models in an effort to correlate the levels to human subjects [186]. This study showed that rats showed similar trends of TMX metabolism and tissue levels compared to humans. Also, the plasma level of 4HT was comparatively lower than EDX due to the less dominant 4-hydroxylation pathway in rats. The elimination $t_{1/2}$ of tamoxifen,

N-desmethyltamoxifen and 4-hydroxytamoxifen in rats following a single oral dose was found to be 10.3, 12.1 and 17.2 hrs respectively.

In another study[164], tamoxifen loaded PLGA microspheres of varying hydrophobicity's were administered subcutaneously in rats with similar levels observed as the present study. The plasma levels of tamoxifen and 4-hydroxytamoxifen was determined after a single subcutaneous dose of 11mg/kg tamoxifen. For the most hydrophilic system (PLGA 50/50 microspheres), the maximum concentration of tamoxifen was obtained within 8 hours reaching levels of 17.1 ng/ml and 4 hydroxy tamoxifen reaching maximum levels of 6.7 ng/ml at 11 hours. For PLGA 50/50 and 75/25 microspheres, the plasma levels of tamoxifen and 4 hydroxy tamoxifen were 36.14 and 8.5 ng/ml respectively but took longer time to reach them (23.5 and 215 hours respectively). When tamoxifen in solution was administered subcutaneously, TMX and 4HT levels were higher (40ng/ml at 8 hours and 24.69 ng/ml at 48 hours respectively). However, on day 4, the presence of tamoxifen and 4HT in plasma decreased and drug was not detected.

The therapeutic levels of 4HT and EDX observed in breast cancer patients taking tamoxifen (20 mg) are found to be in the range of 0.38 - 6.97 ng/ml and 2.98 - 28.05 ng/ml respectively. [182] Taken together, results show that therapeutic levels of TMX were maintained in the breast tissue but not in the plasma. However, EDX and 4HT maintained therapeutic levels in the plasma for PLGA ISG and MS.

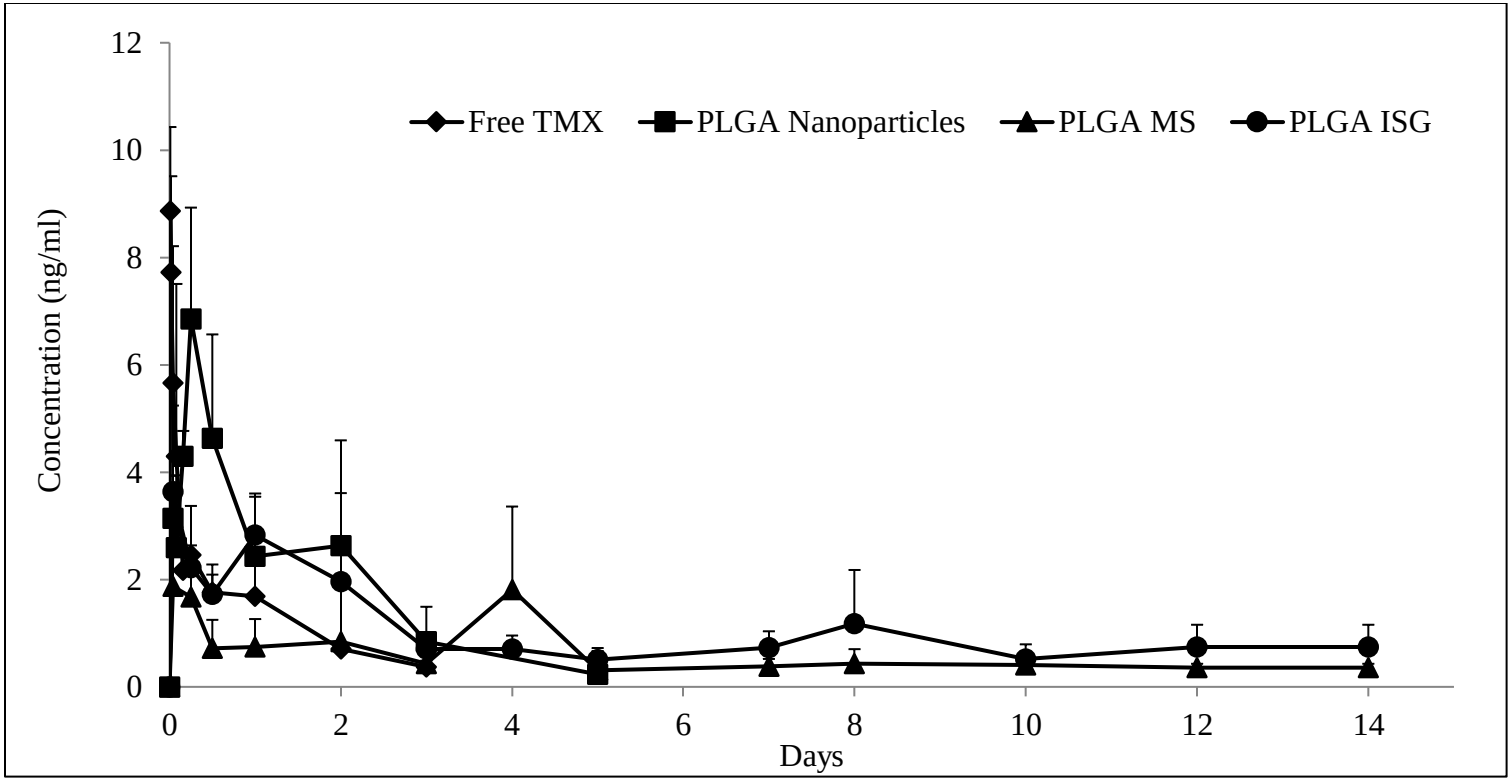

Figure 33: Plasma profile of tamoxifen after intraductal injection of formulations. The plasma concentration was measured for 3 days for free tamoxifen, 5 days for PLGA nanoparticles and 14 days for PLGA microspheres (MS) and in situ gel. ISG is in situ gel. ISG is in-situ gel. Each value is Mean ± SD, n=3

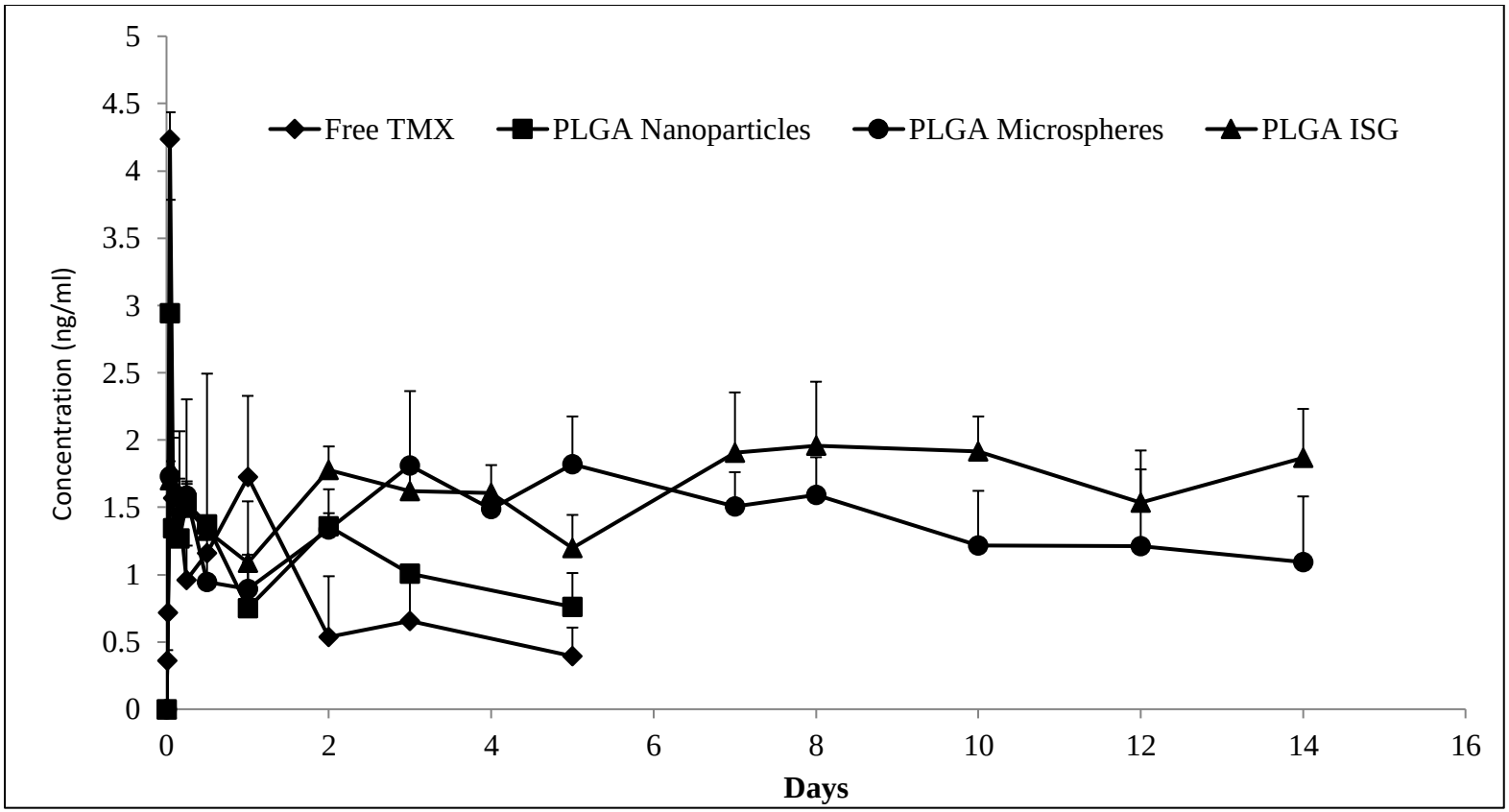

Figure 34: Plasma profile of 4-hydroxytamoxifen after intraductal injection of PLGA formulations. The plasma concentration was measured for 5 days for free tamoxifen, 5 days for PLGA nanoparticles and 14 days for PLGA microspheres and in situ gel. ISG is in situ gel. ISG is in situ gel. Each value is Mean ± SD, n=3. * Significant in comparison to free Tamoxifen ($p<0.05$) by One-way ANOVA followed by Bonferroni post hoc analysis

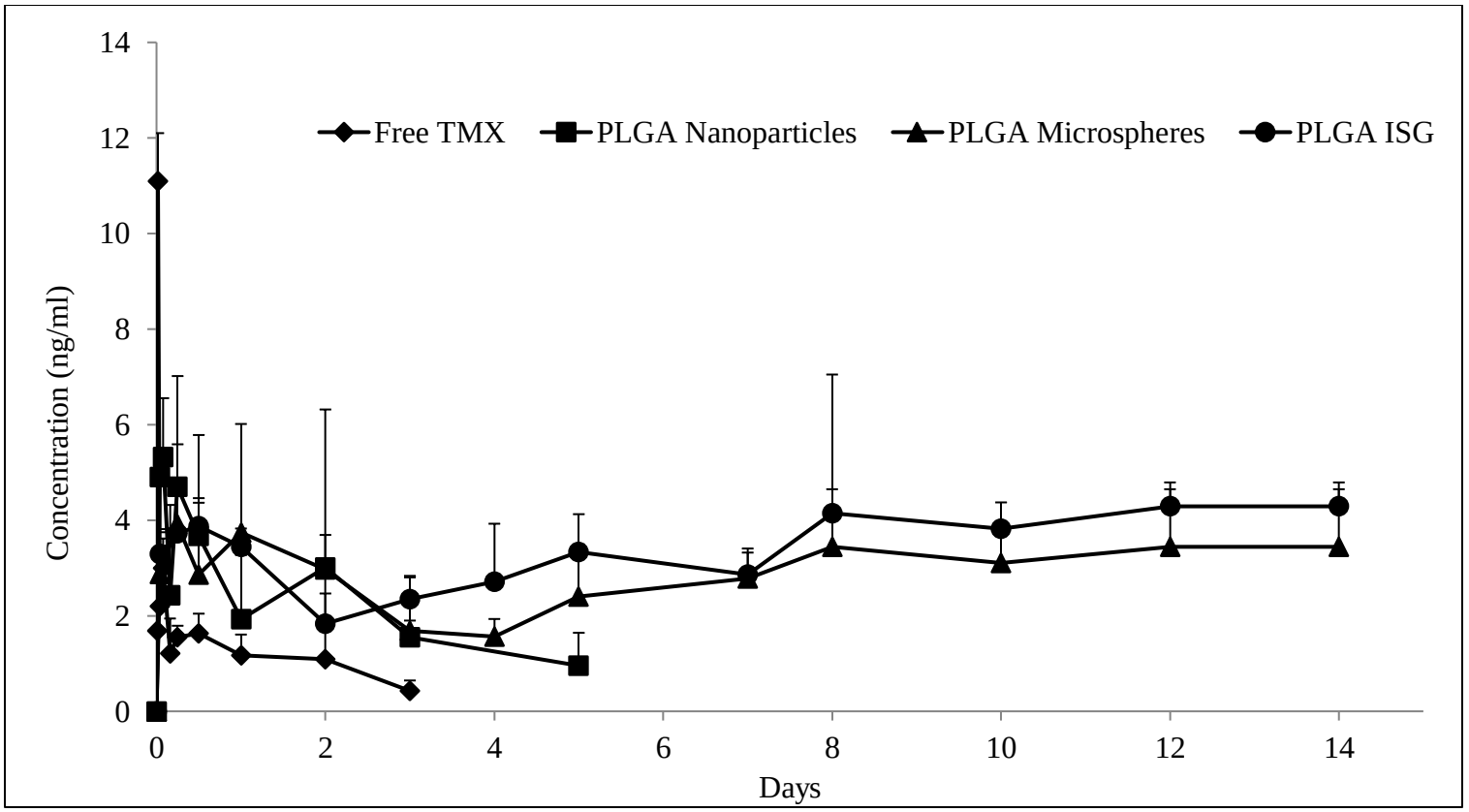

Figure 35: Plasma profile of Endoxifen after intraductal injection of PLGA formulations. The plasma concentration was measured for 3 days for free tamoxifen, 5 days for PLGA nanoparticles and 14 days for PLGA microspheres and in situ gel. ISG is in situ gel. Each Value is Mean ± SD, n=3.

Table 18: Pharmacokinetic parameters of tamoxifen in plasma

	C_{max} (ng/ml)	**T_{max} (hrs)**	**k_e (hrs^{-1})**	**$t_{½}$ (hrs)**	**AUC (ng. hr/ml)**	**AUMC ($ng.\ hr^2/ml$)**	**MRT (hrs)**
Free TMX	8.9 ± 1.55	0.3	0.015 ± 0.002	19.51 ± 4.24	115.8 ± 43.31	4546.37 ± 466.103	38.6 ± 13.10
PLGA NP	6.9 ± 2.1	8 ± 3.4 a	0.0066 ± 0.003 a	56.75 ± 35.33	260.9 ± 35.41	1 * 5.2 ± 466.10	47.7 ± 3.15
PLGA MS	2.9 ± 0.72 ab	72 ab	0.0033 ± 0.0009 a	92.89 ± 26.08 a	211.23 ± 89.43 a	34635.5 ± 25952.3	147.73 ± 59.28 ab
PLGA ISG	3.63 ± 0.15 a	80 ±27.71 ab	0.0028 ±0.0007 a	110.75 ± 31.15 a	575.96 ± 88.14 abc	136427 ± 76773.6 ab	230.2 ± 0.68 ab

$t_{½}$- plasma half-life; k_e - elimination rate constant; C_{max} – peak plasma concentration; T_{max}- time to reach peak plasma concentration; AUC – area under the curve; AUMC- area under the first moment curve; ; MRT- mean residence time. TMX- is tamoxifen; NP is nanoparticle; MS is microsphere; ISG is PLGA in-situ gel. a is significant to Free TMX, b is significant to PLGA NP, c is significant to PLGA MS by One-way Anova followed by Bonferroni post-hoc test.

Table 19: Pharmacokinetic parameters of 4-hydroxytamoxifen in plasma

	C_{max} (ng/ml)	**T_{max} (hrs)**	**k_e (hrs^{-1})**	**$t_{½}$ (hrs)**	**k_e (hrs^{-1})**	**AUC (ng. hr/ml)**	**AUMC (ng. hr^2/ml)**	**MRT (hrs)**
Free TMX	4.2 ± 0.115	1	0.0204 ± 0.011	33.16 ± 20.20	0.0204 ± 0.011	92.56 ± 19.45	4153.8 ± 1094.60	43.56 ± 3.19
Nanoparticles	3.1 ± 0.36 a	4.6 ± 3.6	0.0077 ± 0.0003	38.51 ± 1.83	0.0077 ± 0.0003	168.1 ± 1.80 a	14150.3 ± 1373.2	84.03 ± 7.39
Microspheres	2.36 ± 0.26 ab	112 ± 42.33	0.002 ± 0.0004	157.11 ± 26.29 ab	0.002 ± 0.0004	679.2 ± 169.94 ab	188094.86 ± 77107.74	252.03 ± 49.79 ab
ISG	2.36 ± 0.17 ab	224 ± 42.33 ab	0.0037 ± 0.0011	94.27 ± 23.52	0.0037 ± 0.0011	813.06 ± 97.36 ab	220136.53 ± 52211.86 a	264.66 ± 32.21 ab

$t_{½}$- plasma half-life; k_e - elimination rate constant; C_{max} – peak plasma concentration; T_{max}- time to reach peak plasma concentration; AUC – area under the curve; AUMC- area under the first moment curve; ; MRT- mean residence time. TMX- is tamoxifen; NP is nanoparticle; MS is microsphere; ISG is PLGA in-situ gel. a is significant to Free TMX, b is significant to PLGA NP, c is significant to PLGA MS by One-way Anova followed by Bonferroni post-hoc test

Table 20: Pharmacokinetic parameters of endoxifen in plasma

	C_{max} (ng/ml)	**T_{max} (hrs)**	**k_e (hrs^{-1})**	**$t_{½}$ (hrs)**	**AUC (ng. hr/ml)**	**AUMC ($ng. hr^2/ml$)**	**MRT (hrs)**
Free TMX	11.1 ± 1	2	0.0142 ± 0.0127	34.19 ± 25.42	174.26 ± 19.38	8312.83 ± 2050.43	46.4 ± 5.95
Nanoparticles	4.76 ± 0.26 a	1	0.0083 ± 0.0012	37.92 ± 6.43	219.5 ± 22.3	9967 ± 1628.2	44.9 ± 2.6
Microspheres	5 ± 1.10 a	2.33 ± 0.88	0.0013 ± 0.0003	247.27 ± 90.59	2177.63 ± 580.41 ab	1155923.16 ± 594100.43	472.56 ± 124.02 ab
ISG	5.36 ± 1.10 a	2	0.0013 ± 0.0003	292.30 ± 112.05	3125.06 ± 1050.41 ab	2279641.4 ± 1447487.3	592.93 ± 205.86 ab

$t_{½}$- plasma half-life; k_e - elimination rate constant; C_{max} – peak plasma concentration; T_{max}- time to reach peak plasma concentration; AUC – area under the curve; AUMC- area under the first moment curve; ; MRT- mean residence time. TMX- is tamoxifen; NP is nanoparticle; MS is microsphere; ISG is PLGA in-situ gel. a is significant to Free TMX, b is significant to PLGA NP, c is significant to PLGA MS by One-way Anova followed by Bonferroni post-hoc test.

2.3.7 Organ distribution of TMX

To determine the biodistribution of PLGA formulations, the organs were collected at the end of the study and the concentrations of TMX, 4HT and EDX were determined. Free TMX showed significantly higher systemic exposure of TMX compared PLGA MS and ISG (Figure 36). PLGA MS and ISG showed significantly ($p<0.05$) lower systemic exposure of TMX in all organs compared to free TMX. The levels of TMX in the liver and uterus for free TMX was ~10 fold and 3-fold higher compared to PLGA MS and ISG. PLGA NP showed higher systemic TMX levels than PLGA MS and ISG with higher drug levels present in the lungs and liver.

The organ distribution of EDX was significantly lower for PLGA MS and ISG compared to free TMX (Figure 37). EDX levels were ~3 fold lower with PLGA MS and ISG compared to free TMX. The higher levels of EDX can be due to the relatively higher circulating levels of EDX in the plasma. EDX was found in the highest level in all the organs (Figure 37). The systemic exposure of 4HT was found to be lower than EDX with higher levels present in the liver were higher than TMX (Figure 38). The 4HT organ distribution with the free TMX group was significantly different ($p<0.05$) compared to PLGA MS and ISG. Both the metabolites remained undetectable in the uterus for PLGA MS and ISG while free TMX showed ~6 fold and ~3-fold higher levels of EDX and 4HT with free TMX.

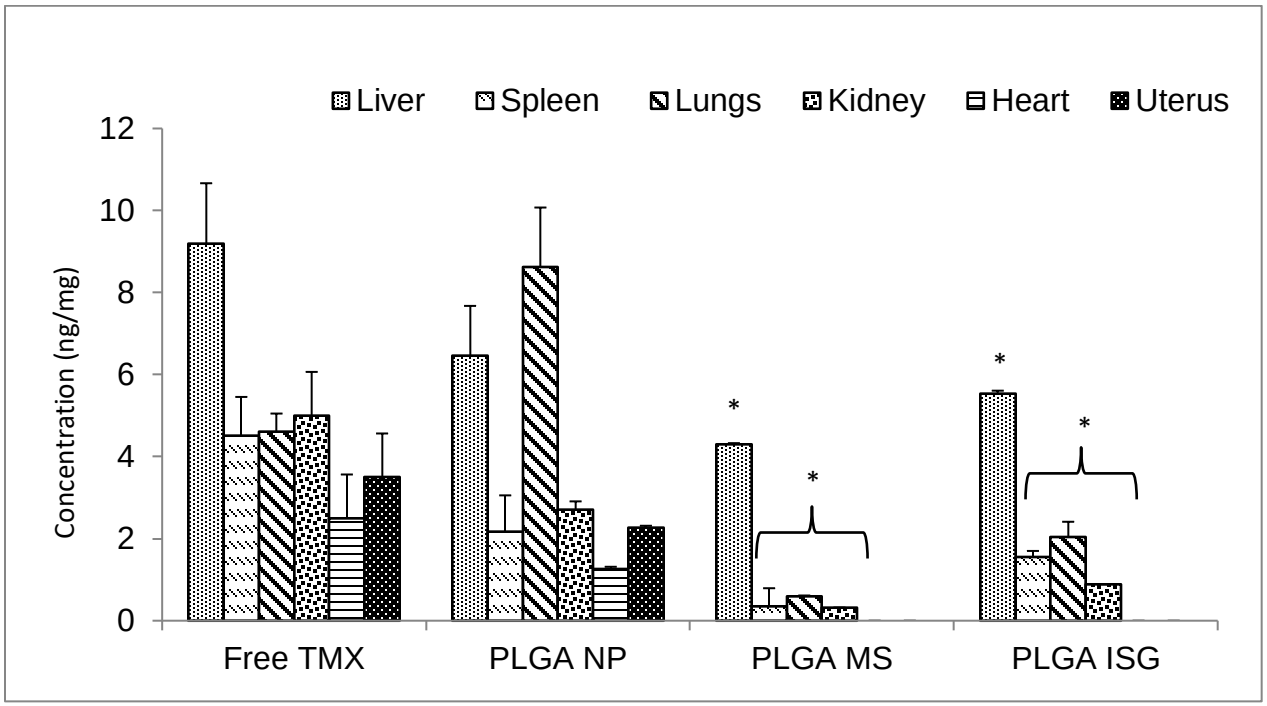

Figure 36: Biodistribution of tamoxifen after intraductal administration of PLGA formulations. Each value is Mean ± SD, n=3. * is significant compared to free TMX

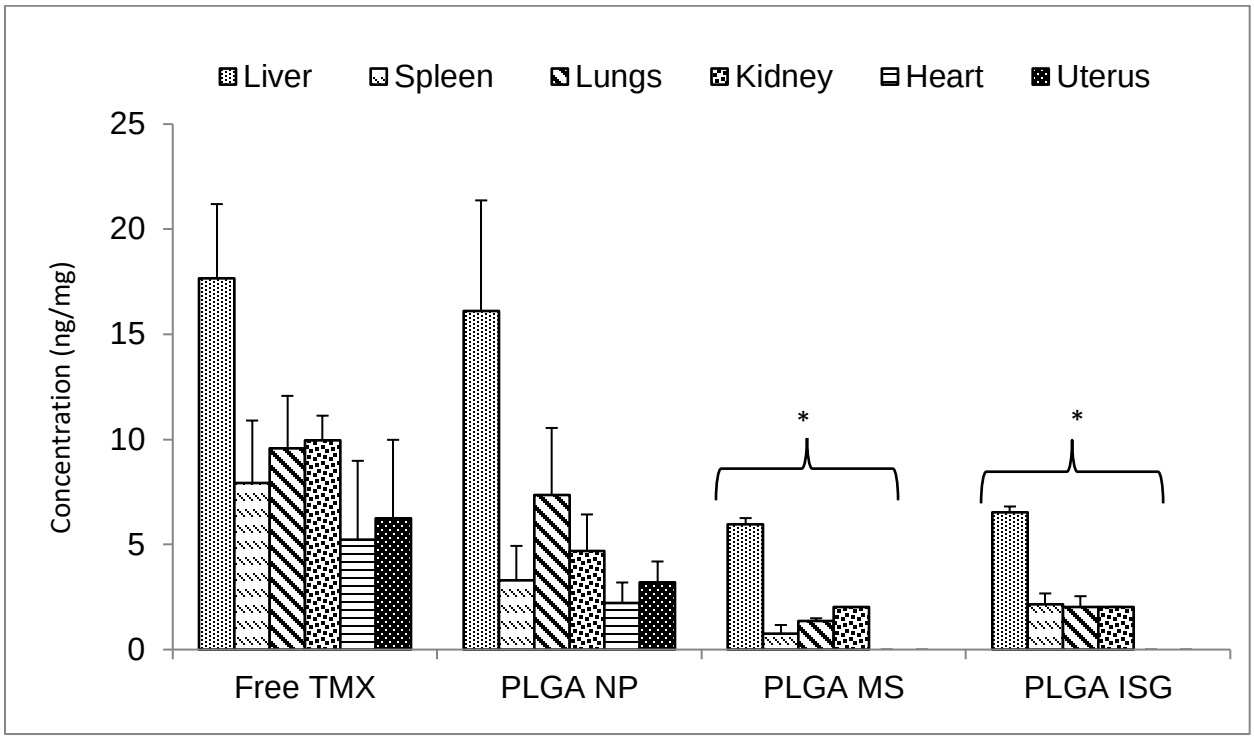

Figure 37: Biodistribution of endoxifen after Intraductal administration of PLGA formulations. Data is Mean ± SD, n=3.* is significant in comparison to free TMX.

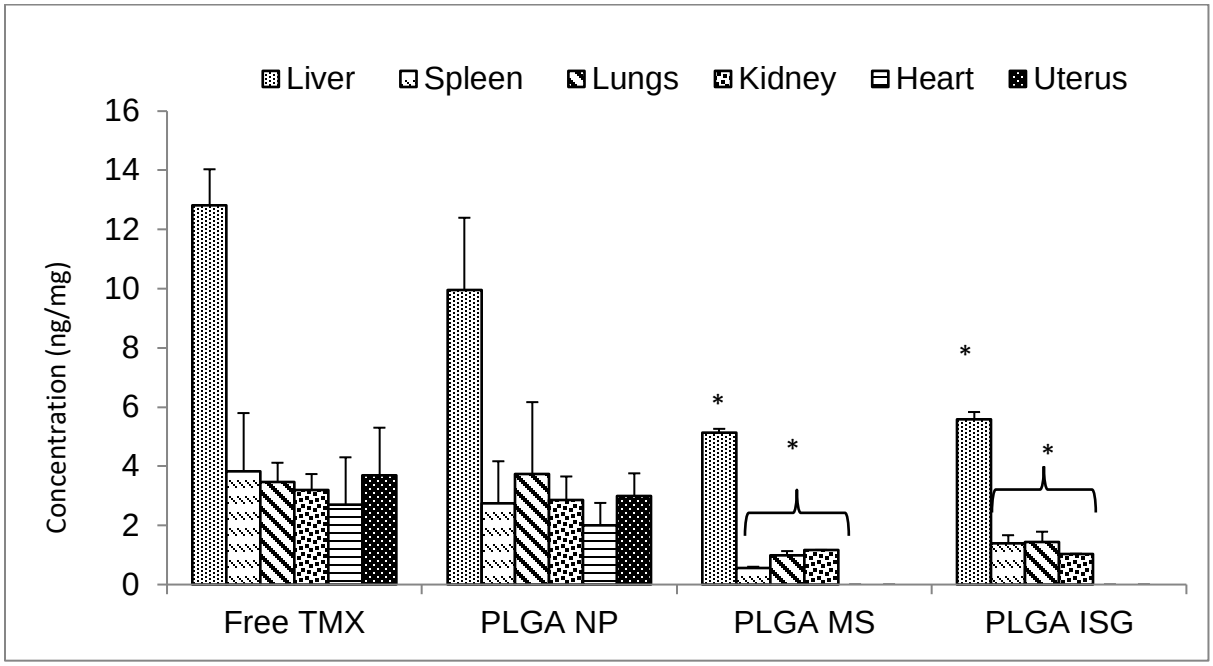

Figure 38: Biodistribution of 4-hydroxytamoxifen after Intraductal administration of PLGA formulations. Each value is Mean ± SD, n=3. * is significant compared to free TMX.

2.4 Conclusions

Tamoxifen (TMX) loaded PLGA microspheres (MS) were formulated with particle size 9.12 ± 3.77 μm with loading and encapsulation efficiencies of 10.22 ± 0.12% and 95.35 ± 2.01% respectively. This formulation sustained TMX release for ~3 weeks. PLGA nanoparticles were formulated with loading and encapsulation efficiencies 6.19±0.17 and 91.28±2.17% respectively. The optimized formulations sustained TMX release for ~2 weeks. 25 wt% PLGA in situ gel with polymer blends resulted in low viscous (25cP) formulations and sustained TMX release for ~3 weeks. PLGA MS and ISG were retained in the mammary glands for 2 weeks and showed >200-fold higher $t_{½}$ compared to free TMX. The levels of TMX in the mammary gland were maintained above the therapeutic levels of TMX for 2 weeks. PLGA MS and ISG generated 4-hydroxytamoxifen in the mammary glands at levels above the therapeutic levels of 4HT for 2 weeks. PLGA MS and ISG showed lower TMX levels in the plasma (<5ng/ml) for 2 weeks. The systemic exposure of free TMX was significantly higher with TMX, EDX and 4HT compared to PLGA MS and ISG. PLGA MS and NP was transported to the regional lymph nodes and was retained for 2 and 14 days respectively with levels significantly higher ($p<0.05$) than Free TMX. Taken together, PLGA MS and ISG formulations enhanced TMX and 4HT retention in the mammary glands for 2 weeks. These formulations resulted in lower systemic exposure and PLGA MS and NP can potentially target regional lymph nodes.

A summary of the findings from this chapter is depicted below.

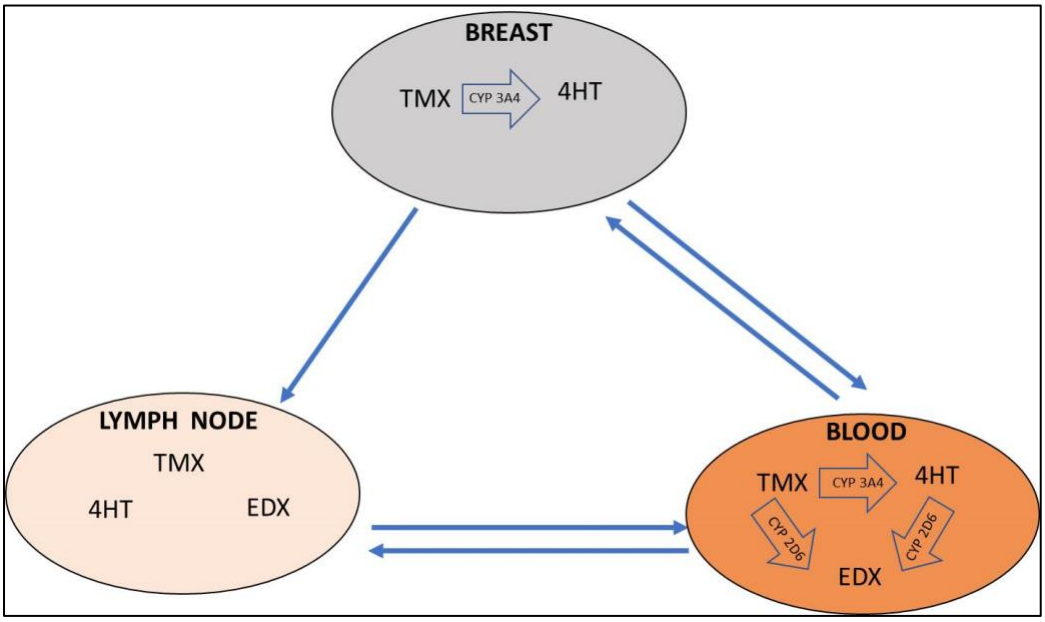

Figure 39: Summary of findings from this chapter

CHAPTER 3

INTRADUCTAL FORMULATIONS OF 4-HYDROXYTAMOXIFEN

3.1. BACKGROUND

For more than 25 years, TMX has been the gold standard for endocrine treatment for all cases of estrogen receptor (ER) positive breast cancer. TMX is also the first SERM that has been successfully used in the clinic to prevent and treat breast cancer. [159] TMX is a prodrug which is extensively metabolized by cytochrome P450 enzymes to form metabolites with higher potencies towards estrogen receptors. 4HT is formed by 4-hydroxylation of tamoxifen requires CYP3A4 for its metabolic conversion. [188] It is reported to have 100-fold more affinity towards ER and 30-100 fold more potent than TMX in suppressing estrogen dependent cell proliferation. [176] EDX is another major metabolite of TMX which has higher potency than the parent compound. [181]

Sukumar et al [109] , investigated chemopreventive effects of intraductal TMX in estrogen receptor–positive, MNU-induced rat mammary tumor model. Intraductal TMX did not show any chemopreventive effect as the metabolic conversion relied mainly on the CYP enzymes in the liver. [189] However, results from the previous chapter suggest that increased drug retention time in the mammary gland will likely have an effect on metabolic conversion of prodrugs like TMX in the breast. The study reports rapid diffusion of small molecules out of the ducts and hence the chemopreventive effects of 4HT might be limited because of poor drug retention in the mammary glands. CYP450 is a key enzyme for metabolic activation of TMX and genetic polymorphism of CYP enzymes influences the plasma concentrations of metabolites and clinical outcomes of patients treated with TMX. [188] Intraductal 4HT further offers the advantage of treating patients who are susceptible to genetic polymorphisms of CYP enzymes. Taken together, the main goal of the study is to develop long-acting formulations of 4HT and study *in vivo* biodistribution.

Based our results from the previous chapter, PLGA MS and ISG were retained in the mammary glands for 14 days. However, PLGA ISG showed signs of local inflammation, likely from the organic solvent (NMP). Therefore, our goal was to develop an aqueous gel to address this issue. Thermoresponsive *in situ* hydrogels are attractive options for long term release of drugs. [190, 191] These are liquid at room temperature and forms a gel at the body temperature[192].

PLGA-PEG-PLGA is an ABA-type triblock copolymer and is the most widely studied thermosensitive gel because of its biodegradable and nontoxic properties. [193] However, for prolonged release, PLGA block is replaced with poly lactic acid (PLA), poly (e-caprolactone) (PCL) and poly (e-caprolactone-co-lactide) (PCLA) blocks. The degradation times for PCLA-PEG-PCLA is much slower than PLGA-PEG-PLGA. Also, the use of CL (e-caprolactone) instead of LA could reduce the effect of acidic degradation products that can arise from using PLA alone. [193-195] In our previous study with TMX, MS and ISG alone sustained drug release for ~2 weeks. In the present study, the goal was to further prolong the retention of 4HT in the mammary gland. The combination of micro or nanocarriers in thermosensitive hydrogels have been reported to further sustain drug release.[196-198] Hence, we chose a combinatorial approach of dispersing PLGA MS in PCLA-PEG-PCLA thermogel to extend the drug release and retention.

The specific aims of the study are:

i) To develop 4HT loaded PLGA microspheres in PCLA-PEG-PCLA thermogel

ii) Determine the pharmacokinetics of 4HT MS in gel (MSG) in rats

3.2. Materials and Methods

PCLA-PEG-PCLA (1700-1500-1700) were purchased from Akina, Inc. (West Lafayette, IN). All the other chemicals were similar to chapters 1 and 2.

3.2.1. Formulation of PLGA microspheres

Microspheres were formulated as described previously in sections 1.2.2.1 and 2.2.1 using 50 mg 4-hydroxytamoxifen.

3.2.2. Determination of encapsulation and loading efficiency

The encapsulation and loading efficiencies were determined as described previously in section 2.2.5.

3.2.3. Formulation of PLGA microspheres in PCLA-PEG-PCLA thermogel

To make the thermogel, the PCLA-PEG-PCLA (1700-1500-1700) was weighed and added to ultrapure DI water to attain a final concentration of 25 % w/v. [191] The solution was stirred for 24 hours at 2-8 ºC. PLGA microspheres were dispersed into PCLA-PEG-PCLA by gentle vortex mixing for 5-10 seconds. Different weight ratios of thermogel and MS were tested for optimal gelling at 37°C. Optimized PLGA microspheres (mg): PCLA: PEG: PCLA (mg) ratio: 1:10 w/w. Vial tilt method[199] was used to confirm the gelling of the polymer at 37ºC. The formulations were transferred to a glass vial and were incubated at 37°C for 10 minutes. Gelling was confirmed if there was no flow of the formulation after inverting the tube for 60 seconds.

3.2.4. *In vitro* release study

PLGA microspheres containing 300 µg 4HT were dispersed in 25% w/v PCLA-PEG-PCLA thermogel at 1:10 % w/w ratio into a 2 ml Eppendorf tube. The formulation was

gently vortexed for 5-10 seconds to disperse the microspheres in thermogel. The formulation was incubated at 37°C for 10 minutes and allowed to gel. Afterwards, 2 ml of pre-warmed release medium (PBS, pH 7.4 containing 0.05 % w/v SDS) was gently added on top of the gel. The tube was placed in an incubator shaker (50 rpm) and 1.8ml of release medium was drawn at each time points and replaced with fresh release medium to maintain sink conditions. The supernatant was then analyzed using HPLC as described in section 2.2.6.

For thermogel alone, 4HT was dissolved in methanol and 300µg of 4HT was added to the thermogel and the release study was performed as described earlier. For PLGA microspheres, microspheres containing 300 µg of 4HT was dispersed in 2 ml release medium (PBS, pH 7.4 containing 0.05 % w/v SDS). At each time point, the tubes were centrifuged at 10,000 rpm for 10 minutes. The supernatant (1.8 ml) was collected and replaced with fresh release medium to maintain sink conditions. The drug concentration was determined using HPLC at γ_{max} 243nm as described in section 2.2.4.

3.2.5. *In vivo* studies

In vivo studies were performed as described previously in section 2.2.7. For pharmacokinetic studies, Female Sprague Dawley rats 4-6 weeks old, 150-200 g were used for the study. 4HT formulations were injected (300µg x 2 teat) into inguinal mammary glands for breast retention studies and into the axillary mammary glands (n=3) for lymph node localization studies. All the animal studies were performed after getting approval from the IACUC at South Dakota State University.

3.2.6. Sampling and tissue preparation

The sampling and tissue preparations were performed using the same methodology as described previously in section 2.2.8.

3.2.7. LC-MS

LCMS method using gradient elution was the same as described previously in section 2.2.9

3.3. RESULTS AND DISCUSSION

3.3.1. Preparation and characterization of formulations

In the present study we chose PLGA of molecular weight 75-85KDa and used homogenization to formulate microspheres of particle size 9.63 ±1.49 µm (Table 21). This formulation resulted in microspheres with spherical morphology (Figure 40), higher drug content (10.46 ± 0.38 %) and encapsulation efficiency (92.46 ± 2.59).This is consistent with previous findings in which a highly lipophilic drug like 4HT (Log P = 6) tends to show higher entrapment in hydrophobic PLGA matrix.[97, 200] PCLA-PEG-PCLA thermogel was chosen as the gel matrix to disperse PLGA MS owing to its slower degradation and ability to sustain drug release.

In the present study, we chose a biodegradable, thermoreversible triblock copolymer poly (ε-caprolactone-co-lactide)-b-poly (ethylene glycol)-b-poly (ε-caprolactone-co-lactide) (PCLA–PEG–PCLA) as month long release profile was preferred. [199] The concentration of PCLA-PEG-PCLA thermogel was 25% w/v. Moreover, thermogel chosen for this study offer the benefit of lower viscosity in their sol state with slower degradation rates. [201] This is critical for intraductal injections where a lower viscosity with sustained release profile is preferred. Several ratios were tried to optimize the amount of 4HT loaded MS that can be dispersed in thermogel (data not shown). Optimized ratio of 4HT loaded MS and PCLA-PEG-PCLA was determined to be 1:10 w/w. Vial tilting method[199] was performed to visually characterize the sol to gel transition after incubation at 37 ºC for 10 minutes. The image (Figure 41) shows the sol to gel transition of MSG after incubation of the formulation for 10 minutes at 37 ºC.

Table: 21. Formulation characteristics of 4HT loaded PLGA microspheres

Formulation	Particle size (µm)	Encapsulation Efficiency (%)	Loading Efficiency (%)
PLGA Microspheres (LA:GA-75:25), Mw – 75-85KDa	9.63 ± 1.49	92.46 ± 2.59	10.46 ± 0.38

PLGA is poly (lactic-co-glycolic acid), LA is lactic acid, GA is Glycolic acid, Mw is molecular weight. Each value represents Mean ± S.D, n=3.

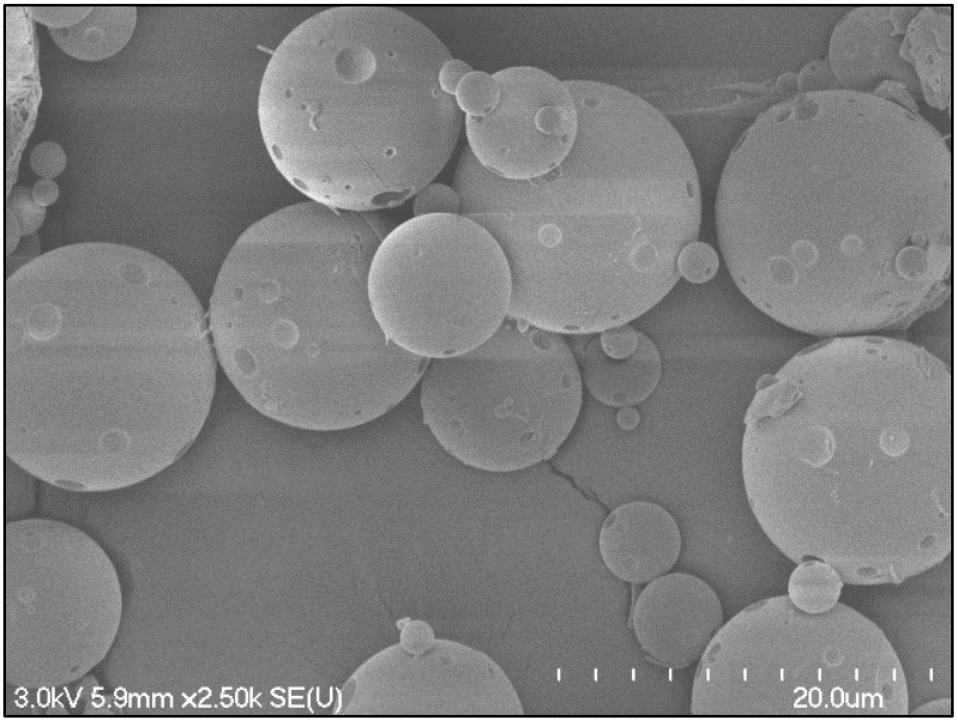

Figure 40: Scanning electron microscopy image of 4HT loaded PLGA microspheres

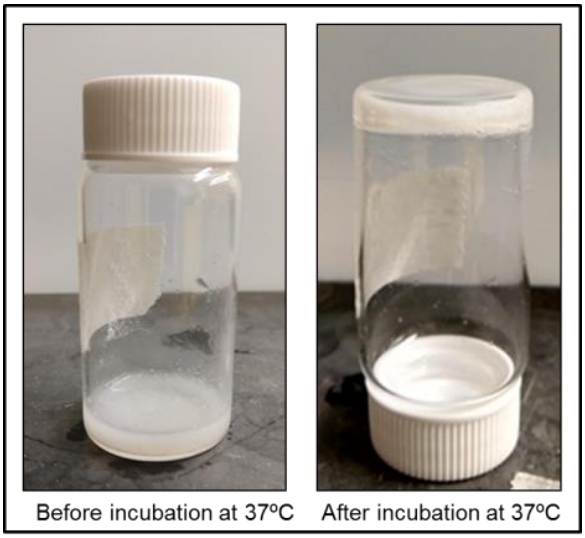

Figure 41: PLGA microspheres dispersed in PCLA-PEG-PCLA thermogel before (left))and after (right) incubation at 37°C.

3.3.2 *In vitro* release

The PLGA MS and thermogel released 4HT for ~ 3 weeks. On the other hand, MSG sustained 4HT release >4 weeks (Figure 42). PLGA MS showed a highest burst release resulting in ~ 30% of 4HT released in 48 hours. Thermogel showed lower burst release (~16 %) compared to MS alone. MSG showed the lowest burst release of 4HT and resulted in ~ 4 fold reduction compared to PLGA MS alone and ~ 2 -fold reduction compared to thermogel (Figure 42). The MSG sustained 4HT release for >30 days. Similar observations were made previously where microspheres when combined with thermogel system resulted in drug release of >30 days. [191] Microspheres dispersed in thermogel provides a dual barrier long-acting formulation. [196-198] and sustained drug release longer than MS or thermogel alone. MSG formulation was chosen for in vivo studies.

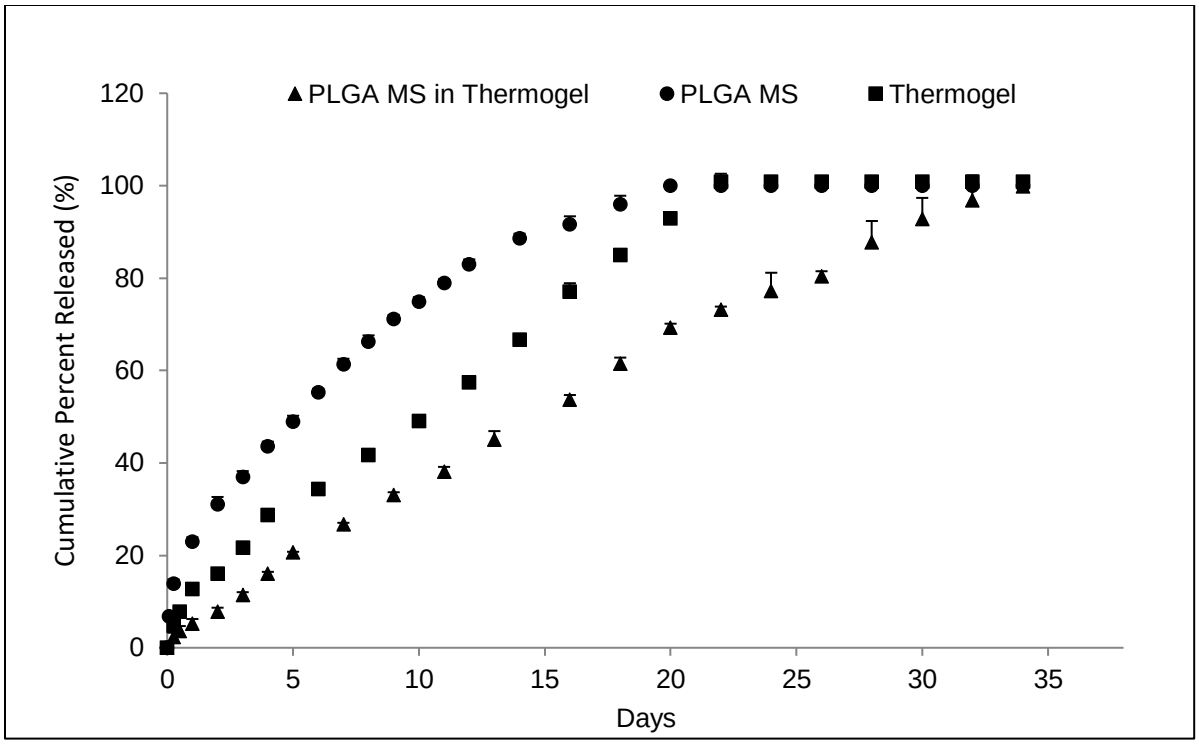

Figure 42: In vitro release profile of 4-hydroxy tamoxifen from PLGA microspheres, Thermogel is PLGA microspheres dispersed in PCLA-PEG-PCLA thermogel; MS is microspheres; PLGA is poly (lactic-co-glycolic acid). Data is Mean ± SD, n=3

3.3.3. Pharmacokinetics and *in vivo* biodistribution

To study the pharmacokinetics, MSG and free 4HT in corn oil was injected into two mammary glands (300 µg per teat x 2 teats) and the concentrations of 4HT and EDX were measured from 0-14 days. The duration study was consistent with previous study with TMX. The axillary mammary glands were chosen to study the lymph node localization of 4HT.

MSG sustained plasma levels for both 4HT and EDX for 14 days, while no 4HT or EDX was detected with free 4HT after days 7 and 9 respectively (Figures 43, 44). For free 4HT, the plasma $t_{½}$ was 31.83 ± 8.08 hrs and this was significantly shorter ($p<0.05$) than MSG (104.12 ± 18.30 hrs). The elimination rate constant (k_e) for MSG was also significantly ($p<0.05$) lower in comparison to free 4HT (Table 22) suggesting a slower diffusion of 4HT from mammary glands treated with MSG. This was also evident from the plasma concentrations where free 4HT showed higher peak plasma levels compared to MSG. Free 4HT exhibited a higher C_{max} of 29.7 ± 2.9 ng.hr/ml and was reached earlier (T_{max} of 2 hrs) compared to the C_{max} observed with MSG (21.5 ± 3.01 ng.hr/ml) with a delayed T_{max} (72 hrs). 4HT was undetectable in the free 4HT group after day 7 (Figure 43), whereas MSG prolonged 4HT levels for 14 days (Figure 43) in the plasma. Similarly, other pharmacokinetic parameters such as $AUC_{0-\alpha}$ and MRT for 4HT were significantly higher for MSG suggesting longer retention of drug in the plasma (Table 22).

EDX is a major metabolite of 4HT and requires CYP enzyme system for its metabolic conversion. [202] EDX levels were found to be higher in the plasma for both free 4HT and MSG (Table 22). The C_{max} for EDX for free 4HT was higher than MSG (Table 23). Free 4HT showed significantly lower ($p<0.05$) $t_{½}$ for EDX (45.43 ± 22.42 hrs) compared to MSG (302.58 ± 41.91 hrs). For free 4HT, no EDX was detected after day 9 (Figure 41), while MSG sustained EDX concentration in the plasma for 14 days (Figure 42).

The therapeutic levels of 4HT and EDX in the plasma observed in breast cancer patients taking tamoxifen (20 mg) are found to be in the range of 0.38 - 6.97 ng/ml and 2.98 - 28.05 ng/ml respectively. The reported IC50 values of 4HT and EDX on MCF-7 cells are reported to be 1.52 - 6.97 ng/ml for 4HT and 2.98 – 70.19 ng/ml for EDX. [182] In the present study, MSG sustained both 4HT and EDX levels within the range of the reported IC50 value for both the drugs. Taken together, MSG sustained therapeutic levels of EDX and 4HT in the plasma.

At day 14, the concentration of 4HT retained in the mammary gland was 5-fold higher than free 4HT (Figure 43). No 4HT was detected with free 4HT at day 14. EDX was detected in the mammary glands treated with MSG at day 14 (Figure 44). Previously, intraductal 4HT did not result the formation of EDX in the mammary glands.[109] However, results from this study suggest that formulations that can sustain 4HT levels in the mammary glands is a critical factor for conversion of 4HT to EDX. Moreover, the levels of EDX in the mammary glands treated with MSG was much higher than the reported IC50 value of EDX

in MCF-7 cells[181]. This was consistent with our observations in the previous chapter where TMX was converted to 4HT in the mammary glands by CYP enzymes[178] treated with MS and ISG.

In vivo biodistribution study after 14 days showed higher levels of EDX compared to 4HT for MSG (Figure 50). No uterine exposure was detected with MSG. At day 14, no 4HT or EDX were detected in organs treated with free 4HT suggesting faster clearance of EDX and 4HT compared to MSG. Lymph node localization study showed that 4HT was transported to the regional lymph nodes and was retained for 14 days in rats treated with MSG (Figure 45). No 4HT was detected in the lymph nodes in free 4HT group. This was consistent with our previous findings where PLGA MS was localized in the regional lymph nodes for 14 days. With MSG, PLGA MS might have possibly diffused out of the gel matrix and transported to the regional lymph nodes. No 4HT was detected in the regional lymph nodes treated with free 4HT. The levels of 4HT observed in the regional lymph nodes were higher than the IC50 value for 4HT on MCF- 7 cells suggesting its clinical significance. Taken together, MSG sustained therapeutic levels of 4HT and EDX in the plasma and mammary glands. Also, PLGA MS from the MSG was transported and retained in the regional lymph nodes for 14 days.

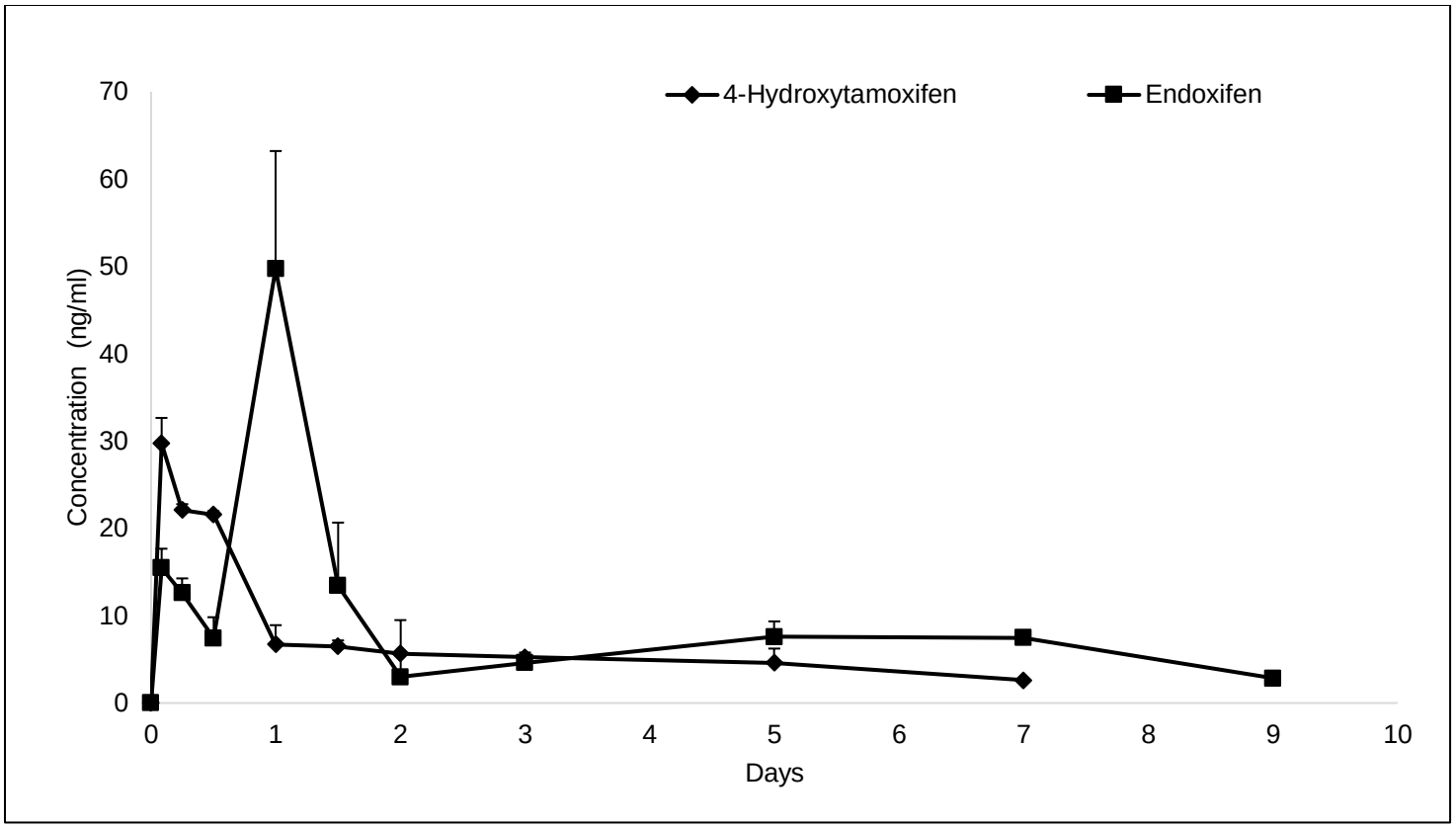

Figure 43: Plasma drug profile of 4-hydroxytamoxifen and endoxifen following treatment with free 4-hydroxytamoxifen formulation. Each data point is Mean ± SD, n=3. The concentration 4-hydroxytamoxifen was undetectable after day 7 and endoxifen was undetectable after day 9. The two groups are not statistically significant by Students t-test ($p<0.05$)

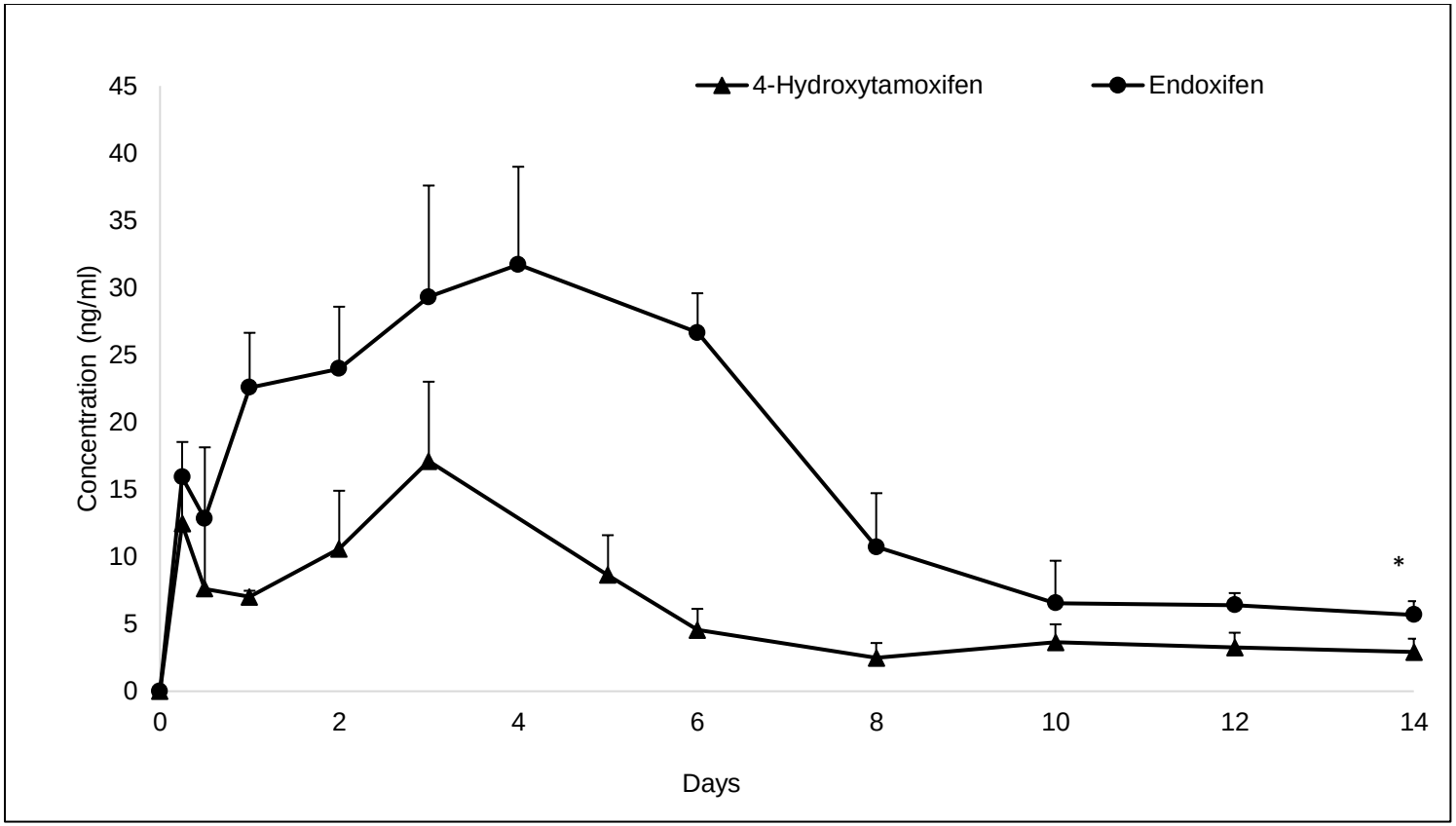

Figure 44: Plasma drug profile of 4-hydroxytamoxifen and endoxifen following treatment with microspheres in thermogel formulation. Each data point is Mean ± SD, n=3.* is significant by Students t-test ($p<0.05$).

Table 22: Pharmacokinetic parameters of 4-hydroxytamoxifen in plasma

Pharmacokinetic parameters of 4-hydroxytamoxifen							
	$t_{½}$ (hrs)	**k_e (hrs^{-1})**	**C_{max} (ng/ml)**	**T_{max} (hrs)**	**AUC (ng. hr/ml)**	**AUMC (ng. hr^2/ml)**	**MRT (hrs)**
Free 4HT	31.83 ± 8.08	0.009 ± 0.002	29.7 ± 2.9	2	1156.53 ± 4.36	72813.93 ± 4744.79	63.4 ± 4.85
MS in Thermogel	104.12 ± 18.39*	0.002 ±0.0004*	21.5 ± 3.01*	72*	2590.3 ± 261.57*	465544 ± 103516.95*	182.66 ± 55.98*

$t_{½}$- plasma half-life; k_e - elimination rate constant; C_{max} – peak plasma concentration; T_{max}- time to reach peak plasma concentration; AUC – area under the curve; AUMC- area under the first moment curve; ; MRT- mean residence time. MS is microspheres; Data is Mean ± SD, n=3; * is significant by Students t-test ($p<0.05$)

Table 23: Pharmacokinetic parameters of endoxifen in plasma

Pharmacokinetic parameters of Endoxifen							
	$t_{½}$ (hrs)	**k_e (hrs^{-1})**	**C_{max} (ng/ml)**	**T_{max} (hrs)**	**AUC (ng. hr/ml)**	**AUMC (ng. hr^2/ml)**	**MRT (hrs)**
Free 4HT	45.43 ± 22.42	0.007 ± 0.002	49.7 ± 13.5	24	1978.76 ± 97.32	174361.1 ± 45850.24	87.53 ± 18.63
MS in Thermogel	302.58 ± 41.91*	0.0009 ± 0.0001*	38.5 ± 0.73	88 ± 13.85*	8145.8 ± 1465.92*	2710550.93 ± 1064850.69*	324.3 ± 74.96*

$t_{½}$- plasma half-life; k_e - elimination rate constant; C_{max} – peak plasma concentration; T_{max}- time to reach peak plasma concentration; AUC – area under the curve; AUMC- area under the first moment curve; ; MRT- mean residence time; MS is microspheres; Data is Mean ± SD, n=3; * is significant by Students t-test ($p<0.05$)

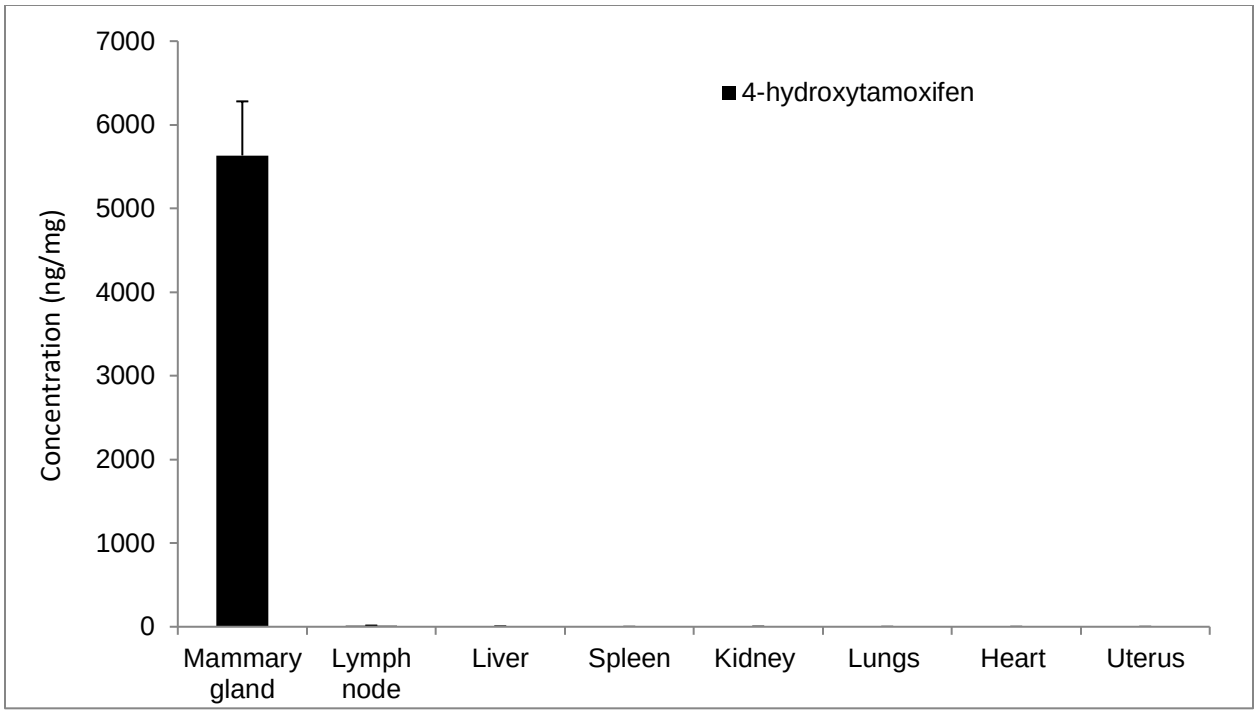

Figure 45: Organ levels of 4HT at the end of study (14 days). Data is Mean ± SD, n=3.

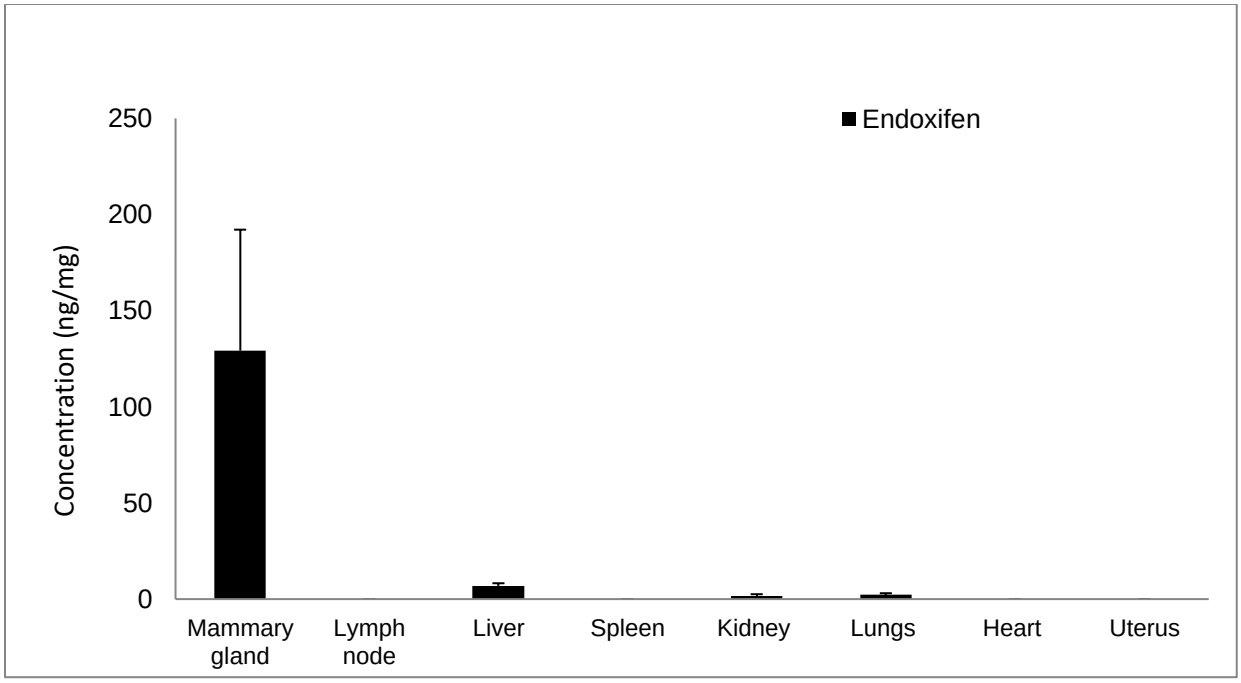

Figure 46: Organ levels of EDX at the end of study (14 days). Data is Mean ± SD, n=3..

3.3.4 Time dependent breast distribution study

To determine the extent of drug retention in the breast, the mammary gland levels of 4HT and EDX were measured on days 7, 14 and 28. Results showed that MSG retained 4HT for 28 days compared to free 4HT (Figure 47). Free 4HT was retained in the mammary glands for 7 days even though the levels were >10 fold lower as observed with MSG (Figure 47). This can be due to the highly lipophilicity of 4HT and the vehicle (corn oil) resulting in drug binding to the adipose tissue in the breast. [97] At day 7, the 4HT concentration was 12-fold higher with MSG compared to free 4HT. At day 28, MSG maintained 4HT concentration of 1.06 µg/mg, which is higher than the reported IC50 value of 4HT for MCF-7 cells. [182]

EDX was generated in the mammary glands treated with MSG possibly due to the biotransformation of 4HT by resident CYP enzymes present in the mammary glands. [178] The mammary gland levels of EDX were highest on day 14 with levels much higher than the therapeutic levels of EDX (Figure 48). The therapeutic levels were maintained in the mammary glands treated with MSG until day 28. The lower levels of EDX on day 7 suggest a time dependent conversion of 4HT to EDX. Previous studies with 4HT shows no enzymatic conversion which might be due to faster diffusion of 4HT out of the mammary glands. Another possibility is the recirculation EDX from the circulation back into the mammary glands. Further studies needs to be conducted to validate our findings and also to test other possibilities like the role of enzyme induction associated with SERM's. [179]

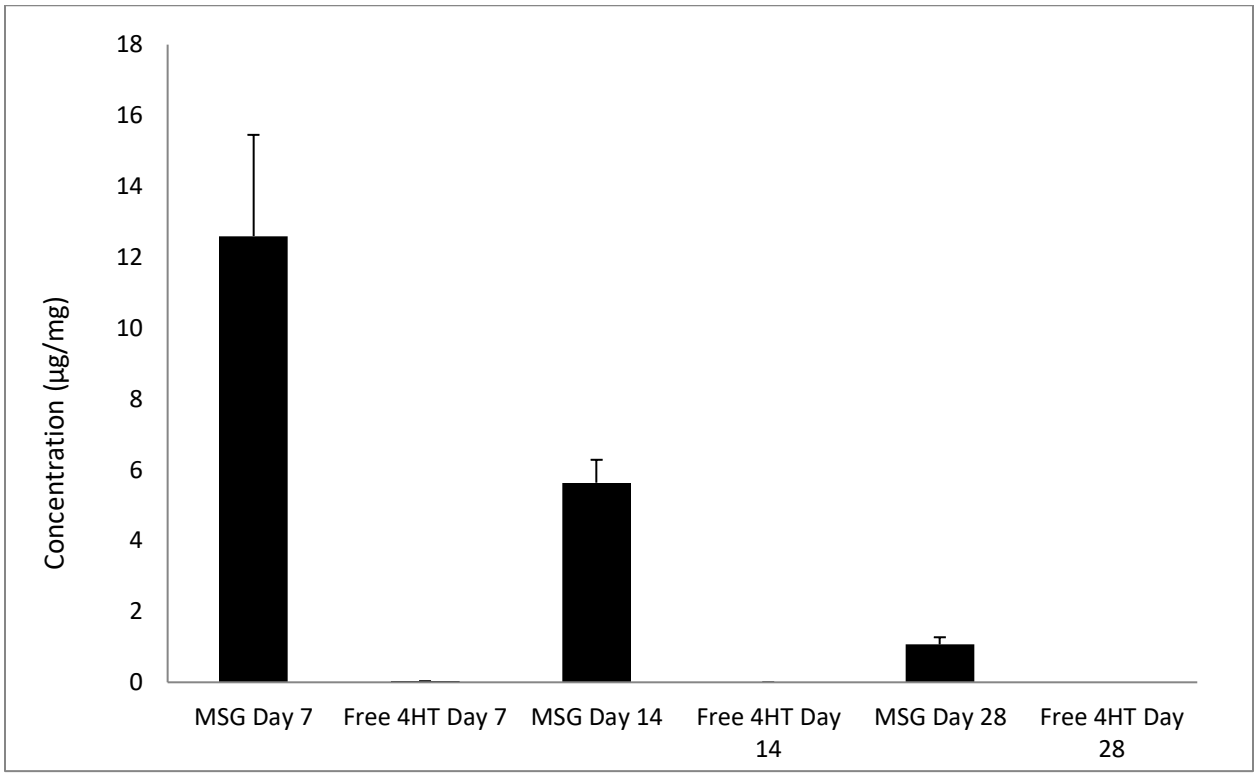

Figure 47: Mammary gland concentration of 4HT treated with MSG and free 4HT on 7, 14 and 28 days. Data is Mean ± SD, n=3.

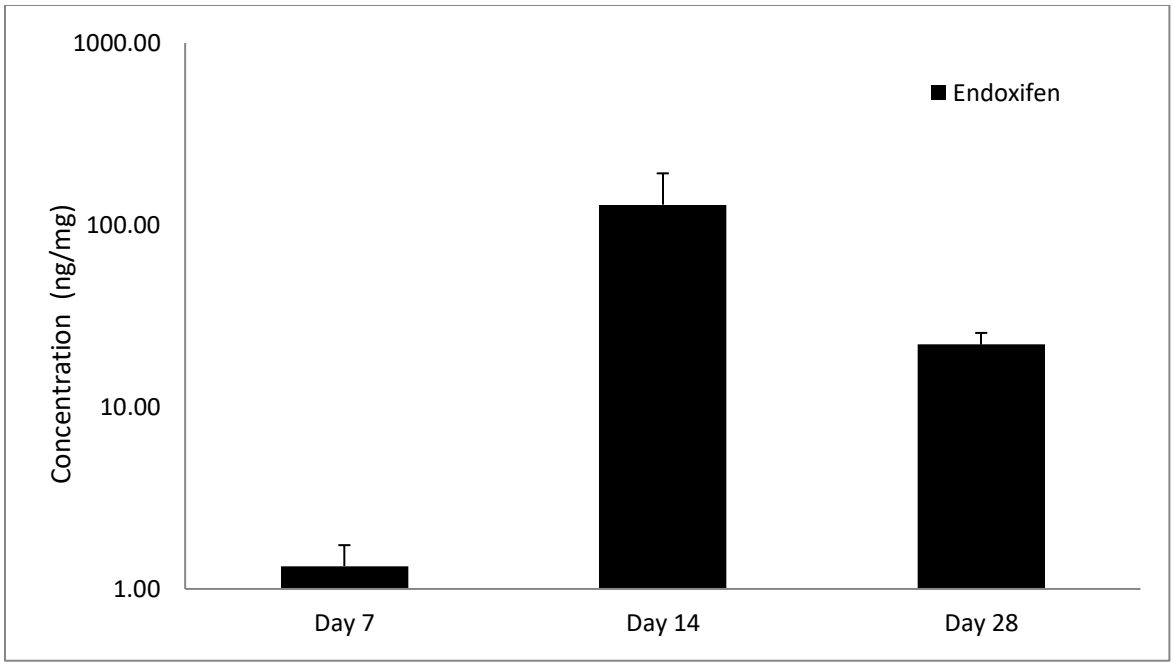

Figure 48: Mammary gland concentration of EDX treated with MSG on 7, 14 and 28 days. Data is Mean ± SD, n=3. No EDX was detected in mammary glands treated with free 4HT.

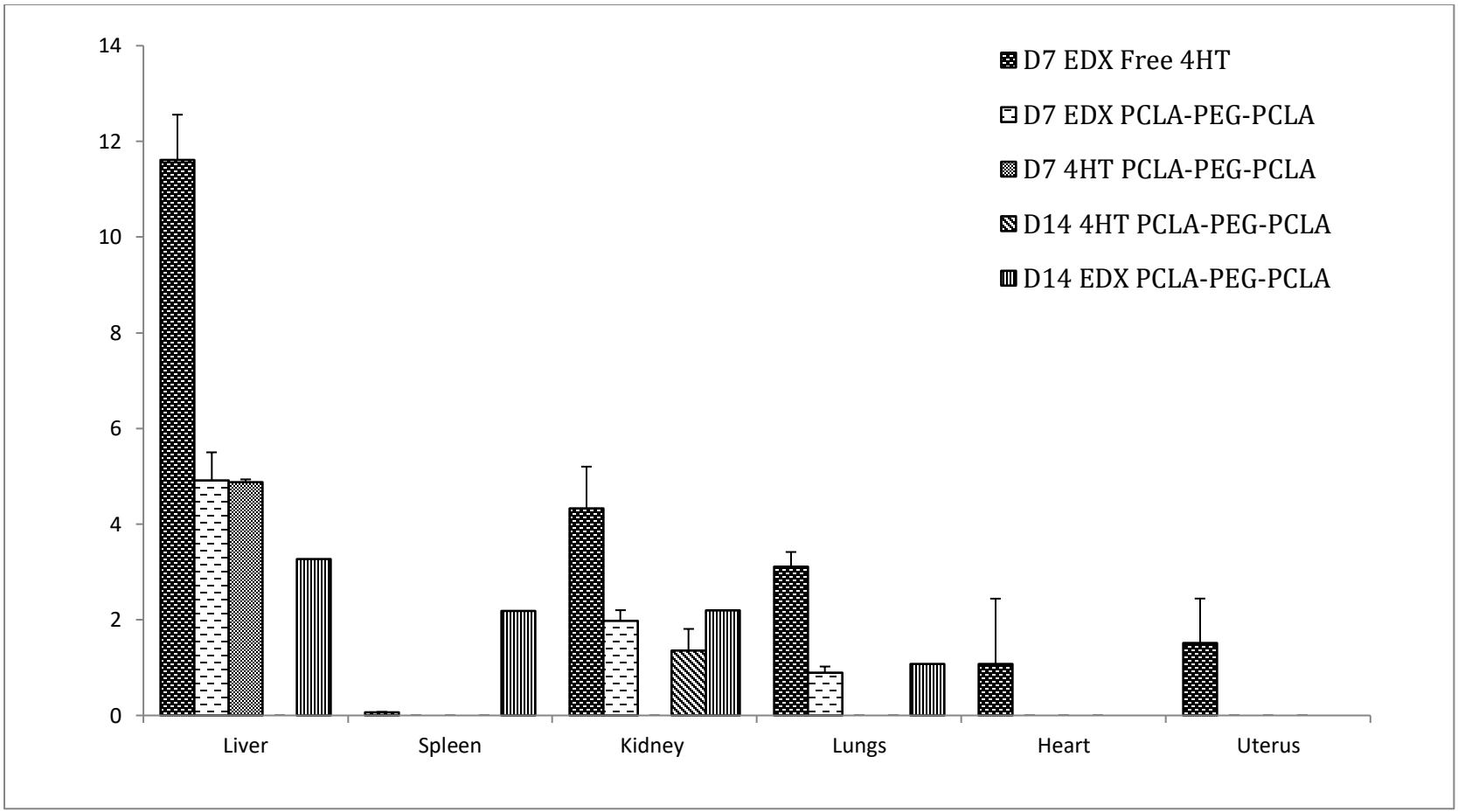

Figure 49: Organ distribution of 4HT and EDX in rats treated with MSG and free 4HT 7, 14 and 28 days.

Both free 4HT and MSG did not show detectable levels at 28 days. Data is Mean ± SD, n=3

3.3.5 Time dependent lymph node retention study

To test the role of regional lymph nodes on the transport of formulations from the breast, we determined the levels of 4HT at the regional lymph nodes at days 7, 14 and 28. As reported in the previous chapter, microsphere drained through the regional lymph nodes and was retained for 14 days (Figure 50). The lymph node levels of 4HT in MSG were 30 and 5-fold higher compared to free 4HT at days 7 and 14 respectively. EDX was present at very low levels in the regional lymph nodes at day 7 in mammary glands treated with MSG (Figure 50). According to previous studies, particle size plays a major role in targeting distinct subsets of immune cells and occupies distinct areas of the lymph nodes. Smaller particles (<200nm) are found to be associated with macrophages and larger particles (>200 μm) are transported to the lymph nodes by dendritic cells.[203, 204]

Studies[205, 206] have reported the improved retention of microparticles >1μm in the lymph node upon oral and subcutaneous administration of microspheres. In a more recent study, microparticles of different particle sizes were injected subcutaneously into the breast of healthy rabbits to characterize lymphatic transport and also to assess the location of the particles in the lymph node relative to the malignant cells[155]. Results showed that 1μm particles were 20 times more retained compared to 100nm nanospheres showing the advantage of micrometric particles for lymph node targeted chemotherapy. This is possibly due to a "washout phenomenon" of the nanoparticles by the efferent lymphatic system where in the particles travel freely to the nodes and then exit from the nodes within the first few hours after injection.

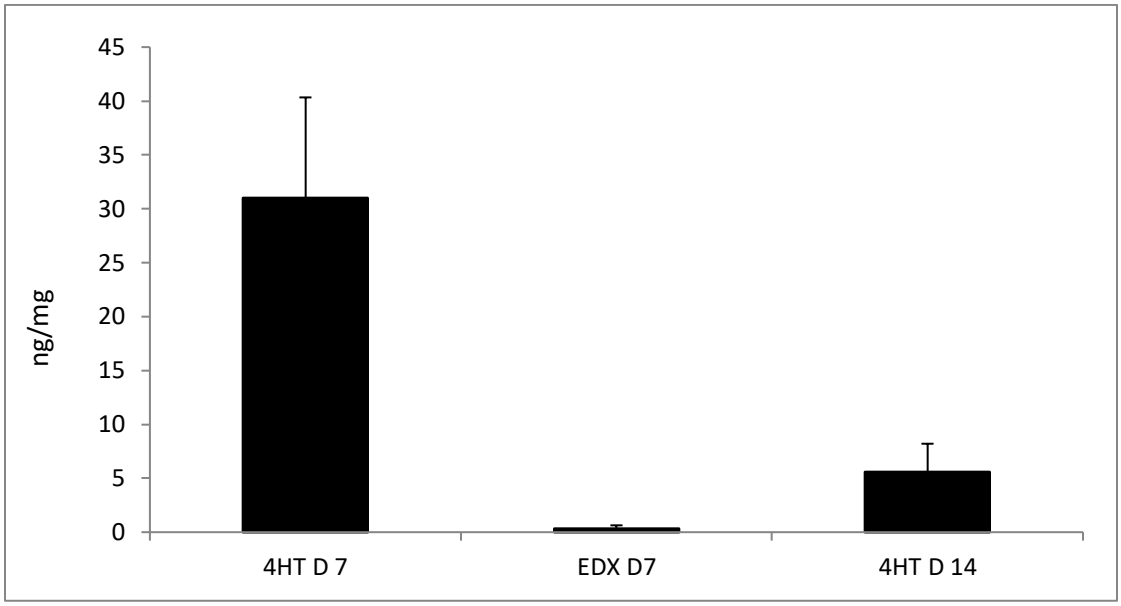

Figure 50: Lymph node concentration of 4HT and EDX in rats treated with MSG on 7, 14 and 28 days. 4HT was undetectable at 28 days. EDX was undetectable after 7 days. Data is Mean ± SD, n=3.

3.4. CONCLUSIONS

4HT loaded PLGA MS with particle size 9.63 ± 1.49 µm and encapsulation and loading efficiencies 92.46 ± 2.59 % and 10.46 ± 0.38 % respectively were prepared. Optimal drug polymer ratio for PLGA microspheres and thermogel was found to be 1:10 % w/w. *In vitro* release study showed sustained release of 4HT from MSG for 1 month. Pharmacokinetic studies showed that MSG sustained therapeutic levels of 4HT and EDX in the mammary glands and plasma for 28 and 14 days respectively. MSG formulation resulted in transport of 4HT to the regional lymph nodes and was retained for 2 weeks. In vivo biodistribution study showed minimal systemic distribution of 4HT and EDX with MSG compared to free 4HT. Taken together, this study demonstrates the feasibility of long-acting intraductal formulations of 4HT that can sustain therapeutic levels in the mammary glands for ~1 month.

A summary of the findings from this chapter is depicted below.

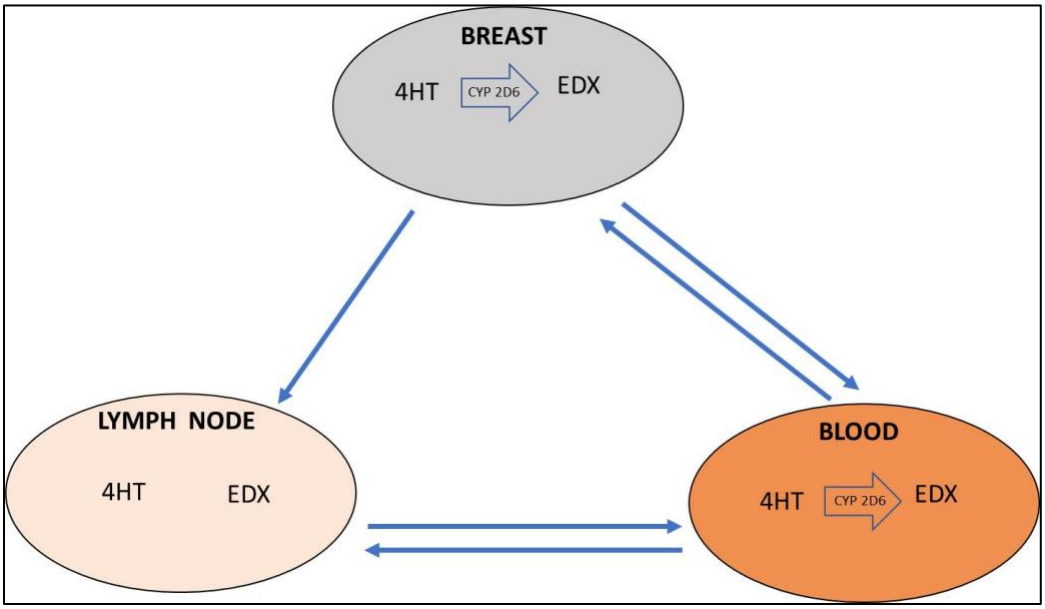

Figure 51: Summary of findings from this chapter

4. SUMMARY

The main goal of this dissertation was to demonstrate the feasibility of long-acting intraductal delivery system for the breast. In the first study, PS particles of 1 µm were retained for 3 days compared to the free dye which retained only few hours. PS particles of 100nm and 500nm were retained only for 2 days. PLGA formulations with particle size ~10µm (microspheres) and *in situ* forming gel systems showed retention of 4 days. Free dye and nanoparticles (200-500 nm) diffused out of the ducts in 2- 4 hours and 24 - 36 hours respectively. The microspheres and *in situ* gel formulations showed reduced systemic biodistribution. The whole mount images confirmed retention of the formulation and distribution of formulation in the ducts. The microspheres and nanoparticles also retained in the regional lymph nodes for 24 and 48 hours respectively. Based on these findings, tamoxifen loaded PLGA microspheres and *in situ* gel formulations were developed. PLGA microspheres and in situ gel retained tamoxifen in the mammary glands for 14 days compared to free tamoxifen and PLGA nanoparticles, which was retained for 3 and 6 days respectively. Also, 4-hydroxytamoxifen, a major metabolite of tamoxifen was formed in the in the mammary glands treated with microspheres and *in situ* gel. The systemic biodistribution study showed reduced systemic exposure with microspheres and *in situ* gel. The TMX loaded PLGA nanoparticles and microspheres were retained in the regional lymph nodes for 2 and 14 days respectively.

Based on these findings, the next objective focused on developing intraductal formulations of 4HT, a potent metabolite of TMX. Further, the goal was to prolong drug retention for 1 month. PLGA microspheres were combined with thermogel to achieve this objective. The microsphere in gel formulation sustained 4-hydroxytamoxifen release 1

month. Time dependent breast distribution study showed that therapeutic levels of 4-hydroxytamoxifen was maintained for ~1 month using this formulation. On the other hand, free 4-hydroxytamoxifen was retained in the breast only for 7 days. Endoxifen, a major metabolite of 4-hydroxytamoxifen, was formed in the breast and the therapeutic levels were maintained for 28 days in the breast. Pharmacokinetic studies showed that 4-hydroxytamoxifen and endoxifen maintained therapeutic levels in the plasma for 14 days, while free 4-hydroxytamoxifen showed no detectable levels of 4-hydroxytamoxifen and endoxifen after 7 and 9 days respectively. Taken together, the findings from this dissertation demonstrated the feasibility of developing long acting intraductal delivery systems for prevention and treatment of breast cancer.

5. FUTURE PROSPECTS

The findings from this dissertation can be used to guide future formulation design and development of long-acting intraductal delivery systems. The future studies should focus on:

- Developing other formulation approaches such as drug-polymer conjugates and combinatorial approaches with microspheres and/or in-situ gels to further sustain drug release and prolong the drug levels in the breast for > 1 month
- Mechanistic studies to understand the transport kinetics and pathways from the breast to lymph nodes
- Efficacy studies using suitable animal models including metastatic breast cancer models.
- Study the pharmacokinetics of long-acting formulations in a clinically translatable animal model such as pig
- Conduct long-term preclinical safety studies in animals
- Develop and test intraductal formulations for macromolecules (biologics) and test the retention in mammary glands

6. BIBLIOGRAPHY

1. Jesinger, R. A. Breast Anatomy for the Interventionalist. *Techniques in Vascular and Interventional Radiology* **2014,** *17*, (1), 3-9.
2. Ellis, H., Colborn, G.L. and Skandalakis, J.E. Surgical embryology and anatomy of the breast and its related anatomic structures. *The Surgical clinics of North America* **1993,** *73*, (4), 611-632.
3. Pandya, S., and Richard G. Moore. Breast development and anatomy. *Clinical obstetrics and gynecology* **2011,** *54*, (1), 91-95.
4. Fwu, P. T.; Chen, J.-H.; Li, Y.; Chan, S.; Su, M.-Y. Quantification of Regional Breast Density in Four Quadrants Using 3D MRI—A Pilot Study. *Translational Oncology* **2015,** *8*, (4), 250-257.
5. Hassiotou, F.; Geddes, D. Anatomy of the human mammary gland: Current status of knowledge. *Clinical Anatomy* **2013,** *26*, (1), 29-48.
6. PE, H., *The breast and breast-feeding*. 4 ed.; Scientifc Foundations of Obstetrics and Gynaecology: 1991.
7. L A Venta, C. M. D., C G Salomon, M E Flisak. Sonographic evaluation of the breast. *Radiographics* **1994,** *14*, (1), 29-50.
8. Love, S. M.; Barsky, S. H. Anatomy of the nipple and breast ducts revisited. *Cancer* **2004,** *101*, (9), 1947-1957.
9. OW Sartorius, P. M., DL Benedict, HS Smith. Contrast ductography for recognition and localization of benign and malignant breast lesions: an improved technique. *Breast Cacinoma* **1977**.

10. Going, J. J.; Mohun, T. J. Human breast duct anatomy, the ‘sick lobe’ hypothesis and intraductal approaches to breast cancer. *Breast Cancer Research and Treatment* **2006,** *97*, (3), 285-291.

11. Tot, T. The theory of the sick breast lobe and the possible consequences. *International Journal of Surgical Pathology* **2007** *15*, (4), 369-375.

12. Bland, K. I., Copeland, E.M., Klimberg, V.S. and Gradishar, W.J., *The breast: comprehensive management of benign and malignant diseases*. Elsevier Inc.: 2017.

13. Sappey, P. C. Anatomie, physiologie, pathologie des vesseaux lymphatiques consideres chez l'homme et les vertebres. *Paris A* **1885**.

14. Alitalo, K., Tammela, T. and Petrova, T.V. Lymphangiogenesis in development of human disease. *Nature* **2005,** *438*, (7070), 946.

15. Kirby I. Bland, E. M. C., V. Suzanne Klimberg, William J Gradishar, *The breast: comprehensive management of benign and malignant diseases*. Elsevier Inc: 2017.

16. Brunicardi, F., Andersen, Dana, Billiar, Timothy, Dunn, David, Hunter, John, Pollock, Raphael E., *Schwartz’s Principles of Surgery*. 8 ed.; The McGraw-Hill Medical Publishing Division: New York, 2004.

17. Ellis, H.; Mahadevan, V. Anatomy and physiology of the breast. *Surgery (Oxford)* **2013,** *31*, (1), 11-14.

18. Siegel, R. L.; Miller, K. D.; Jemal, A. Cancer statistics, 2019. *CA: A Cancer Journal for Clinicians* **2019,** *69*, (1), 7-34.

19. Davies, E. L. Breast cancer. *Medicine* **2012,** *40*, (1), 5-9.

20. Lukong, K. E. Understanding breast cancer – The long and winding road. *BBA Clinical* **2017,** *7*, 64-77.

21. McPherson, K., Steel, C. and Dixon, J.M. ABC of breast diseases: breast cancer—epidemiology, risk factors, and genetics. *British Medical Journal* **2000,** *321*, (7261), p.624.

22. Gu, Z.; Gao, D.; Al-Zubaydi, F.; Li, S.; Singh, Y.; Rivera, K.; Holloway, J.; Szekely, Z.; Love, S.; Sinko, P. J. The effect of size and polymer architecture of doxorubicin–poly(ethylene) glycol conjugate nanocarriers on breast duct retention, potency and toxicity. *European Journal of Pharmaceutical Sciences* **2018,** *121*, 118-125.

23. Walsh, T., Casadei, S., Coats, K.H., Swisher, E., Stray, S.M., Higgins, J., Roach, K.C., Mandell, J., Lee, M.K., Ciernikova, S. and Foretova, L. Spectrum of mutations in BRCA1, BRCA2, CHEK2, and TP53 in families at high risk of breast cancer. *Jama* **2006,** *295*, (12), pp.1379-1388.

24. Turner, N., Tutt, A. and Ashworth, A. Targeting the DNA repair defect of BRCA tumours. *Current opinion in pharmacology* **2005,** *5*, (4), 388-393.

25. Carol E. DeSantis, F. B., Jacques Ferlay, Joannie Lortet-Tieulent, Benjamin O. Anderson and Ahmedin Jemal. International variation in female breast cancer incidence and mortality rates. *Cancer Epidemiology and Prevention Biomarkers* **2015,** *24*, (10), 1495-1506.

26. Emilio González-Jiménez PhD, P. A. G. P., María José Aguilar PhD, Carlos A Padilla MD, Judit Álvarez MD. Breastfeeding and the prevention of breast

cancer: a retrospective review of clinical histories. *Journal of clinical nursing* **2014,** *23*, (17), 2397-2403.

27. Sunil R. Lakhani , M. J. v. d. V., Jocelyne Jacquemier , Thomas J. Anderson , Peter P. Osin , Lesley McGuffogDouglas F. Easton. The pathology of familial breast cancer: predictive value of immunohistochemical markers estrogen receptor, progesterone receptor, HER-2, and p53 in patients with mutations in BRCA1 and BRCA2. *Journal of clinical oncology* **2002,** *20*, (9), 2310-2318.

28. Jacques Ferlay, I. S., Rajesh Dikshit, Sultan Eser, Colin Mathers, Marise Rebelo, Donald Maxwell Parkin, David Forman, Freddie Bray. Cancer incidence and mortality worldwide: sources, methods and major patterns in GLOBOCAN 2012. *International journal of cancer* **2015,** *136*, (5), E359-E386.

29. Burstein, H. J., Polyak, K., Wong, J.S., Lester, S.C. and Kaelin, C.M. Ductal carcinoma in situ of the breast. *New England Journal of Medicine* **2004,** *350,* (14), 1430-1441.

30. Kawada, K.; Taketo, M. M. Significance and Mechanism of Lymph Node Metastasis in Cancer Progression. *Cancer Research* **2011,** *71*, (4), 1214-1218.

31. Maughan, K. L., Lutterbie, M.A. and Ham, P.S. Treatment of breast cancer. *Chemotherapy* **2010,** *51*, (53).

32. Klevos, G. A.; Ezuddin, N. S.; Vinyard, A.; Ghaddar, T.; Gort, T.; Almuna, A.; Abisch, A.; Welsh, C. F. A Breast Cancer Review: Through the Eyes of the Doctor, Nurse, and Patient. *Journal of Radiology Nursing* **2017,** *36*, (3), 158-165.

33. Eroles, P.; Bosch, A.; Alejandro Pérez-Fidalgo, J.; Lluch, A. Molecular biology in breast cancer: Intrinsic subtypes and signaling pathways. *Cancer Treatment Reviews* **2012,** *38*, (6), 698-707.

34. Murawa, P.; Murawa, D.; Adamczyk, B.; Połom, K. Breast cancer: Actual methods of treatment and future trends. *Reports of Practical Oncology & Radiotherapy* **2014,** *19*, (3), 165-172.

35. Dai, X., Li, T., Bai, Z., Yang, Y., Liu, X., Zhan, J. and Shi, B. Breast cancer intrinsic subtype classification, clinical use and future trends. *American journal of cancer research* **2015,** *5*, (10), p.2929.

36. Kennecke, H.; Yerushalmi, R.; Woods, R.; Cheang, M. C. U.; Voduc, D.; Speers, C. H.; Nielsen, T. O.; Gelmon, K. Metastatic Behavior of Breast Cancer Subtypes. *Journal of Clinical Oncology* **2010,** *28*, (20), 3271-3277.

37. Guarneri, V.; Conte, P. Metastatic Breast Cancer: Therapeutic Options According to Molecular Subtypes and Prior Adjuvant Therapy. *The Oncologist* **2009,** *14*, (7), 645-656.

38. Ross, J. S., Fletcher, J.A., Bloom, K.J., Linette, G.P., Stec, J., Symmans, W.F., Pusztai, L. and Hortobagyi, G.N. Targeted therapy in breast cancer: the HER-2/neu gene and protein. *Molecular & Cellular Proteomics* **2004,** *3*, (4), 379-398.

39. Ross, J. S.; Slodkowska, E. A.; Symmans, W. F.; Pusztai, L.; Ravdin, P. M.; Hortobagyi, G. N. The HER-2 Receptor and Breast Cancer: Ten Years of Targeted Anti-HER-2 Therapy and Personalized Medicine. *The Oncologist* **2009,** *14*, (4), 320-368.

40. Gianni, L., Dafni, U., Gelber, R.D., Azambuja, E., Muehlbauer, S., Goldhirsch, A., Untch, M., Smith, I., Baselga, J., Jackisch, C. and Cameron, D. Treatment with trastuzumab for 1 year after adjuvant chemotherapy in patients with HER2-positive early breast cancer: a 4-year follow-up of a randomised controlled trial. . *The lancet oncology* **2011,** *12*, (3), pp.236-244.

41. Park, J. H., Ahn, J.H. and Kim, S.B. How shall we treat early triple-negative breast cancer (TNBC): from the current standard to upcoming immuno-molecular strategies. . *ESMO open* **2018,** *3*, (Suppl 1), p.e000357.

42. Fong, P. C., Boss, D.S., Yap, T.A., Tutt, A., Wu, P., Mergui-Roelvink, M., Mortimer, P., Swaisland, H., Lau, A., O'Connor, M.J. and Ashworth, A. Inhibition of poly (ADP-ribose) polymerase in tumors from BRCA mutation carriers. . *New England Journal of Medicine* **2009,** *361*, (2), 123-134.

43. Bilal, E., Dutkowski, J., Guinney, J., Jang, I.S., Logsdon, B.A., Pandey, G., Sauerwine, B.A., Shimoni, Y., Vollan, H.K.M., Mecham, B.H. and Rueda, O.M. Improving breast cancer survival analysis through competition-based multidimensional modeling. *PLoS computational biology* **2013,** *9*, (5), p.e1003047.

44. Miller, E.; Lee, H. J.; Lulla, A.; Hernandez, L.; Gokare, P.; Lim, B. Current treatment of early breast cancer: adjuvant and neoadjuvant therapy. *F1000Research* **2014,** *3*, 198.

45. Young, W. W., Marks, S.M., Kohler, S.A. and Hsu, A.Y. Dissemination of clinical results: mastectomy versus lumpectomy and radiation therapy. *Medical care* **1996,** *34*, (10), pp.1003-1017.

46. Lasry, J. C. M., Margolese, R.G., Poisson, R., Shibata, H., Fleischer, D., Lafleur, D., Legault, S. and Taillefer, S. Depression and body image following mastectomy and lumpectomy. *Journal of Chronic Diseases* **1987,** *40*, (6), pp.529-534.

47. John R Benson, I. J., Martin Keisch, Francisco J Esteva, Andreas Makris, V Craig Jordan. Early breast cancer. *The Lancet* **2009,** *373* 1463-1479.

48. Lichter, A. S., Lippman, M.E., Danforth, D.N., d'Angelo, T., Steinberg, S.M., DeMoss, E., MacDonald, H.D., Reichert, C.M., Merino, M. and Swain, S.M. Mastectomy versus breast-conserving therapy in the treatment of stage I and II carcinoma of the breast: a randomized trial at the National Cancer Institute. *J Clin oncol* **1992,** *10*, (6), pp.976-983.

49. Norum, J., Olsen, J.A. and Wist, E.A. Lumpectomy or mastectomy? Is breast conserving surgery too expensive?. *Breast Cancer Research and Treatment* **1997,** *45*, (1), 07-14.

50. Hindie, E.; Groheux, D.; Brenot-Rossi, I.; Rubello, D.; Moretti, J. L.; Espie, M. The Sentinel Node Procedure in Breast Cancer: Nuclear Medicine as the Starting Point. *Journal of Nuclear Medicine* **2011,** *52*, (3), 405-414.

51. Furdui, C. M. Ionizing Radiation: Mechanisms and Therapeutics. *Antioxidants & Redox Signaling* **2014,** *21*, (2), 218-220.

52. Espié, M. The management of breast cancer. *Diagnostic and Interventional Imaging* **2014,** *95*, (7-8), 753-757.

53. Senkus-Konefka, E.; Jassem, J. Complications of Breast-cancer Radiotherapy. *Clinical Oncology* **2006,** *18*, (3), 229-235.

54. Rodin, D.; Knaul, F. M.; Lui, T. Y.; Gospodarowicz, M. Radiotherapy for breast cancer: The predictable consequences of an unmet need. *The Breast* **2016,** *29*, 120-122.

55. Corrie, P. G. Cytotoxic chemotherapy: clinical aspects. *Medicine* **2011,** *39*, (12), 717-722.

56. Bhosle, J.; Hall, G. Principles of cancer treatment by chemotherapy. *Surgery (Oxford)* **2009,** *27*, (4), 173-177.

57. Group, E. B. C. T. C. Polychemotherapy for early breast cancer: an overview of the randomised trials. *The Lancet* **1998,** *352*, (9132), 930-942.

58. Group, E. B. C. T. C. Tamoxifen for early breast cancer: an overview of the randomised trials. *The Lancet* **1998,** *351*, (9114), 1451-1467.

59. Henderson, I. C., Berry, D. A., Demetri, G. D., Cirrincione, C. T., Goldstein, L. J., Martino, S., ... & Fleming, G. . Improved outcomes from adding sequential paclitaxel but not from escalating doxorubicin dose in an adjuvant chemotherapy regimen for patients with node-positive primary breast cancer. *Journal of clinical oncology* **2003,** *21*, (6), 976-983.

60. Tao, J. J.; Visvanathan, K.; Wolff, A. C. Long term side effects of adjuvant chemotherapy in patients with early breast cancer. *The Breast* **2015,** *24*, S149-S153.

61. Osborne, C. K. Steroid hormone receptors in breast cancer management. *Breast cancer research and treatment* **1998,** *51*, (3), 227-238.

62. Abraham, J.; Staffurth, J. Hormonal therapy for cancer. *Medicine* **2011,** *39*, (12), 723-727.

63. Dutertre, M. a. S., C.L. Molecular mechanisms of selective estrogen receptor modulator (SERM) action. *Journal of Pharmacology and Experimental Therapeutics* **2000,** *295*, (2), 431-437.

64. Trunet, P. F., Vreeland, F., Royce, C., Chaudri, H.A., Cooper, J. and Bhatnagar, A.S. Clinical use of aromatase inhibitors in the treatment of advanced breast cancer. *The Journal of steroid biochemistry and molecular biology* **1997,** *61*, (3-6), 241-245.

65. Amir, E., Seruga, B., Niraula, S., Carlsson, L. and Ocaña, A. Toxicity of adjuvant endocrine therapy in postmenopausal breast cancer patients: a systematic review and meta-analysis. *Journal of the National Cancer Institute* **2011,** *103*, (17), 1299-1309.

66. Patel, H. K.; Bihani, T. Selective estrogen receptor modulators (SERMs) and selective estrogen receptor degraders (SERDs) in cancer treatment. *Pharmacology & Therapeutics* **2018,** *186*, 1-24.

67. Park, W. C. a. J., V.C. Selective estrogen receptor modulators (SERMS) and their roles in breast cancer prevention. *Trends in molecular medicine* **2002,** *8*, (2), 82-88.

68. Osborne, C. K. Tamoxifen in the treatment of breast cancer. *New England Journal of Medicine* **1998,** *339*, (22), 1609-1618.

69. Chumsri, S.; Howes, T.; Bao, T.; Sabnis, G.; Brodie, A. Aromatase, aromatase inhibitors, and breast cancer. *The Journal of Steroid Biochemistry and Molecular Biology* **2011,** *125*, (1-2), 13-22.

70. Smith, I. E. a. D., M. Aromatase inhibitors in breast cancer. *New England Journal of Medicine* **2003,** *348*, (24), 2431-2442.

71. Lyman, G. H., Giuliano, A.E., Somerfield, M.R., Benson III, A.B., Bodurka, D.C., Burstein, H.J., Cochran, A.J., Cody III, H.S., Edge, S.B., Galper, S. and Hayman, J.A., 2005. . American Society of Clinical Oncology guideline recommendations for sentinel lymph node biopsy in early-stage breast cancer. *Journal of clinical oncology* **2005,** *23*, (30), 7703-7720.

72. Normanno, N.; Morabito, A.; De Luca, A.; Piccirillo, M. C.; Gallo, M.; Maiello, M. R.; Perrone, F. Target-based therapies in breast cancer: current status and future perspectives. *Endocrine-Related Cancer* **2009,** *16*, (3), 675-702.

73. Olayioye, M. A., Neve, R.M., Lane, H.A. and Hynes, N.E. The ErbB signaling network: receptor heterodimerization in development and cancer. *The EMBO journal* **2000,** *19*, (3), 3159-3167.

74. Higgins, M. J.; Baselga, J. Targeted therapies for breast cancer. *Journal of Clinical Investigation* **2011,** *121*, (10), 3797-3803.

75. Slamon, D. J., Gary M. Clark, Steven G. Wong, Wendy J. Levin, Axel Ullrich, and William L. McGuire. . Human breast cancer: correlation of relapse and survival with amplification of the HER-2/neu oncogene. *Science* **1987,** *235*, (4785), 177-182.

76. Geyer, C. E., John Forster, Deborah Lindquist, Stephen Chan, C. Gilles Romieu, Tadeusz Pienkowski, Agnieszka Jagiello-Gruszfeld et al. Lapatinib plus capecitabine for HER2-positive advanced breast cancer. *New England Journal of Medicine* **2006,** *355*, (26), 2733-2743.

77. Nahta, R., Mien-Chie Hung, and Francisco J. Esteva. The HER-2-targeting antibodies trastuzumab and pertuzumab synergistically inhibit the survival of breast cancer cells. *Cancer research* **2004,** *64*, (7), 2343-2346.

78. O'Reilly, K. E., Rojo, F., She, Q.B., Solit, D., Mills, G.B., Smith, D., Lane, H., Hofmann, F., Hicklin, D.J., Ludwig, D.L. and Baselga, J. mTOR inhibition induces upstream receptor tyrosine kinase signaling and activates Akt. *Cancer research* **2006,** *66*, (3), 1500-1508.

79. Perez, E. A.; Spano, J.-P. Current and emerging targeted therapies for metastatic breast cancer. *Cancer* **2012,** *118*, (12), 3014-3025.

80. Prausnitz, M. R.; Mitragotri, S.; Langer, R. Current status and future potential of transdermal drug delivery. *Nature Reviews Drug Discovery* **2004,** *3*, (2), 115-124.

81. Ita, K. B. Transdermal drug delivery: progress and challenges. *Journal of Drug Delivery Science and Technology* **2014,** *24*, (3), 245-250.

82. Prausnitz, M. R., Mitragotri, S. and Langer, R. Current status and future potential of transdermal drug delivery. *Nature reviews Drug discovery* **2004,** *3*, (2), 115.

83. Naik, A., Kalia, Y.N. and Guy, R.H. Transdermal drug delivery: overcoming the skin's barrier function. *Pharmaceutical science & technology today* **2000,** *3*, (9), 318-326.

84. Prausnitz, M. R.; Langer, R. Transdermal drug delivery. *Nature Biotechnology* **2008,** *26*, (11), 1261-1268.

85. Marwah, H.; Garg, T.; Goyal, A. K.; Rath, G. Permeation enhancer strategies in transdermal drug delivery. *Drug Delivery* **2014,** *23*, (2), 564-578.

86. Ng, K. W. a. L., W.M. Skin deep: the basics of human skin structure and drug penetration. In Percutaneous penetration enhancers chemical methods in penetration enhancement *Springer* **2015**, 3-11.

87. Davis, A. F. a. H., J. Supersaturated solutions as topical drug delivery systems. *Drugs and the pharmaceutical sciences* **1993,** *59*, 243-267.

88. Osborne, D. W., Ward, A.J.I. and O'NEILL, K.J. Surfactant association colloids as topical drug delivery vehicles. *Drugs and the pharmaceutical sciences* **1990**, (42), 349-379.

89. Uster, P. S. Liposome-based vehicles for topical delivery. *Drugs and the pharmaceutical sciences* **1990,** *42*, 327-348.

90. Hadgraft, J. a. W., K.A. Skin penetration enhancement. *Journal of dermatological treatment* **1994,** *5*, (1), 43-47.

91. Pujol, H., Girault, J., Rouanet, P., Fournier, S., Grenier, J., Simony, J., Fourtillan, J.B. and Pujol, J.L. Phase I study of percutaneous 4-hydroxy-tamoxifen with analyses of 4-hydroxy-tamoxifen concentrations in breast cancer and normal breast tissue. *Cancer chemotherapy and pharmacology* **1995,** *36*, (6), 493-498.

92. Mauvais-Jarvis, P., Baudot, N., Castaigne, D., Banzet, P. and Kuttenn, F. trans-4-Hydroxytamoxifen concentration and metabolism after local percutaneous administration to human breast. . *Cancer research* **1986,** *46*, (3), 1521-1525.

93. Lee, O.; Ivancic; Chatterton, R.; Rademaker; Khan. In vitro human skin permeation of endoxifen: potential for local transdermal therapy for primary prevention and carcinoma in situ of the breast. *Breast Cancer: Targets and Therapy* **2011**, 61.

94. Sauvez, F., Drouin, D.S., Attia, M., Bertheux, H. and Forster, R. Cutaneously applied 4-hydroxytamoxifen is not carcinogenic in female rats. *Carcinogenesis* **1999,** *20*, (5), 843-850.

95. Lee, O.; Ivancic, D.; Allu, S.; Shidfar, A.; Kenney, K.; Helenowski, I.; Sullivan, M. E.; Muzzio, M.; Scholtens, D.; Chatterton, R. T.; Bethke, K. P.; Hansen, N. M.; Khan, S. A. Local transdermal therapy to the breast for breast cancer prevention and DCIS therapy: preclinical and clinical evaluation. *Cancer Chemotherapy and Pharmacology* **2015,** *76*, (6), 1235-1246.

96. Soe, L., Wurz, G.T., Mäenpää, J.U., Hubbard, G.B., Cadman, T.B., Wiebe, V.J., Theon, A.P. and DeGregorio, M.W. Tissue distribution of transdermal toremifene. *Cancer chemotherapy and pharmacology* **1997,** *39*, (6), 513-520.

97. Güngör, S.; Delgado-Charro, M. B.; Masini-Etévé, V.; Potts, R. O.; Guy, R. H. Transdermal flux predictions for selected selective oestrogen receptor modulators (SERMs): Comparison with experimental results. *Journal of Controlled Release* **2013,** *172*, (3), 601-606.

98. Lee, L. M.; Davison, Z.; Heard, C. M. In vitro delivery of anti-breast cancer agents directly via the mammary papilla (nipple). *International Journal of Pharmaceutics* **2010,** *387*, (1-2), 161-166.

99. Dave, K.; Averineni, R.; Sahdev, P.; Perumal, O. Transpapillary Drug Delivery to the Breast. *PLoS ONE* **2014,** *9*, (12), e115712.

100. Dave, K.; Alsharif, F. M.; Perumal, O. Transpapillary (Nipple) Delivery of Macromolecules to the Breast: Proof of Concept Study. *Molecular Pharmaceutics* **2016,** *13*, (11), 3842-3851.

101. Alsharif, F. M.; Dave, K.; Samy, A. M.; Saleh, K. I.; Amin, M. A.; Perumal, O. Influence of Hydroalcoholic Vehicle on In Vitro Transport of 4-Hydroxy Tamoxifen Through the Mammary Papilla (Nipple). *AAPS PharmSciTech* **2016,** *18*, (4), 1366-1373.

102. Kurtz, S. L.; Lawson, L. B. Nanoemulsions Enhance in vitro Transpapillary Diffusion of Model Fluorescent Dye Nile Red. *Scientific Reports* **2019,** *9*, (1).

103. Kurtz, S. L.; Lawson, L. B. Liposomes Enhance Dye Localization within the Mammary Ducts of Porcine Nipples. *Molecular Pharmaceutics* **2019,** *16*, (4), 1703-1713.

104. Dave, K.; Alsharif, F. M.; Islam, S.; Dwivedi, C.; Perumal, O. Chemoprevention of Breast Cancer by Transdermal Delivery of α-Santalol through Breast Skin and Mammary Papilla (Nipple). *Pharmaceutical Research* **2017,** *34*, (9), 1897-1907.

105. Cooper, B. a. P., A. On the anatomy of the breast. **1840,** *1*.

106. N.Gould, D. R. M. a. M. Rat mammary carcinogenesis induced by in situ expression of constitutive Raf kinase activity is prevented by tethering Raf to the plasma membrane. *Carcinogenesis* **2003,** *26* (6), 1149 - 1153.

107. Lakshmi Sivaraman, J. G., Susan G Hilsenbeck, H David Shine, Orla M Conneely, Daniel Medina, and Bert W O'Malley. Effect of selective ablation of proliferating mammary epithelial cells on MNU induced rat mammary tumorigenesis. *Breast Cancer Research and Treatment 73: .* **2002,** *73*, 75–83.

108. Homa Okugawa, D. Y., Yoshiko Uemura, Noriko Sakaida, Akihide Tanano, Kanji Tanaka and Yasuo Kamiyama. Effect of perductal paclitaxel exposure on

the development of MNU-induced mammary carcinoma in female S–D rats. *Breast Cancer Research and Treatment* **2005,** *91*, 29–34.

109. Murata, S.; Kominsky, S. L.; Vali, M.; Zhang, Z.; Garrett-Mayer, E.; Korz, D.; Huso, D.; Baker, S. D.; Barber, J.; Jaffee, E.; Reilly, R. T.; Sukumar, S. Ductal Access for Prevention and Therapy of Mammary Tumors. *Cancer Research* **2006,** *66*, (2), 638-645.

110. Stearns, V.; Mori, T.; Jacobs, L. K.; Khouri, N. F.; Gabrielson, E.; Yoshida, T.; Kominsky, S. L.; Huso, D. L.; Jeter, S.; Powers, P.; Tarpinian, K.; Brown, R. J.; Lange, J. R.; Rudek, M. A.; Zhang, Z.; Tsangaris, T. N.; Sukumar, S. Preclinical and Clinical Evaluation of Intraductally Administered Agents in Early Breast Cancer. *Science Translational Medicine* **2011,** *3*, (106), 106ra108-106ra108.

111. Migotto, A.; Carvalho, V. F. M.; Salata, G. C.; da Silva, F. W. M.; Yan, C. Y. I.; Ishida, K.; Costa-Lotufo, L. V.; Steiner, A. A.; Lopes, L. B. Multifunctional nanoemulsions for intraductal delivery as a new platform for local treatment of breast cancer. *Drug Delivery* **2018,** *25*, (1), 654-667.

112. Chun, Y. S.; Yoshida, T.; Mori, T.; Huso, D. L.; Zhang, Z.; Stearns, V.; Perkins, B.; Jones, R. J.; Sukumar, S. Intraductally administered pegylated liposomal doxorubicin reduces mammary stem cell function in the mammary gland but in the long term, induces malignant tumors. *Breast Cancer Research and Treatment* **2012,** *135*, (1), 201-208.

113. Chun, Y. S.; Bisht, S.; Chenna, V.; Pramanik, D.; Yoshida, T.; Hong, S.-M.; de Wilde, R. F.; Zhang, Z.; Huso, D. L.; Zhao, M.; Rudek, M. A.; Stearns, V.; Maitra, A.; Sukumar, S. Intraductal administration of a polymeric nanoparticle

formulation of curcumin (NanoCurc) significantly attenuates incidence of mammary tumors in a rodent chemical carcinogenesis model: Implications for breast cancer chemoprevention in at-risk populations. *Carcinogenesis* **2012,** *33*, (11), 2242-2249.

114. Zhang, B.; Love, S. M.; Chen, G.; Wang, J.; Gao, J.; Xu, X.; Wang, Z.; Wang, X. The safety parameters of the study on intraductal cytotoxic agent

delivery to the breast before mastectomy. *Chin J Cancer Res* **2014,** *26*, 579-587.

115. Brock, A.; Krause, S.; Li, H.; Kowalski, M.; Goldberg, M. S.; Collins, J. J.; Ingber, D. E. Silencing HoxA1 by Intraductal Injection of siRNA Lipidoid Nanoparticles Prevents Mammary Tumor Progression in Mice. *Science Translational Medicine* **2014,** *6*, 217ra2-217ra2.

116. Takahiro Yoshida, K. J., Hong Song, Sunju Park, David L. Huso, Zhe Zhang, Han Liangfeng, Charles Zhu, Frank Bruchertseifer, Alfred Morgenstern, George Sgouros, Saraswati Sukumar. Effective treatment of ductal carcinoma in situ with a HER-2-targeted alpha-particle emitting radionuclide in a preclinical model of human breast cancer. *Oncotarget* **2016,** *7*, (22), 33306 - 33315.

117. Groot, J. S. d.; Pan, X.; Youssef; Hoeve, N. D. t.; Bruin, A. d.; Diest, P. J. v.; Jonkers, J.; Amersfoort, M. v.; Rosing, H.; Wall, E. v. d.; Beijnen, J. H.; Vlug, E. J.; A, S.; W.B., P.; Derksen. Intraductal cisplatin treatment in a BRCA-associated breast cancer mouse model attenuates tumor development but leads to systemic tumors in aged female mice. *Oncotarget* **2017,** *8* 60750-60763.

118. Carvalho, V. F. M.; Salata, G. C.; de Matos, J. K. R.; Costa-Fernandez, S.; Chorilli, M.; Steiner, A. A.; de Araujo, G. L. B.; Silveira, E. R.; Costa-Lotufo, L.

V.; Lopes, L. B. Optimization of composition and obtainment parameters of biocompatible nanoemulsions intended for intraductal administration of piplartine (piperlongumine) and mammary tissue targeting. *International Journal of Pharmaceutics* **2019,** *567*, 118460.

119. Wang, G.; Chen, C.; Pai, P.; Korangath, P.; Sun, S.; Merino, V. F.; Yuan, J.; Li, S.; Nie, G.; Stearns, V.; Sukumar, S. Intraductal fulvestrant for therapy of ERα-positive ductal carcinoma in situ of the breast: a preclinical study. *Carcinogenesis* **2019,** *40*, (7), 903-913.

120. Leonard, G. D.; Swain, S. M. Ductal Carcinoma In Situ, Complexities and Challenges. *JNCI Journal of the National Cancer Institute* **2004,** *96*, (12), 906-920.

121. Shapiro, C. L.; Recht, A. Side effects of adjuvant treatment of breast cancer. *New England Journal of Medicine* **2001,** *344.26*, 1997-2008.

122. Palesh, O.; Scheiber, C.; Kesler, S.; Mustian, K.; Koopman, C.; Schapira, L. Management of side effects during and post-treatment in breast cancer survivors. *The breast journal* **2018,** *24.2*, 167-175.

123. Love, S. M.; Zhang, W.; Gordon, E. J.; Rao, J.; Yang, H.; Li, J.; Zhang, B.; Wang, X.; Chen, G.; Zhang, B. A Feasibility Study of the Intraductal Administration of Chemotherapy. *Cancer Prevention Research* **2012,** *6*, (1), 51-58.

124. Yashveer Singh, D. G., Zichao Gu, Shike Li, Kristia A. Rivera, Stanley Stein, Susan Love, Patrick J. Sinko. Influence of Molecular Size on the Retention of Polymeric Nanocarrier Diagnostic Agents in Breast Ducts. *Pharm Research* **2012,** *29*, 2377–2388.

125. Makadia, H. K.; Siegel, S. J. Poly Lactic-co-Glycolic Acid (PLGA) as Biodegradable Controlled Drug Delivery Carrier. *Polymers* **2011,** *3*, (3), 1377-1397.

126. Murata, N., Takashima, Y., Toyoshima, K., Yamamoto, M., & Okada, H. Anti-tumor effects of anti-VEGF siRNA encapsulated with PLGA microspheres in mice. *Journal of Controlled Release* **2008,** *126*, (3), 246-254.

127. Avgoustakis, K. Polylactic-co-glycolic acid (PLGA). *Encyclopedia of Biomaterials and Biomedical Engineering* **2008**, 2259-2269.

128. Colzani, B.; Pandolfi, L.; Hoti, A.; Iovene, P. A.; Natalello, A.; Avvakumova, S.; Colombo, M.; Prosperi, D. Investigation of antitumor activities of trastuzumab delivered by PLGA nanoparticles. *International Journal of Nanomedicine* **2018,** *Volume 13*, 957-973.

129. Fung, L. K. a. S., W.M. Polymeric implants for cancer chemotherapy. *Advanced drug delivery reviews* **1997,** *26*, (2-3), 209-230.

130. Kim, K. K.; Pack, D., Microspheres for Drug Delivery. In *BioMEMS and Biomedical Nanotechnology.* , M, F.; A.P, L.; L.J, L., Eds. Springer: Boston, MA, 2006 Microspheres for Drug Delivery. In: Ferrari M., Lee A.P., Lee L.J. (eds)

131. Kempe, S.; Mäder, K. In situ forming implants — an attractive formulation principle for parenteral depot formulations. *Journal of Controlled Release* **2012,** *161*, (2), 668-679.

132. Love, S. M.; Zhang, B.; Zhang, W.; Zhang, B.; Yang, H.; Rao, J. Local drug delivery to the breast: a phase 1 study of breast cytotoxic agent administration prior to mastectomy. *BMC Proceedings* **2009,** *3*, (Suppl 5), S29.

133. Choi, H. S., Seo, S.A., Khang, G., Rhee, J.M. and Lee, H.B. Preparation and characterization of fentanyl-loaded PLGA microspheres: in vitro release profiles. *International journal of pharmaceutics* **2002,** *234*, (1-2), 195-203.

134. Mainardes, R. M.; Evangelista, R. C. PLGA nanoparticles containing praziquantel: effect of formulation variables on size distribution. *International Journal of Pharmaceutics* **2005,** *290*, (1-2), 137-144.

135. Parent, M.; Nouvel, C.; Koerber, M.; Sapin, A.; Maincent, P.; Boudier, A. PLGA in situ implants formed by phase inversion: Critical physicochemical parameters to modulate drug release. *Journal of Controlled Release* **2013,** *172*, (1), 292-304.

136. Ravivarapu, H. B., Moyer, K.L. and Dunn, R.L. Parameters affecting the efficacy of a sustained release polymeric implant of leuprolide. *International journal of pharmaceutics* **2000,** *194*, (2), 181-191.

137. Solorio, L.; Olear, A. M.; Hamilton, J. I.; Patel, R. B.; Beiswenger, A. C.; Wallace, J. E.; Zhou, H.; Exner, A. A. Noninvasive Characterization of the Effect of Varying PLGA Molecular Weight Blends on In Situ Forming Implant Behavior Using Ultrasound Imaging. *Theranostics* **2012,** *2*, (11), 1064-1077.

138. Ruan, S.; Hea, Q.; Gao, H. Matrix metalloproteinase triggered size-shrinkable gelatin-gold fabricated nanoparticles for tumor microenvironment sensitive penetration and diagnosis of glioma." *Nanoscale* **2015,** *7.21* 9487-9496.

139. Xu, Q.; Hashimoto, M.; Dang, T. T.; Hoare, T.; Kohane, D. S.; Whitesides, G. M.; Langer, R.; Anderson, D. G. Preparation of Monodisperse Biodegradable Polymer Microparticles Using a Microfluidic Flow-Focusing Device for Controlled Drug Delivery. *Small* **2009,** *5*, (13), 1575-1581.

140. Sahoo, S. K., Panyam, J., Prabha, S. and Labhasetwar, V. Residual polyvinyl alcohol associated with poly (D, L-lactide-co-glycolide) nanoparticles affects their physical properties and cellular uptake. *Journal of controlled release* **2002,** *82*, (1), 105-114.

141. Allegra, C. J., Aberle, D.R., Ganschow, P., Hahn, S.M., Lee, C.N., Millon-Underwood, S., Pike, M.C., Reed, S.D., Saftlas, A.F., Scarvalone, S.A. and Schwartz, A.M. NIH state-of-the-science conference statement: diagnosis and management of ductal carcinoma in situ (DCIS) *NIH consensus and state-of-the-science statements* **2009,** *26*, (2), 1-27.

142. Darby, S. C., McGale, P., Taylor, C.W. and Peto, R. Long-term mortality from heart disease and lung cancer after radiotherapy for early breast cancer: prospective cohort study of about 300 000 women in US SEER cancer registries. *The lancet oncology* **2005,** *6*, (8), 557-565.

143. Reisch, A. a. K., A.S. Fluorescent polymer nanoparticles based on dyes: seeking brighter tools for bioimaging. *Small* **2016** *12*, (15), 1968-1992.

144. Tyler, B.; Gullotti, D.; Mangraviti, A.; Utsuki, T.; Brem, H. Polylactic acid (PLA) controlled delivery carriers for biomedical applications. *Advanced Drug Delivery Reviews* **2016,** *107*, 163-175.

145. Eliaz, R. E.; Szoka, F. C. Robust and prolonged gene expression from injectable polymeric implants. *Gene Therapy* **2002,** *9*, (18), 1230-1237.

146. Graves, R. A.; Pamujula, S.; Moiseyev, R.; Freeman, T.; Bostanian, L. A.; Mandal, T. K. Effect of different ratios of high and low molecular weight PLGA

blend on the characteristics of pentamidine microcapsules. *International Journal of Pharmaceutics* **2004,** *270*, (1-2), 251-262.

147. Mittal, G.; Sahana, D. K.; Bhardwaj, V.; Ravi Kumar, M. N. V. Estradiol loaded PLGA nanoparticles for oral administration: Effect of polymer molecular weight and copolymer composition on release behavior in vitro and in vivo. *Journal of Controlled Release* **2007,** *119*, (1), 77-85.

148. Budhian, A.; Siegel, S. J.; Winey, K. I. Controlling the in vitro release profiles for a system of haloperidol-loaded PLGA nanoparticles. *International Journal of Pharmaceutics* **2008,** *346*, (1-2), 151-159.

149. Lee, M. S., Kim, Y.H., Kim, Y.J., Kwon, S.H., Bang, J.K., Lee, S.M., Song, Y.S., Hahm, D.H., Shim, I., Han, D. and Her, S. Pharmacokinetics and biodistribution of human serum albumin-TIMP-2 fusion protein using near-infrared optical imaging. *Journal of Pharmacy & Pharmaceutical Sciences* **2011,** *14*, (3), 368-377.

150. Gu, Z.; Al-Zubaydi, F.; Adler, D.; Li, S.; Johnson, S.; Prasad, P.; Holloway, J.; Szekely, Z.; Love, S.; Gao, D.; Sinko, P. J. Evaluation of intraductal delivery of poly(ethylene glycol)-doxorubicin conjugate nanocarriers for the treatment of ductal carcinoma in situ (DCIS)-like lesions in rats. *Journal of Interdisciplinary Nanomedicine* **2018,** *3*, (3), 146-159.

151. Luo, Y.; Li, S.; Bolund, L.; Li, J.; Liu, Y.; Yang, H.; Lin, L.; Du, Y.; Li, S.; Yang, H.; Vajta, G.; Callesen, H.; Bolund, L.; Sørensen, C. B. High efficiency of BRCA1 knockout using rAAV-mediated gene targeting: developing a pig model for breast cancer. *Transgenic Res* **2011,** *20*, 975–988.

152. Rahman, M.; Mohammed, S. Breast cancer metastasis and the lymphatic system. *Oncology Letters* **2015,** *10*, (3), 1233-1239.

153. Xie, Y., Bagby, T.R., Cohen, M.S. and Forrest, M.L. Drug delivery to the lymphatic system: importance in future cancer diagnosis and therapies. *Expert opinion on drug delivery* **2009,** *6*, (8), 785-792.

154. Tanis, P. J., Nieweg, O.E., Olmos, R.A.V. and Kroon, B.B. Anatomy and physiology of lymphatic drainage of the breast from the perspective of sentinel node biopsy 1. *Journal of the American College of Surgeons* **2001,** *192*, (3), 399-409.

155. Pascale, F.; Bédouet, L.; Fazel, A.; Namur, J.; Ghegediban, S. H.; Cornil, I. S.; Wassef, M.; Moine, L.; Laurent, A. Lymphatic Transport and Lymph Node Location of Microspheres Subcutaneously Injected in the Vicinity of Tumors in a Rabbit Model of Breast Cancer. *Pharmaceutical Research* **2018,** *35*, (10).

156. Taghian, N. R.; Miller, C. L.; Jammallo, L. S.; O'Toole, J.; Skolny, M. N. Lymphedema following breast cancer treatment and impact on quality of life: A review. *Critical Reviews in Oncology/Hematology* **2014,** *92*, (3), 227-234.

157. Nguyen, T. T.; Hoskin, T. L.; Day, C. N.; Habermann, E. B.; Goetz, M. P.; Boughey, J. C. Factors Influencing Use of Hormone Therapy for Ductal Carcinoma In Situ: A National Cancer Database Study. *Annals of Surgical Oncology* **2017,** *24*, (10), 2989-2998.

158. Fisher, B.; Dignam, J.; Wolmark, N.; Wickerham, D. L.; Fisher, E. R.; Mamounas, E.; Smith, R.; Begovic, M.; Dimitrov, N. V.; Margolese, R. G.; Kardinal, C. G.; Kavanah, M. T.; Fehrenbacher, L.; Oishi, R. H. Tamoxifen in

treatment of intraductal breast cancer: National Surgical Adjuvant Breast and Bowel Project B-24 randomised controlled trial. *The Lancet* **1999,** *353*, (9169), 1993-2000.

159. Peng, J., Sengupta, S. and Jordan, V.C. Potential of selective estrogen receptor modulators as treatments and preventives of breast cancer. *Anti-Cancer Agents in Medicinal Chemistry (Formerly Current Medicinal Chemistry-Anti-Cancer Agents)* **2009,** *9*, (5), 481-499.

160. Jordan, V. C. Tamoxifen: a most unlikely pioneering medicine. *Nature Reviews Drug Discovery* **2003,** *2*, (3), 205-213.

161. Jordan, V. New insights into the metabolism of tamoxifen and its role in the treatment and prevention of breast cancer. *Steroids* **2007,** *72*, (13), 829-842.

162. Rao, U. S., Fine, R.L. and Scarborough, G.A. Antiestrogens and steroid hormones: substrates of the human P-glycoprotein. *Biochemical pharmacology* **1994** *48*, (2), 287-292.

163. Gant, T. W., Oconnor, C.K., Corbitt, R., Thorgeirsson, U. and Thorgeirsson, S.S. In vivo induction of liver P-glycoprotein expression by xenobiotics in monkeys. *Toxicology and applied pharmacology* **1995,** *133*, (2), 269-276.

164. Fernández-Olleros, A. M.; Olmo, R.; Muñíz, E.; Lozano, R.; Teijón, J. M.; Blanco, M. D. In-vivo evaluation of tamoxifen-loaded microspheres based on mixtures of poly (D,L-lactide-co-glycolide) and poly (D,L-lactide) polymers. *Anti-Cancer Drugs* **2014**, 1.

165. Chollet, J.; Mermelstein, F.; Rocamboli, S. C.; Friend, D. R. Vaginal tamoxifen for treatment of vulvar and vaginal atrophy: Pharmacokinetics and local tolerance

in a rabbit model over 28 days. *International Journal of Pharmaceutics* **2019,** *570*, 118691.

166. Chaurasia, S.; Mounika, K.; Bakshi, V.; Prasad, V. 3-month parenteral PLGA microsphere formulations of risperidone: Fabrication, characterization and neuropharmacological assessments. *Materials Science and Engineering: C* **2017,** *75*, 1496-1505.

167. Teunissen, S. F.; Rosing, H.; Koornstra, R. H. T.; Linn, S. C.; Schellens, J. H. M.; Schinkel, A. H.; Beijnen, J. H. Development and validation of a quantitative assay for the analysis of tamoxifen with its four main metabolites and the flavonoids daidzein, genistein and glycitein in human serum using liquid chromatography coupled with tandem mass spectrometry. *Journal of Chromatography B* **2009,** *877*, (24), 2519-2529.

168. Freiberg, S.; Zhu, X. X. Polymer microspheres for controlled drug release. *International Journal of Pharmaceutics* **2004,** *282*, (1-2), 1-18.

169. de Jalón, E. G., Blanco-Príeto, M.J., Ygartua, P. and Santoyo, S. Topical application of acyclovir-loaded microparticles: quantification of the drug in porcine skin layers. *Journal of controlled release* **2001,** *75*, ((1-2)), 191-197.

170. Chaiyasat, P.; Pholsrimuang, P.; Boontung, W.; Chaiyasat, A. Influence of Poly(L-lactic acid) Molecular Weight on the Encapsulation Efficiency of Urea in Microcapsule Using a Simple Solvent Evaporation Technique. *Polymer-Plastics Technology and Engineering* **2016,** *55*, (11), 1131-1136.

171. Berkland, C., Kim, K.K. and Pack, D.W. PLG microsphere size controls drug release rate through several competing factors. *Pharmaceutical research* **2003,** *20*, (7), 1055-1062.

172. Jain, R. A., Rhodes, C.T., Railkar, A.M., Malick, A.W. and Shah, N.H. Controlled release of drugs from injectable in situ formed biodegradable PLGA microspheres: effect of various formulation variables. *European journal of pharmaceutics and biopharmaceutics* **2000,** *50*, (2), 257-262.

173. Huang, W.; Tsui, C. P.; Tang, C. Y.; Gu, L. Effects of Compositional Tailoring on Drug Delivery Behaviours of Silica Xerogel/Polymer Core-shell Composite Nanoparticles. *Scientific Reports* **2018,** *8*, (1).

174. Huang, X. a. B., C.S. On the importance and mechanisms of burst release in matrix-controlled drug delivery systems. *Journal of controlled release* **2001,** *73*, (2-3), 121-136.

175. Lambert, W. J. a. P., K.D. Development of an in situ forming biodegradable poly-lactide-coglycolide system for the controlled release of proteins. *Journal of Controlled Release* **1995,** *33*, (1), 189-195.

176. Jordan, V. C., COLLINS, M.M., ROWSBY, L. and Prestwich, G. A monohydroxylated metabolite of tamoxifen with potent antioestrogenic activity *Journal of Endocrinology* **1977,** *75*, (2), 305-316.

177. Lien, E. A., Solheim, E., Lea, O. A., Lundgren, S., Kvinnsland, S., & Ueland, P. M. . Distribution of 4-hydroxy-N-desmethyltamoxifen and other tamoxifen metabolites in human biological fluids during tamoxifen treatment. *Cancer research* **1989,** *49*, (8), 2175-2183.

178. Huang, Z., Fasco, M.J., Figge, H.L., Keyomarsi, K. and Kaminsky, L.S. Expression of cytochromes P450 in human breast tissue and tumors. *Drug metabolism and disposition* **1996,** *24*, (8), 899-905.

179. Desai, P. B., Nallani, S.C., Sane, R.S., Moore, L.B., Goodwin, B.J., Buckley, D.J. and Buckley, A.R.,. Induction of cytochrome P450 3A4 in primary human hepatocytes and activation of the human pregnane X receptor by tamoxifen and 4-hydroxytamoxifen. *Drug metabolism and disposition* **2002,** *30*, (5), 608-612.

180. Mandlekar, S., Yu, R., Tan, T.H. and Kong, A.N.T. Activation of caspase-3 and c-Jun NH2-terminal kinase-1 signaling pathways in tamoxifen-induced apoptosis of human breast cancer cells. *Cancer research* **2000,** *60*, (21), 5995-6000.

181. Lim, Y. C.; Desta, Z.; Flockhart, D. A.; Skaar, T. C. Endoxifen (4-hydroxy-N-desmethyl-tamoxifen) has anti-estrogenic effects in breast cancer cells with potency similar to 4-hydroxy-tamoxifen. *Cancer Chemotherapy and Pharmacology* **2005,** *55*, (5), 471-478.

182. de Vries Schultink, A. H. M.; Alexi, X.; van Werkhoven, E.; Madlensky, L.; Natarajan, L.; Flatt, S. W.; Zwart, W.; Linn, S. C.; Parker, B. A.; Wu, A. H. B.; Pierce, J. P.; Huitema, A. D. R.; Beijnen, J. H. An Antiestrogenic Activity Score for tamoxifen and its metabolites is associated with breast cancer outcome. *Breast Cancer Research and Treatment* **2016,** *161*, (3), 567-574.

183. Zou, Y.; Bateman, T. J.; Adreani, C.; Shen, X.; Cunningham, P. K.; Wang, B.; Trinh, T.; Christine, A.; Hong, X.; Nunes, C. N.; Johnson, C. V.; Zhang, A. S.; Staskiewicz, S. J.; Braun, M.; Kumar, S.; Reddy, V. B. G. Lymphatic Absorption,

Metabolism, and Excretion of a Therapeutic Peptide in Dogs and Rats. *Drug Metabolism and Disposition* **2013,** *41*, (12), 2206-2214.

184. Chen, J., Wang, L., Yao, Q., Ling, R., Li, K. and Wang, H. Drug concentrations in axillary lymph nodes after lymphatic chemotherapy on patients with breast cancer. *Breast Cancer Research* **2004,** *6*, (4), p.R474.

185. Johnson, M. D., Zuo, H., Lee, K. H., Trebley, J. P., Rae, J. M., Weatherman, R. V., ... & Skaar, T. C. Pharmacological characterization of 4-hydroxy-N-desmethyl tamoxifen, a novel active metabolite of tamoxifen. *Breast cancer research and treatment* **2004,** *85*, (2), 151-159.

186. Robinson, S. P., Langan-Fahey, S. M., Johnson, D. A., & Jordan, V. C. . Metabolites, pharmacodynamics, and pharmacokinetics of tamoxifen in rats and mice compared to the breast cancer patient. *Drug Metabolism and Disposition* **1991,** *19*, (1), 36-43.

187. Lien, E. A., Solheim, E., & Ueland, P. M. . Distribution of tamoxifen and its metabolites in rat and human tissues during steady-state treatment. *Cancer research* **1991,** *51*, (18), 4837-4844.

188. Kiyotani, K.; Mushiroda, T.; Nakamura, Y.; Zembutsu, H. Pharmacogenomics of Tamoxifen: Roles of Drug Metabolizing Enzymes and Transporters. *Drug Metabolism and Pharmacokinetics* **2012,** *27*, (1), 122-131.

189. Desta, Z. Comprehensive Evaluation of Tamoxifen Sequential Biotransformation by the Human Cytochrome P450 System in Vitro: Prominent Roles for CYP3A and CYP2D6. *Journal of Pharmacology and Experimental Therapeutics* **2004,** *310*, (3), 1062-1075.

190. Ward, M. A.; Georgiou, T. K. Thermoresponsive Polymers for Biomedical Applications. *Polymers* **2011,** *3*, (3), 1215-1242.

191. Mohammadi, M.; Patel, K.; Alaie, S. P.; Shmueli, R. B.; Besirli, C. G.; Larson, R. G.; Green, J. J. Injectable drug depot engineered to release multiple ophthalmic therapeutic agents with precise time profiles for postoperative treatment following ocular surgery. *Acta Biomaterialia* **2018,** *73*, 90-102.

192. Zhang, Z.; Ni, J.; Chen, L.; Yu, L.; Xu, J.; Ding, J. Biodegradable and thermoreversible PCLA–PEG–PCLA hydrogel as a barrier for prevention of post-operative adhesion. *Biomaterials* **2011,** *32*, (21), 4725-4736.

193. Wang, P.; Zhuo, X.; Chu, W.; Tang, X. Exenatide-loaded microsphere/thermosensitive hydrogel long-acting delivery system with high drug bioactivity. *International Journal of Pharmaceutics* **2017,** *528*, (1-2), 62-75.

194. Petit, A., Müller, B., Bruin, P., Meyboom, R., Piest, M., Kroon-Batenburg, L.M., de Leede, L.G., Hennink, W.E. and Vermonden, T. Modulating rheological and degradation properties of temperature-responsive gelling systems composed of blends of PCLA–PEG–PCLA triblock copolymers and their fully hexanoyl-capped derivatives. *Acta biomaterialia* **2012,** *8*, (12), 4260-4267.

195. Sandker, M. J., Petit, A., Redout, E.M., Siebelt, M., Müller, B., Bruin, P., Meyboom, R., Vermonden, T., Hennink, W.E. and Weinans, H. In situ forming acyl-capped PCLA–PEG–PCLA triblock copolymer based hydrogels. *Biomaterials* **2013,** *34*, (32), 8002-8011.

196. Cai, X., Luan, Y., Jiang, Y., Song, A., Shao, W., Li, Z. and Zhao, Z. Huperzine A–phospholipid complex-loaded biodegradable thermosensitive polymer gel for

controlled drug release. *International journal of pharmaceutics* **2012,** *433*, (1-2), 102-111.

197. Duvvuri, S., Janoria, K.G., Pal, D. and Mitra, A.K. Controlled delivery of ganciclovir to the retina with drug-loaded Poly (d, L-lactide-co-glycolide)(PLGA) microspheres dispersed in PLGA-PEG-PLGA Gel: a novel intravitreal delivery system for the treatment of cytomegalovirus retinitis. *Journal of ocular pharmacology and therapeutics* **2007,** *23*, (3), 264-274.

198. Hirani, A., Grover, A., Lee, Y.W., Pathak, Y. and Sutariya, V. Triamcinolone acetonide nanoparticles incorporated in thermoreversible gels for age-related macular degeneration. *Pharmaceutical development and technology* **2016,** *21*, (1), 61-67.

199. Petit, A.; Sandker, M.; Müller, B.; Meyboom, R.; van Midwoud, P.; Bruin, P.; Redout, E. M.; Versluijs-Helder, M.; van der Lest, C. H. A.; Buwalda, S. J.; de Leede, L. G. J.; Vermonden, T.; Kok, R. J.; Weinans, H.; Hennink, W. E. Release behavior and intra-articular biocompatibility of celecoxib-loaded acetyl-capped PCLA-PEG-PCLA thermogels. *Biomaterials* **2014,** *35*, (27), 7919-7928.

200. Barichello, J. M., Morishita, M., Takayama, K. and Nagai, T.. . Encapsulation of hydrophilic and lipophilic drugs in PLGA nanoparticles by the nanoprecipitation method. *Drug development and industrial pharmacy* **1999,** *25*, (4), 471-476.

201. Liow, S. S.; Dou, Q.; Kai, D.; Karim, A. A.; Zhang, K.; Xu, F.; Loh, X. J. Thermogels: In Situ Gelling Biomaterial. *ACS Biomaterials Science & Engineering* **2016,** *2*, (3), 295-316.

202. Johnson, M. D., Zuo, H., Lee, K.H., Trebley, J.P., Rae, J.M., Weatherman, R.V., Desta, Z., Flockhart, D.A. and Skaar, T.C. Pharmacological characterization of 4-hydroxy-N-desmethyl tamoxifen, a novel active metabolite of tamoxifen. *Breast cancer research and treatment* **2004,** *85*, (2), 151-159.

203. Manolova, V.; Flace, A.; Bauer, M.; Schwarz, K.; Saudan, P.; Bachmann, M. F. Nanoparticles target distinct dendritic cell populations according to their size. *European Journal of Immunology* **2008,** *38*, (5), 1404-1413.

204. Oussoren, C. a. S., G. Liposomes to target the lymphatics by subcutaneous administration. *Advanced drug delivery reviews* **2001,** *50*, ((1-2)), pp.143-156.

205. Ueno, H., Hihara, J., Shimizu, K., Osaki, A., Yamashita, Y., Yoshida, K. and Toge, T. Experimental study on fluorescent microspheres as a tracer for sentinel node detection. *Anticancer research* **2005,** *25*, (2A), pp.821-825.

206. Damge, C., Aprahamian, M., Marchais, H., Benoit, J.P. and Pinget, M. Intestinal absorption of PLAGA microspheres in the rat. *Journal of anatomy* **1996,** *189*, (3), p.491.